

Dissertation zur Erlangung des Doktorgrades
der Fakultät für Chemie und Pharmazie,
Ludwig-Maximilians-Universität München



The role of impaired cGMP homeostasis
in cone photoreceptor degeneration

Mirja Annika Koch

aus Karlsruhe

2016

Erklärung

Diese Dissertation wurde im Sinne von § 7 der Promotionsordnung vom 28. November 2011 von Herrn Prof. Dr. Martin Biel betreut.

Eidesstattliche Versicherung

Diese Dissertation wurde eigenständig und ohne unerlaubte Hilfe erarbeitet.

München, den 15.07.2016

(Mirja Annika Koch)

Dissertation eingereicht am	<u>15.07.2016</u>
1. Gutachter:	Prof. Dr. Martin Biel
2. Gutachter:	PD Dr. Stylianos Michalakis
Mündliche Prüfung am	<u>23.09.2016</u>

Table of contents

Table of contents.....	4
Abbreviations.....	8
1 Introduction.....	11
1.1 Vision.....	11
1.2 Achromatopsia.....	15
1.3 The role of cGMP in photoreceptor degeneration.....	18
1.4 Animal models to study retinal degeneration.....	22
1.5 Gene therapy for Achromatopsia.....	25
1.6 Aim of this thesis.....	27
2 Materials and Methods.....	28
2.1 Animals.....	28
2.2 Chemicals, solutions and buffers.....	28
2.3 Genotyping.....	28
2.4 Agarose gel electrophoresis.....	30
2.5 Retina dissection.....	31
2.6 RNA extraction.....	31
2.7 cDNA synthesis.....	32
2.8 Microarray analysis.....	32
2.9 Gene regulation networks.....	33
2.10 Functional analyses.....	33
2.11 Real-time quantitative PCR (qPCR).....	33
2.12 Retina dissection (IHC).....	34
2.13 Retinal cryosections.....	35

2.14	Immunohistochemistry	35
2.15	Terminal deoxynucleotidyl transferase dUTP nick end labeling (TUNEL)-assay.....	37
2.16	Cloning.....	37
2.16.1	Cloning of the catalytic domain of cGKI	38
2.16.2	Cloning of shRNAs	40
2.16.3	Restriction analysis	40
2.16.4	Ligation.....	41
2.16.5	Transformation	41
2.16.6	Inoculation of bacterial cells and mini preparation of plasmid DNA.....	42
2.17	AAV production.....	43
2.17.1	Transfection and harvest.....	43
2.17.2	Purification of rAAVs via iodixanol gradient centrifugation.....	44
2.17.3	Purification of rAAVs via anion exchange chromatography.....	46
2.17.4	Concentration of rAAVs.....	47
2.17.5	rAAV titer determination via quantitative real-time PCR	47
2.18	Cell culture and plasmid transfection	48
2.19	shRNA validation.....	50
2.20	Subretinal injection	50
2.21	Ophthalmological examinations.....	51
2.22	SDS-polyacrylamide electrophoresis (SDS-PAGE)	52
2.23	Whole cell protein lysates.....	53
2.24	Western blotting	54
2.25	Co-immunoprecipitation (Co-IP)	55
2.26	Retina dissociation	56
2.27	Fluorescence-activated cell sorting (FACS)	57

Table of contents

2.28	Phospho-enrichment of Proteins	57
2.29	Mass-spectrometry	58
2.30	Statistics	59
3	Results.....	60
3.1	Transcriptional changes in the retina of <i>Cnga3</i> KO mice	60
3.2	cGMP accumulation in cones of <i>Cnga3</i> KO mice	60
3.3	Knock-down of guanylyl cyclase during degeneration	63
3.4	cGMP dependent kinases (cGKs) in the retina.....	65
3.5	Overexpression of cGK in wild type mice	66
3.6	Knockout of cGK during degeneration delays cone degeneration in <i>Cnga3</i> KO mice .	68
3.7	Knock-down of cGK II	72
3.8	cGKII signalling in the retina.....	72
3.8.1	Mass spectrometry based analysis of proteins expressed in cone photoreceptors. .	72
3.8.2	cGK-dependent phosphoprotein analysis.....	76
4	Discussion	78
4.1	Pathway analysis	78
4.2	cGMP accumulation and cell death	79
4.3	Role of cGMP-dependent kinases in cone degeneration	81
4.4	Cell death signalling in photoreceptors	82
4.5	cGKII signalling	84
4.6	Therapeutic applications.....	86
5	Conclusion and Outlook	87
6	Summary.....	88
7	Zusammenfassung	90
8	Appendix.....	92

8.1	Sequences	92
8.2	References.....	98
9	Danksagung	113

Abbreviations

ACHM	Achromatopsia
ANOVA	analysis of variance
Bp	basepair
Ca ²⁺	Calcium
cAMP	cyclic adenosinemonophosphate
Cap	Capsid
cDNA	complementary DNA
cGKI	cGMP dependent kinase type 1
cGKII	cGMP dependent kinase type 2
cGMP	Cyclic guanosine monophosphate
CNBD	cyclic nucleotide-binding domain
CNG	cyclic nucleotide gated
CNS	central nervous system
DKO	double knockout
DMEM	Dulbecco's modified eagle medium
DNA	desoxyribonucleinacid
dNTPs	Desoxyribonucleotide
ERG	Elektroretinogramm
FBS	fetal bovine serum
GCAP	guanylyl cyclase activating protein
GCL	ganglion cell layer
GCL	ganglion cell layer
GFAP	glial fibrillary acidic protein
GKAP	cGMP-dependent kinase anchoring proteins
GUCY	guanylyl cyclase
Glypho	glycogen
HEK cells	human embryonic kidney cells

hmc	hydroxy-methy-cytosine
ILM	inner limiting membrane
INL	inner nuclear layer
IPL	inner plexiform layer
IPL	inner plexiform layer
IS	inner segment
ITRs	inverted terminal repeats
kDa	kilodalton
KO	knockout
Na ⁺	sodium
OCT	optical coherence tomography
OD	oculus dexter/right
ON	optic nerve
ONL	outer nuclear layer
OLM	outer limiting membrane
OPL	outer plexiform layer
ORI	origin of replication
OS	oculus sinister/left
OS	outer segment
PB	phosphatpuffer
PCR	polymerase chain reaction
PDE	phosphodiesterase
PDE	phosphodiesterase
PFA	paraformaldehyd
qPCR	quantitative polymerase chain reaction
rAAV	recombinant adeno-associated virus
Rep	replication
RG	red/green opsin
Rho	rhodopsin
RNA	ribonucleotideacid
RP	Retinitis pigmentosa

Abbreviations

RPE	retinal pigment epithelium
rpm	revolutions per minute
SDS	sodium dodecylsulfate
shRNA	silence haripin RNA
cSLO	confocal laser scanning ophthalmoscopy
SV40	simian Virus 40
SWS	short wave-lengths
TEMED	tetramethylethylendiamin
TMD	trans membrane domain
TRIS	Tris-(hydroxymethyl)-aminomethan
UPR	unfolded protein response

1 Introduction

1.1 Vision

The light sensitive part of the eye is the retina, a thin three-dimensional network of neurons covering the back surface of the eye. The retina is considered as an outgrowth of the developing brain and can be seen as a part of the central nervous system (CNS). It is connected to the visual cortex via the optic nerve and the optic chiasm through the lateral geniculate nucleus.

In mammals vision begins in the outer layer of the retina in so called photoreceptors. To reach them, light has to pass the cornea, the lens, the vitreous body (Figure 1.1) and all layers of the retina (Figure 1.2). Vision relies not only on proper functioning of photoreceptors itself, but also on a proper interconnection between all different types of neurons in the retina. The retina is structured in a three cell layer dimension. These layers are termed: the ganglion cell layer (GCL), the inner nuclear layer (INL) and the outer nuclear layer (ONL) (Figure 1.2). The GCL is

composed of the cell bodies of ganglion and displaced amacrine cells, while in the INL the cell bodies of bipolar, horizontal, amacrine, as well as Müller glia cells are located. The ONL on the other hand is assembled by the cell bodies of the two types of photoreceptor: rods and cones (Figure 1.2). These three nuclear layers are separated by dense networks of neuronal synapses creating three further layers: the outer plexiform layer (OPL), the inner plexiform layer (IPL) and the nerve fibre layer (NFL) (Figure 1.2). In the OPL the projections of rods and cones synapse via rod spherules and cone pedicles to the dendrites of bipolar and horizontal cells. In the IPL axon terminals of bipolar cells and dendrites of ganglion and amacrine cells connect to each other. In the nerve fibre layer (NFL) the axonal fibres of ganglion cells merge in the optic nerve and connect the retina to the brain.

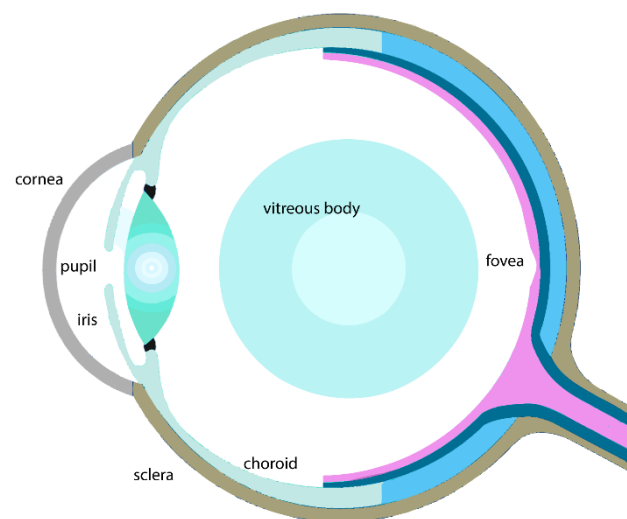


Figure 1.1: Anatomy of the human eye. The eye is protected from the outside by the sclera, in the choroid the blood vessels are located which supply blood to the retina. The inner layer of the eye is the light-sensitive retina with the fovea, responsible for sharp vision.

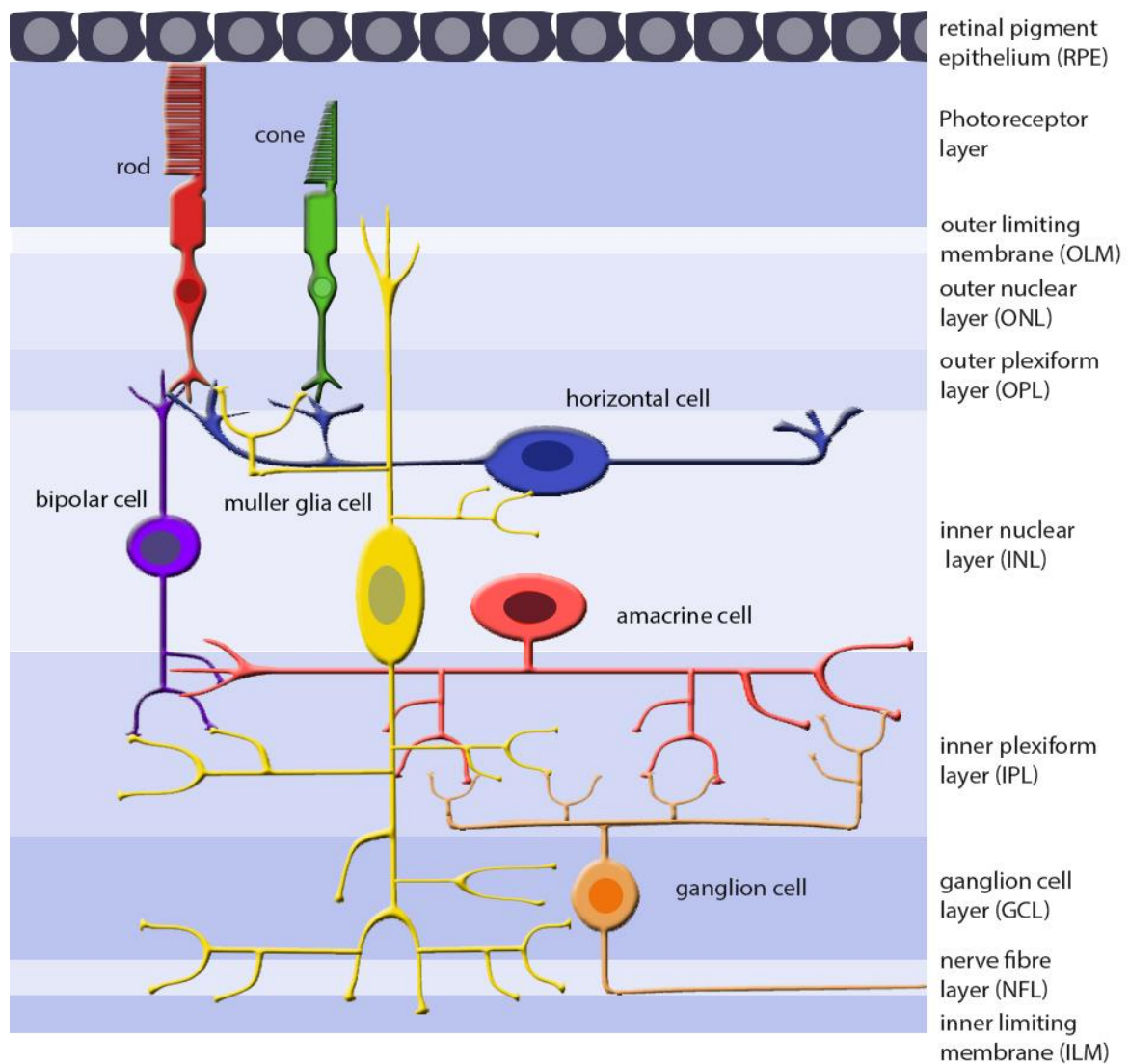


Figure 1.2: Retinal structure: Ten layers are incorporated in the highly complex structure of the retina. The retinal pigment epithelium (RPE) is responsible for nutrients supply for the retina, embedding the light-sensing rod and cone photoreceptors in the outermost layer of the retina. In the inner nuclear layer (INL) the connecting neurons: amacrine, bipolar and horizontal cell can be found. At the innermost layer the ganglion cells are located, which are directly connected to the brain through the optic nerve.

Temporal to the optic nerve the macula is located comprising the fovea centralis which encloses the highest density of cones. 10 % of the 4.5 million cones existing in the retina are situated in the fovea where no rods are present (Figure 1.1). This part is responsible for sharp central vision. Furthermore the vitreous body is separated from the retina by astrocytes and the end feet of Müllerth glia cells, forming the innermost layer, the inner limiting membrane (ILM) (Figure 1.2).

At the bases of rods and cones there is the outer limiting membrane (OLM), separating the nuclei of photoreceptors from the outer segments (Figure 1.2). At last the outer segments in the photoreceptor layer are embedded in the outermost layer of the retina, the retinal pigment epithelium (RPE).

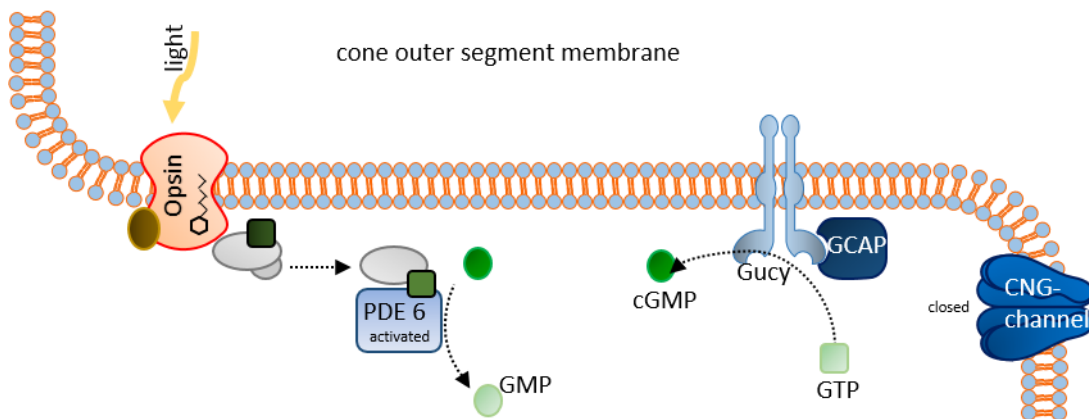
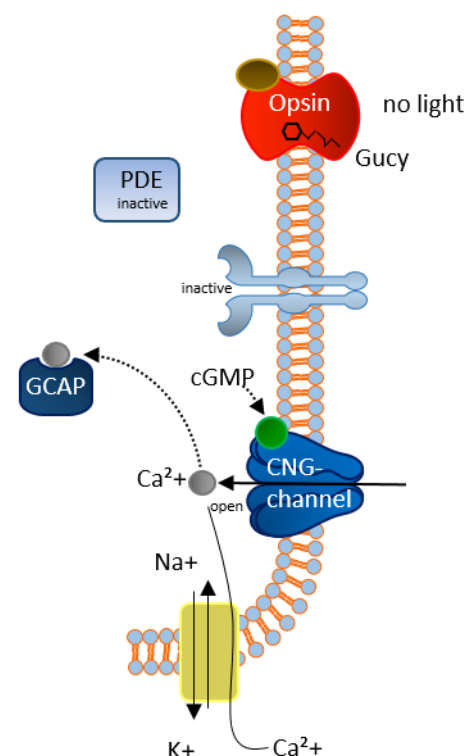


Figure 1.3: The phototransduction cascade:

The bound chromophore of the opsin gets photoisomerized by light and activates the coupled G-protein transducin. The transducin α -subunit then activates the phosphodiesterase (PDE6), which degrades cGMP to GMP. Due to the drop of cGMP level, the cyclic nucleotide-gated (CNG) channels close, causing a shutdown of Ca^{2+} influx and a hyperpolarization of the outer segment membrane potential. Due to decrease of intracellular Ca^{2+} levels, Ca^{2+} -free guanylate-cyclase-activating protein (GCAP) stimulates the guanylate cyclase (GC) for increased synthesis of cGMP. As soon as the light stimulus stops, cGMP-levels are rapidly restored, since PDE is inactive. Additionally GCs are inactive again and CNG channels are opened causing a depolarization of the membrane. This is called “dark current”.



Vision begins in the outer segments of the photoreceptors where light is transformed into an electrical signal. Located in the outer segments of photoreceptors light sensitive G-protein

Introduction

coupled receptors, so called opsins, transform into a new conformation upon interaction with a photon and activate a downstream cascade resulting in signalling action potentials. This conformational change is triggered by the photoreactive part of the opsins the retinal chromophore. In the well-studied rod opsin called rhodopsin, the chromophore 11-cis-retinal isomerizes and transforms rhodopsin to metarhodopsin II and a release of all-trans-retinal. Caused by the conformational change the associated G-protein transducin gets activated. In cones one of the respective cone opsins (S-, M- or L-Opsin) undergoes a similar conformational change. The number of activated transducins is directly linked to the intensity of the light stimulus. Upon

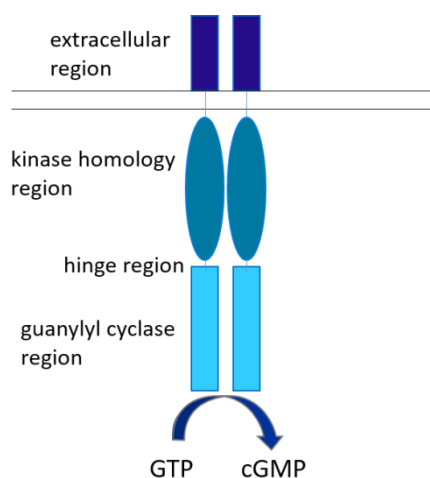


Figure 1.4: Structure of the membrane bound guanylyl cyclase (GC). GCs are anchored in the membrane. This transmembrane region combines an extracellular region, which can be bound by ligands and the intracellular domain. This domain has a protein-kinase like, hinge and catalytic region (Kuhn, 2003).

activation transducins in turn stimulate the phosphodiesterase 6 (PDE6), a cGMP hydrolysing enzyme, thus, leading to a drop of the intracellular level of this second messenger.

The second messenger cGMP plays a central role in the visual cascade. It is a modulator of the cyclic nucleotide-gated (CNG) channel, a nonselective cation channel, located in the plasma membrane of the photoreceptor outer segment. Upon binding, cGMP gates the CNG channel open, leading to a sodium (Na^+) and calcium (Ca^{2+}) ion influx. Upon light stimulation, the cGMP degrading PDE is activated leading to a fast decay of cGMP and closure of the CNG channels. The intracellular calcium concentrations declines and the photoreceptor cell hyperpolarises from -40 mV to -70 mV. As a consequence presynaptic voltage-dependent

calcium channels close and the synaptic glutamate-release is terminated (Arshavsky and Burns, 2012, Luo et al., 2008). The guanylyl cyclase activating protein (GCAP) is regulated by calcium. It has two intracellular Ca^{2+} binding sites: if these binding sites are unoccupied, GCAP stimulates the cGMP-production by activation of guanylyl cyclase (Gucy) (Yang et al., 1999, Palczewski et al., 2004, Lowe et al., 1995, Laura and Hurley, 1998).

Gucys can be membrane bound or soluble enzymes synthesizing cGMP from GTP. Membrane bound Guccys have an extracellular ligand binding domain, a short transmembrane region and an

intracellular catalytic domain (Figure 1.4). The activity of the membrane bound Gucys present in photoreceptors is not dependent on gaseous molecules (NO/CO₂) like soluble Gucys but rather on small proteins. Gucy-E which is expressed in rod and cones and Gucy-F, only present in rods, are both activated by small retinal-specific molecules, the guanylyl-cyclase-activating-proteins (GCAP) 1, 2 and 3 (Kuhn, 2003).

The activity of Gucys is crucial for a fast recovery of the dark current. During a light stimulus PDE hydrolyses the newly synthesized cGMP but as soon as the light stimulus ends PDEs are inactivated and cGMP levels increase - thereby gating the CNG-channel causing an influx of Ca²⁺ and Na⁺. This fast reaction causes a depolarisation of the outer segments plasma membrane (-40mV), which in turn activates presynaptic voltage-dependent calcium channels and triggers transmitter release at the synapse. GCAP now binds calcium and guanylyl cyclase is inhibited (Kuhn, 2003). Hence further cGMP production is interrupted and the cGMP level remains stable until a new light stimulus follows.

1.2 Achromatopsia

Genetic disruption of proteins involved in the photo-transduction cascade are known to lead to photoreceptor degeneration (Biel and Michalakakis, 2007, Boye et al., 2013, Roosing et al., 2014, Schon et al., 2013, Wright et al., 2010) Several retinal diseases have already been associated to a genetic cause. Non- and missense mutations have been identified in human patients suffering from retinal dystrophy affecting either rods or cones. The most common form of inherited retinal degenerative disease is Retinitis Pigmentosa (RP), causing a degeneration of rod photoreceptors while secondary a loss of cones is observed (Hartong et al., 2006). Achromatopsia (ACHM) is a retinal degenerative disorder affecting cone photoreceptors. ACHM shows an autosomal-recessive inheritance and has a prevalence of roughly 1 of 30,000 worldwide (Sundin et al., 2000, Pokorny et al., 1982).

Introduction

As for all other inherited degenerative retinal diseases, there is currently no treatment available. Currently, there are six known ACHM causing genes *CNGA3*, *CNGB3*, *GNAT2*, *PDE6C*, *PDE6H* and *ATF6*. Most of them encode important proteins involved in the cone photo transduction cascade like *CNGA3*, *CNGB3*, *GNAT2*, *PDE6C* and *PDE6H* (Trifunovic et al., 2010). The most recent addition to the ACHM gene list, is *ATF6* encoding for a protein involved in the unfolded protein response (UPR) process (Kohl et al., 2015). The UPR process fixes misshaped or falsely folded proteins. If these proteins are not fixed by the UPR process they not only do not work properly but furthermore might accumulate in the cell and cause cell stress (Kohl et al., 2015).



Figure 1.5: Vision of an Achromatopsia patient (B) compared to a healthy individual (A). Achromatopsia is a disease causing degeneration of photoreceptors in the retina. As a result of this degeneration, patients lack colour-vision. They furthermore suffer from light-sensitivity and blurry vision.

Patients suffering from ACHM are lacking cone photoreceptor function by birth thus, struggling with strongly compromised daylight vision (Figure 1.5). In addition to their inability to distinguish between colours, patients suffer from very low visual acuity, pendular nystagmus and eccentric fixation (Figure 1.5). Moreover, their cone photoreceptors degenerate over time. The subsequent loss of cones causes a sustained activation of rods and as a consequence patients experience an increased sensitivity to light, termed ‘photophobia’ (Pokorny et al., 1982, Kohl et al., 1998, Eksandh et al., 2002).

Diseased patients show only residual or absent cone function in full-field electroretinography (ERG) measurements (Kohl et al., 2000). Monitoring the morphology of diseased retina by spectral domain optical coherence tomography (OCT) a loss of inner and outer segments of cones can be seen at earlier stages (Figure 1.6 B), while a complete loss of cones in the photoreceptor layer (Figure 1.6 C) and an atrophy of retinal pigment epithelium (RPE) is

apparent at later stages of the disease (Figure 1.6 D) (Genead et al., 2011, Thiadens et al., 2010b).

A disruption in the *CNGB3* locus is the most common affected locus in the Western world with a prevalence of approximately 50 % (Kohl et al., 2005). Roughly 25-30 % of ACHM patients carry a genetic disruption in the locus of the CNGA3 subunit, involving over 100 different mutations (Thiadens et al., 2010a, Ma et al., 2013). Less than 2 % of ACHM patients carry a GNAT2,

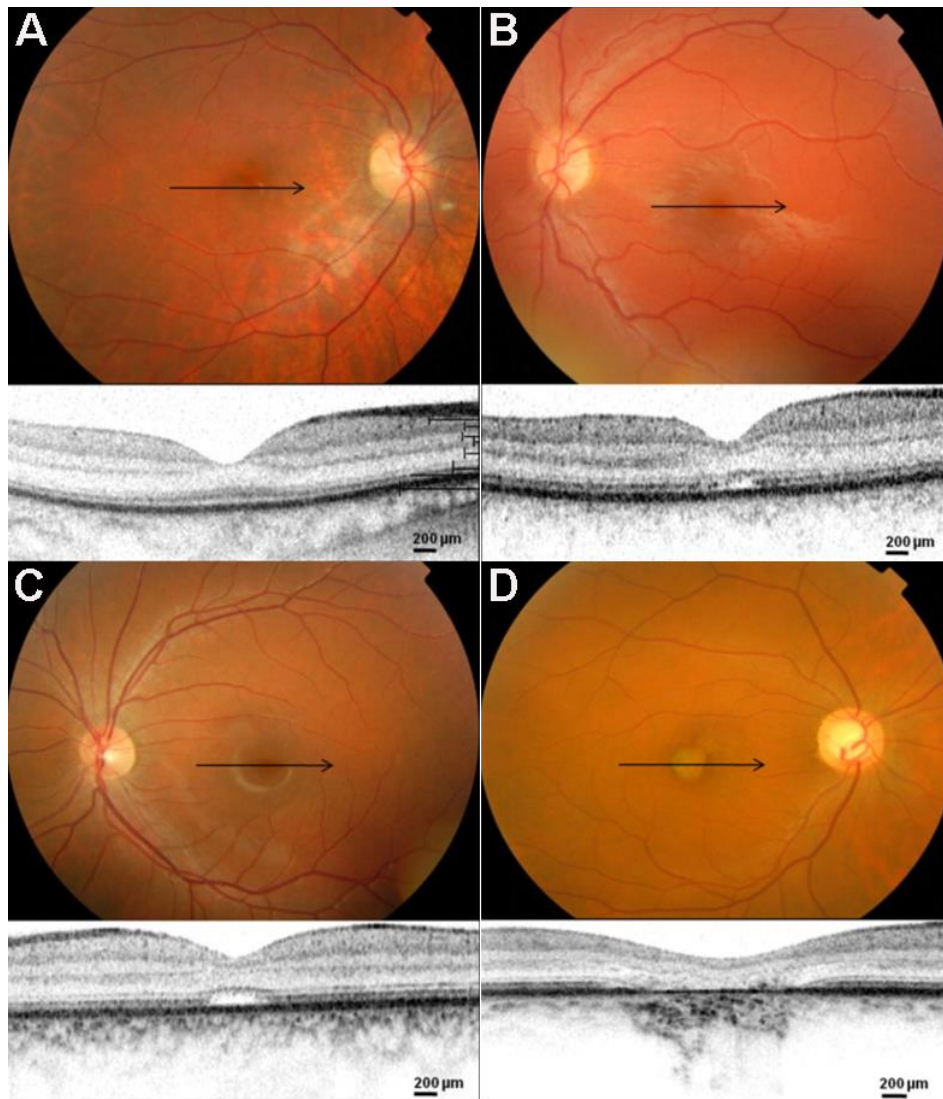


Figure 1.6: Fundus and Optical coherence tomography (OCT) images of Achromatopsia patients at different stages of the disease (A) Normal OCT and fundus images of a nine-year-old patient with a *CNGA3* mutation. (B) The OCT image of an eight-year-old Achromatopsia patient carrying *CNGB3* mutations displays the absence of inner and outer segments of cones while the fundus still shows a normal appearance of the macula. (C) In a 15-year-old patient with *CNGB3* mutations, bubbles in the fovea of the OCT image show a complete loss of cones. The fundus image shows no abnormal morphology. (D) Images of a patient also carrying *CNGB3* mutations in a later stage show a complete loss of cones and macular retinal pigment epithelium (RPE) atrophy. Images adapted from (adapted from Thiadens et al., 2010b)

Introduction

PDE6C or PDE6H mutation (Schon et al., 2013), only very few cases of an ATF6-mutation are known (Kohl et al., 2015). Other mutations still remain unknown.

CNG channels are heterotetrameric non-selective cation channels expressed in the outer segments of photoreceptors. The composition of the four subunits is tissue-specific and each subunit is formed by six transmembrane domains (TMD 1-6, Figure 1.6) (Yu et al., 2005). The cone specific CNG channel consists of three CNGA3 and one CNGB3 subunits and is modulated by cGMP (Figure 1.6) (Peng et al., 2004, Shuart et al., 2011).

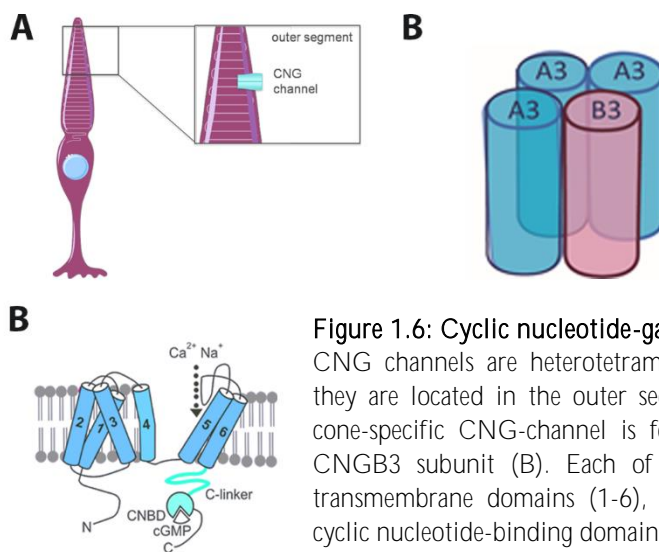


Figure 1.6: Cyclic nucleotide-gated (CNG) channel.

CNG channels are heterotetrameric cation channels. In the retina they are located in the outer segments of photoreceptors (A). The cone-specific CNG-channel is formed by three CNGA3 and one CNGB3 subunit (B). Each of these subunits is composed of 6 transmembrane domains (1-6), C = Carboxy terminus, CNBD = cyclic nucleotide-binding domain; N = amino-terminus (C).

1.3 The role of cGMP in photoreceptor degeneration

In 1974 already Farber and Lolley suggested that cGMP is an essential factor in the degeneration of photoreceptors (Farber and Lolley, 1974). In their study they were able to show an accumulation of this second messenger in cyclic nucleotide phosphodiesterase activity deficiency and assumed that this accumulation might result in an imbalance of the photoreceptor metabolism. More recent studies show an accumulation of cGMP in photoreceptors of mice suffering from different kinds of retinal degeneration (Xu et al., 2013, Paquet-Durand et al., 2009, Michalakakis et al., 2010, Bowes et al., 1990). Although this phenomenon has been described for the first time almost four decades ago it is still not known whether cGMP directly contributes to the degeneration process of photoreceptors.

In mammals cGMP is involved in various physiological functions ranging from contractility of cardiac and smooth muscles, cellular growth, neuronal excitability and neuronal plasticity, immune response and inflammation, as well as sensory transduction (Feil et al., 2005, Kemp-Harper and Feil, 2008). In the retina cGMP is the central second messenger of the phototransduction cascade. Disruption in the decay of this essential molecule is known to lead to photoreceptor dysfunction. Mutations in the *PDE6b* gene have been detected in autosomal recessive RP patients (McLaughlin et al., 1993). Moreover inbred laboratory mice strains termed “*rd^T*” showed a severe early onset retinal degeneration and were later shown to also carry a nonsense mutation in the *Pde6b* locus (Drager and Hubel, 1978, Pittler and Baehr, 1991). Interference with the production of cGMP by knocking out the guanylyl cyclase was also shown to lead to dysfunction and changes in the viability of cones while rods showed no change in morphology up to one year after birth (Yang et al., 1999). Interference with the transcription of

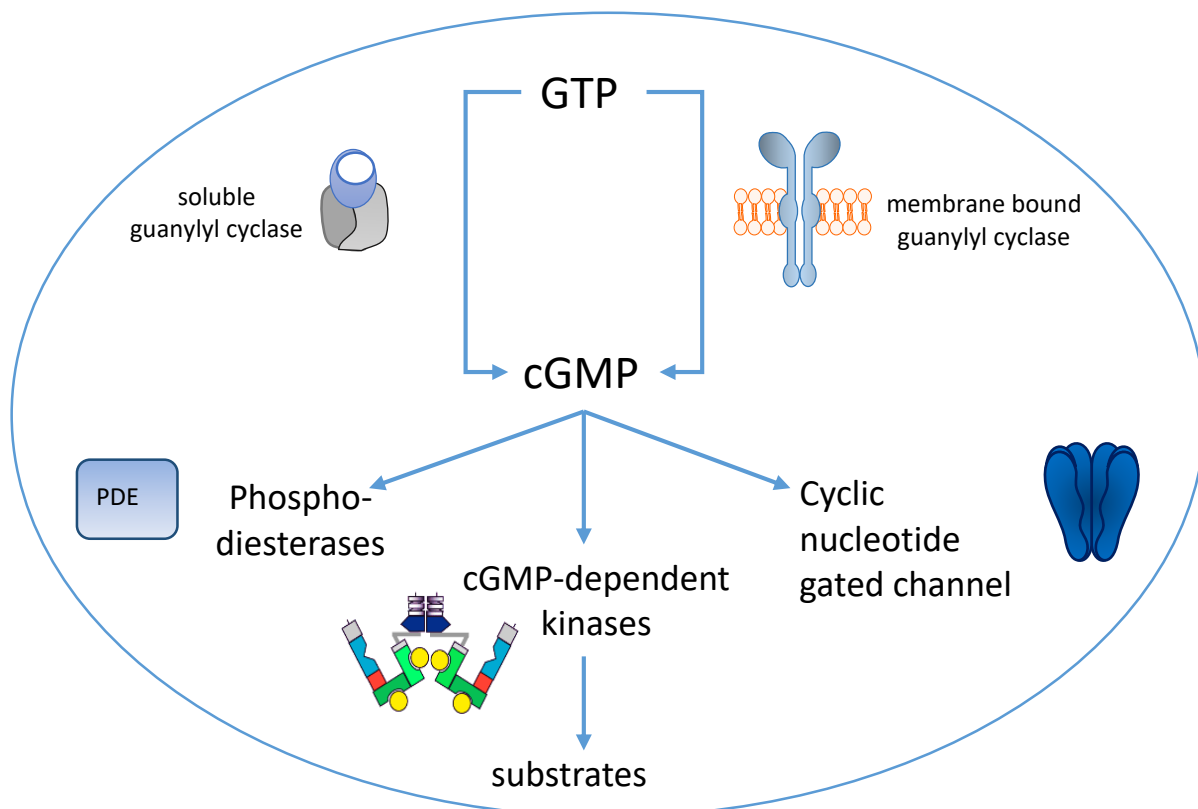


Figure 1.7: cGMP signalling pathway. cGMP is synthesized from GTP by the guanylyl cyclase (Gucy). Guccys can be either soluble or membrane-bound. The major difference between these two types is that the soluble GC gets activated by NO and the membrane-bound GC has an external ligand binding domain. Known targets of cGMP are cyclic-nucleotide-gated (CNG) channels, phosphodiesterases (PDEs) and cGMP dependent kinases (cGKs) which in turn phosphorylate protein substrates. Not all cGK-substrates are identified yet. Especially substrates in the CNS and the retina remain to be elucidated.

Introduction

the guanylyl cyclase activating protein (GCAP) has yet been shown to result in progressive cone-loss in mice (Payne et al., 1998). These studies further support the theory that malfunction of the vision cascade results in cell death in photoreceptors. However the question remains whether cGMP-levels influence the viability of cones.

The main cGMP effectors in the retina are the CNG channel and the phosphodiesterases (Figure 1.7) (Zhang and Cote, 2005). In addition, the cGMP dependent kinases (cGK) are also expressed in photoreceptors, but their function in this cell type is not understood (Figure 1.7) (Zhang and Cote, 2005). The cGKs are serine/threonine kinases phosphorylating the amino acids (AA) serine and threonine of their protein targets in the context of the general -R/K(2-3)-X-S/T-X motif {Kennelly, 1991 #295}. In mammals two genes are known: *Prkg1* coding for the cGK type 1 (cGKI) and *Prkg2* encoding the membrane bound kinase cGK type 2 (cGKII). In *Prkg1*, alternative splicing of exons encoding the N-terminus results in two different isoforms (cGKI alpha 671 AA, 76 kDa and cGKI beta 686 AA, 78 kDa) with distinct functions and cellular distribution (Hofmann and Wegener, 2013, Ruth et al., 1997). Both cGKI isoforms are located in the cellular cytoplasm (Wernet et al., 1989), while the N-terminus of cGKII is anchored in the cell membrane (Vaandrager et al., 1996, Jarchau et al., 1994). All cGKs share a similar structure (Figure 1.8). They are homodimers consisting of three functional domains: the N-terminus, the regulatory domain and the catalytic domain (Hofmann et al., 2006, Gamm et al., 1995). The N-terminal domain is essential for dimerization, inhibition of the kinase activity

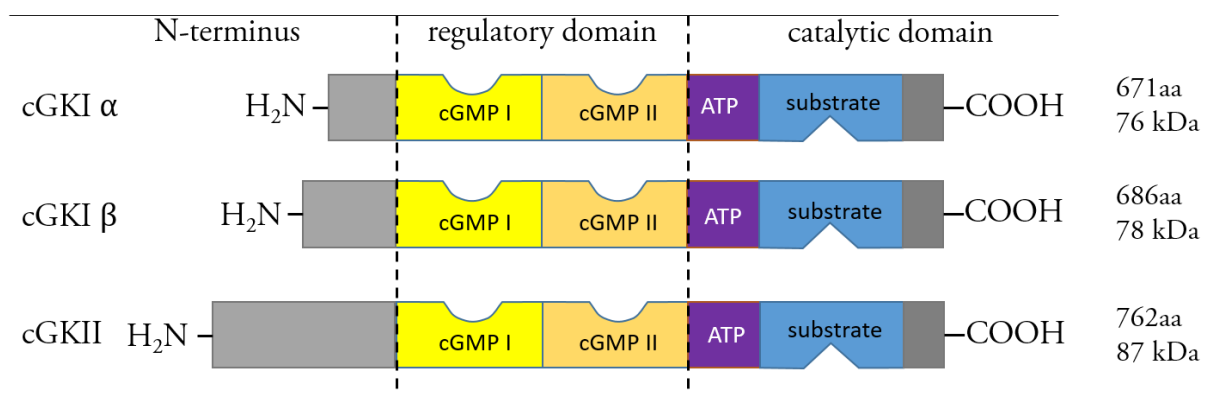
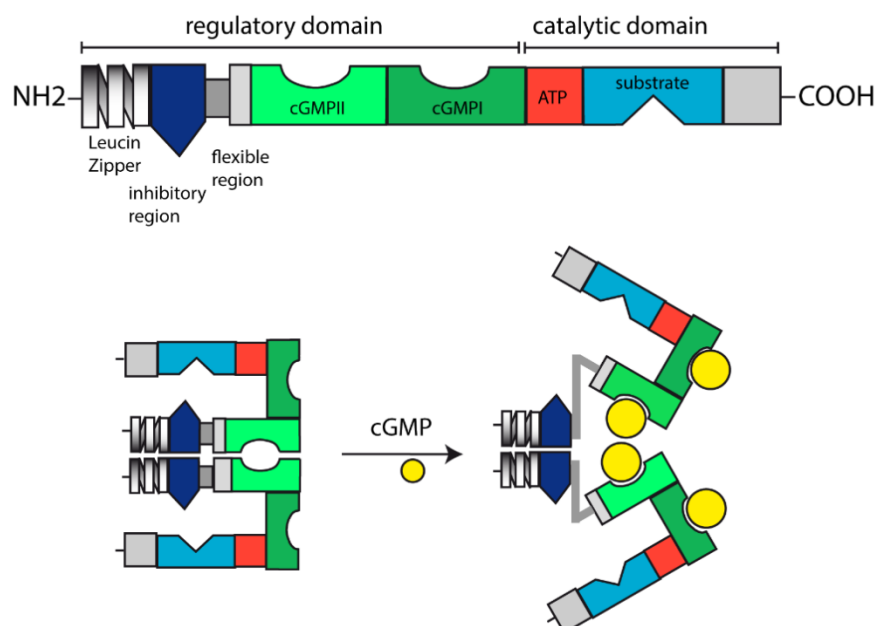


Figure 1.8: Structure of the cGMP-dependent kinases (cGKs). Structurally cGKs have a very similar composition: They have a N-terminus responsible for the dimerization, inhibition and substrate-specificity, a regulatory domain made out of two cGMP-binding domains and a catalytic domain with an ATP- and a substrate-binding pocket. The major difference between the kinases can be detected in the variable N-terminus.

and substrate specific targeting (Gamm et al., 1995, Kim et al., 2011, Landgraf et al., 1990). It contains the major structural difference between the kinases. Its leucine zipper, a protein-protein interaction domain, can dimerize the homomers and bind cGMP-dependent kinase anchoring proteins (GKAPs) (Casteel et al., 2010). The auto-inhibitory domain which is located between the leucine zipper and the regulatory domain prevents the activity of the phosphotransferase in absence of cGMP. Furthermore, the N-terminus targets the kinase to different subcellular localisations and comprises several auto-phosphorylating-sites. Upon cGMP-binding Thr59/Ser64 and Ser80 are auto-phosphorylated and increase the spontaneous activity of cGK and enhances its activity upon phosphorylation (Ruth et al., 1997).

At the regulatory domain two cGMP binding pockets are located. One of these domains has a high affinity for cGMP and the other shows a markedly lower affinity. As soon as both binding pockets are bound by cGMP the kinase undergoes a conformational change revealing the catalytic domain for substrate-binding (Figure 1.9) (Kim et al., 2011, Landgraf et al., 1990, Ruth et al., 1997). The C-terminal catalytic domain is the ‘active’ site of the kinase. It comprises a binding region for MgATP and for the substrate. Upon binding, ATP and the substrate are in close proximity and a phosphate group can be transferred by the catalytic domain to a serine or threonine (Figure 1.9) (Pfeifer et al., 1999, Hofmann, 2005).

Figure 1.9:
Conformational change of the cGMP-dependent kinases upon cGMP binding. At the regulatory domain two cGMP binding pockets are located. One of these sequences has highly affinity for cGMP and the other markedly lower affinity. Only if both sequences are occupied the secondary structure undergoes a conformational change unveiling the catalytic domain for substrate-binding.



Introduction

After truncation of the N-terminal regulatory domain of cGKI, the kinase is no longer subject to auto-inhibitory domain-mediated repression and can continuously phosphorylate proteins, the kinase is then constitutive active (Ruth et al., 1997, Boerth and Lincoln, 1994, Deguchi et al., 2004). Most of these previous structural investigations have solely focused on the cGKI. Due to the high sequence homology it can be assumed that the structural composition of cGKII would be very similar.

For the functional analysis of the cGKs, knock out mouse lines have been generated. cGKI knock-out mice have a severely decreased life expectancy and die about six weeks after birth due to acute problems in the smooth muscle formation (Wegener et al., 2002). This short life expectancy makes long-term studies impossible. Thus cGKI KO mice were generated carrying a rescue knock in the smooth muscle cells (Weber et al., 2007). Caused by the knock-in both isoforms are expressed in the smooth muscle cells and the mice have a significantly higher life expectancy (Weber et al., 2007). cGKII knockout mice on the other hand exhibit less severe pathological effects upon the phenotype (Pfeifer et al., 1996). They have a normal life expectancy, are resistant against enterotoxin STa but are in general 30 % smaller compared to their littermates caused by a deficit in the skeleton growth (Pfeifer et al., 1996).

1.4 Animal models to study retinal degeneration

Animal models are vital for ophthalmologic research and have already helped improving our understanding about retinal diseases. They are indispensable means to unravel genetic and biochemical mechanisms in the retina, especially, since currently *in vitro* retinal cell and tissue culture models cannot sufficiently mimic the highly complex *in vivo* situation.

As previously mentioned, there are naturally occurring mouse models carrying a mutation leading to retinal degeneration like for example the *rd1* mouse discovered in 1976 leading to rod degeneration (Drager and Hubel, 1978, Pittler and Baehr, 1991) and the *Gnat2* mouse model which resembles the Achromatopsia phenotype (Jobling et al., 2013). Over the past forty years several dog breeds have been diagnosed to suffer from retinal degeneration like the Labrador retriever (Kommonen et al., 1994), the Swedish briard (Narfstrom et al., 1989, Wrigstad et al., 1994, Veske et al., 1999) or the Irish setter (Aquirre et al., 1978, Farber and Lolley, 1974, Suber

et al., 1993). In the Alaskan malamute and the German shorthaired pointer deletion and missense mutations in the *Cngb3* locus could be detected. These dogs also show characteristics similar to ACHM patients (Komaromy et al., 2010, Sidjanin et al., 2002) Furthermore an Israeli sheep breed was recently found to carry a premature stop codon in the *Cnga3* subunit which also has been shown to lead to ACHM (Shamir et al., 2010, Reicher et al., 2010).

Larger animals are very useful tools for clinical trial-enabling translational studies focusing on efficacy and safety of treatments. Eyes of dogs or pigs are anatomically more similar to the human eye and harbour a greater proportion of cones than the rodent retina (Li et al., 1998b, Petters et al., 1997). In addition the larger size makes surgical procedures and follow-up examinations easier and more precise. The canine retina contains an area called 'visual streak', similar to the human macula, enriched with cones, making the canine eye favourable compared to other species (Mowat et al., 2008).

Mice on the other hand have always been a popular option for animal experiments. Considering their short gestation time they do not only provide more offspring but also allow fast cross-breeding possibilities with other mouse lines. Due to the accelerated life span of these animals it is possible to examine diseases at late stages and to examine long-term effects in a short timeframe. The biggest advantages are probably that a vast diversity of mouse lines is already available for studying retinal diseases and that new transgenic mice can be easily generated.

Since mutations in the loci encoding the A3 and B3 CNG subunits are the most common mutations identified in ACHM-patients (Kohl et al., 1998, Sundin et al., 2000), the most widely used ACHM mouse models are mice with a knock out (KO) of the corresponding genes *Cnga3* and *Cngb3*, respectively (Biel et al., 1999, Ding et al., 2009). Like human patients these mice lack (*Cnga3* ko) or have strongly compromised (*Cngb3* KO) cone function by birth as detected in Electroretinography (ERG) measurements (Figure 1.10D) (Biel et al., 1999, Ding et al., 2009). Comparing these two mouse models one key-difference is the residual cone function observed in the scotopic (cone) ERG recordings of *Cngb3* KO mice while *Cnga3* KO mice show no recordable cone ERG. Residual cone-ERG in *Cngb3* KO mice is a result of a small number of homomeric CNGA3 channels in the membrane of the outer segments (Ding et al., 2009). Another characteristic difference of these two mouse models is the speed of degeneration. The loss of the *Cnga3* subunit leads to a faster progression of cone death compared to *Cngb3* loss

Introduction

(Arango-Gonzalez et al., 2014). Moreover the degeneration process is not equally progressing in the retina of *Cnga3* KO mice. Ventral cones degenerate more rapidly compared to dorsal ones (Figure 1.10 A/B). The retina of a three month old *Cnga3* KO mouse in comparison to a wild type retina clearly illustrates the gradient of degeneration (eGFP positive cones in Figure 1.10 A/B).

In mice eye opening occurs between 12 and 13 days after birth (P12-13) but the maturation of the eye is not completed until one week after eye opening (P19-21) (Okawa et al., 2014, Hoon et al., 2014). The peak of cell death in *Cnga3* KO mice was initially determined at three weeks after birth (P21) (Michalakis et al., 2005) but a more recent paper suggests the peak to be rather around P35 (Fig 1.10C) (Arango-Gonzalez et al., 2014).

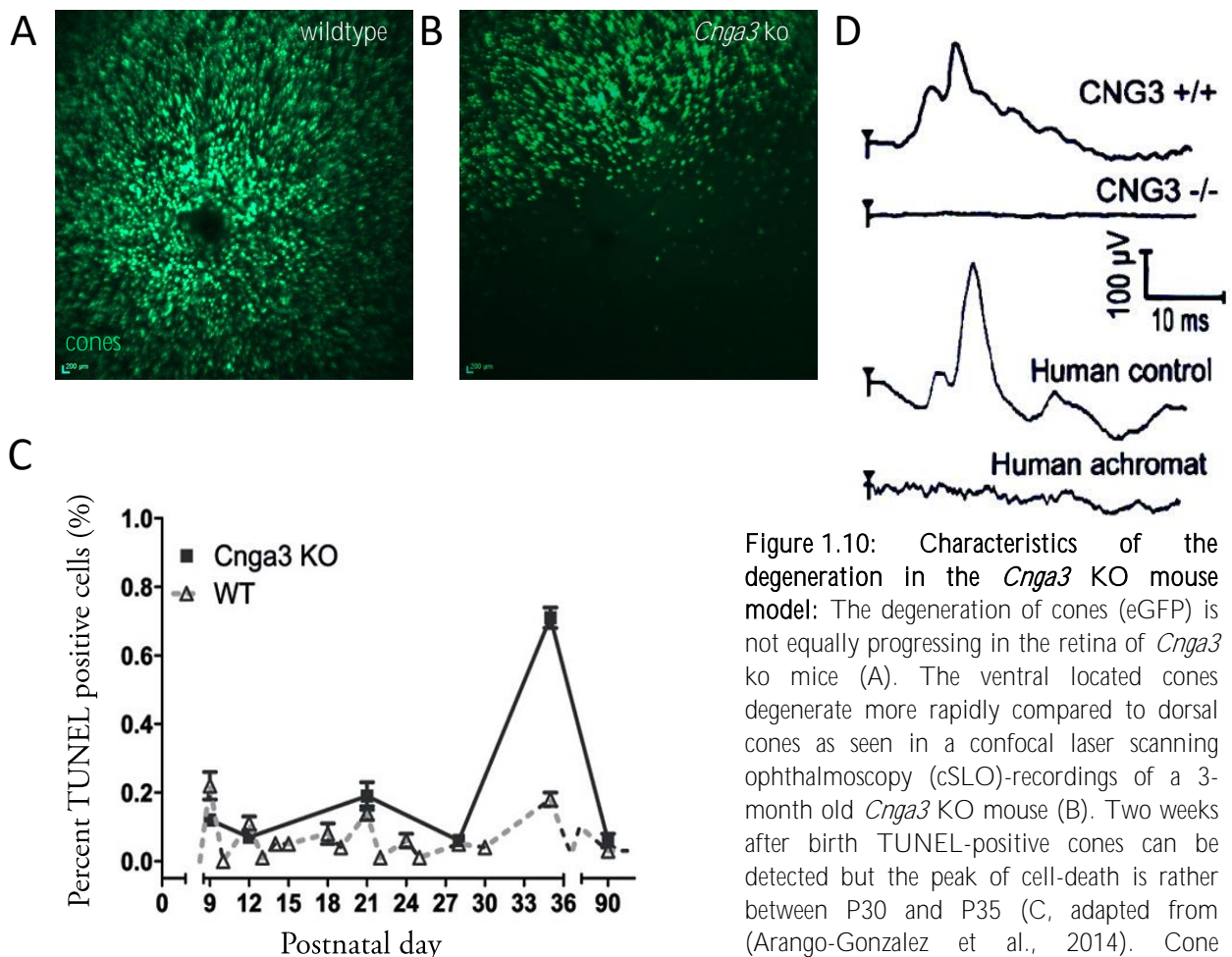


Figure 1.10: Characteristics of the degeneration in the *Cnga3* KO mouse model: The degeneration of cones (eGFP) is not equally progressing in the retina of *Cnga3* ko mice (A). The ventral located cones degenerate more rapidly compared to dorsal cones as seen in a confocal laser scanning ophthalmoscopy (cSLO)-recordings of a 3-month old *Cnga3* KO mouse (B). Two weeks after birth TUNEL-positive cones can be detected but the peak of cell-death is rather between P30 and P35 (C, adapted from (Arango-Gonzalez et al., 2014)). Cone photoreceptors are non-functional from birth and thus no scotopic (cone) ERG can be detected (D, adapted from Biel et al., 1999)

1.5 Gene therapy for Achromatopsia

Over the past ten years gene therapy approaches received a lot of attention in ophthalmology research and became an important tool for research (Schon et al., 2013, Kaufmann et al., 2013, Zulliger et al., 2015). With its exceptional immune privilege and the feasible accessibility the eye is an ideal experiment subject for gene therapy approaches (Medawar, 1948, Zulliger et al., 2015, Klassen, 2016, Willett and Bennett, 2013). Compared to other tissues, like for example the brain,

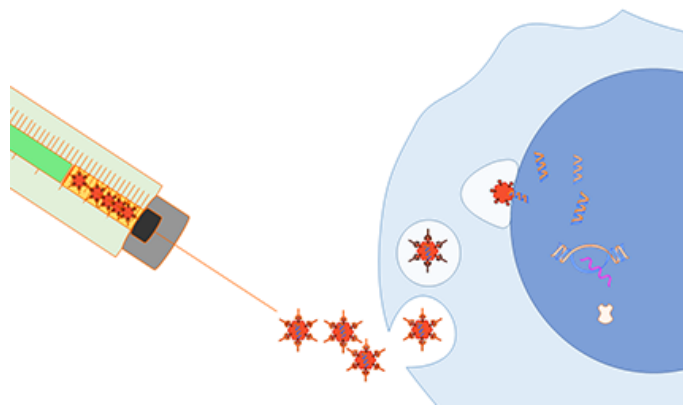


Figure 1.11 Recombinant Adeno-associated virus (rAAV) gene delivery has become an important tool of ophthalmic research due to their excellent efficacy, their good immune response and long-term success in retinal gene delivery. Furthermore rAAVs have a promising safety profile. They stay predominantly episomal after transduction and still achieve strong expression rates of their target gene.

the retina is easy to access for viral application by minimal-invasive procedures and specific regions or specific cell-types can be easily targeted by viral particles. For retinal gene delivery recombinant adeno-associated viruses (rAAVs) seem to be the most promising tool for gene delivery given their low immunogenicity and their high efficacy profile (Figure 1.11) (Boye et al., 2013, Carvalho and Vandenberghe, 2015, Trapani et al., 2014).

There are already several gene therapy approaches using rAAVs to cure inherited retinal diseases. In 2010 Michalakis et al. showed distinctive visual improvements in *Cnga3* KO mice after gene therapy. rAAVs expressing mouse *Cnga3* under a cone-specific promoter improved and maintained the visual ability of mice for at least eight months after treatment (Michalakis et al., 2010, Michalakis et al., 2012). This crucial work provided evidence that *CNGA3* supplementation might be a potential treatment for human ACHM patients (Mamasuew et al., 2010, Michalakis et al., 2012). In 2012 another study confirmed that *Cnga3*-gene therapy can be successful in a naturally occurring *Cnga3*-mutation of the cpfl5 mouse (Pang et al., 2012, Pang et al., 2010). In two other studies *Cngb3* KO mice and a canine *Cngb3* ACHM model were treated by gene therapy (Carvalho et al., 2011, Komaromy et al., 2010). These studies demonstrate that also other genetic loci are suitable for gene replacement with *Cngb3*. An age-dependency was

Introduction

observed during treatment of CNGB3-dependent ACHM (Carvalho et al., 2011, Komaromy et al., 2010) which might limit the application of such AAV-mediated gene replacement therapy to younger patients. Thus there is a limited time window where treatment can be successful.

Additionally, the newly discovered *Cnga3* sheep breed from Israel showed a recovery of cone function after treatment with either human or mouse *CNGA3* packed in an AAV5 serotype applied by unilateral subretinal delivery. Most importantly cone function was maintained in treated sheep for over three years (Ezra-Elia et al., 2014, Banin et al., 2015).

All these studies show highly promising data for gene therapy treatment in the retina. However when the first clinical trial of ophthalmic research completed clinical phase I and II the results were rather disappointing (Cideciyan et al., 2013, Jacobson et al., 2015a). Based on numerous animal experiments, a clinical study aimed to treat the retinal degenerative disease Leber's congenital amaurosis (LCA) (Acland et al., 2005, Acland et al., 2001, Dejneka et al., 2004, Jacobson et al., 2005, Narfstrom et al., 2005, Narfstrom et al., 1989). Even though all clinical trials reported visual improvements and no severe side-effects in patients, the significance of improvement and the efficacy differed vastly (Boye et al., 2013, Cideciyan, 2010). One study even reported a decline in previously detected visual improvements during follow-up examinations (Bainbridge et al., 2015, Jacobson et al., 2015b) and other studies detected that photoreceptor degeneration did not decrease in treated patients (Cideciyan et al., 2013, Jacobson et al., 2015a, Cideciyan, 2010). These results clearly emphasize the medical need for neuroprotection before and during retinal gene therapy

Already studies in *Cngb3* animals showed that a decisive factor for the success of gene-therapy is the time point of treatment (e.g. age) indicating that the ongoing degeneration diminishes the success of gene therapy (Carvalho et al., 2011, Komaromy et al., 2010). Accordingly a very important issue of retinal degeneration research is to arrest photoreceptor cell death and increase the time window where gene-therapy treatment is successful.

1.6 Aim of this thesis

The mechanisms leading to photoreceptor death are poorly understood in Achromatopsia. The time window where gene therapy is successful seems to be limited due to the ongoing photoreceptor cell death. Thus aim of this thesis is to arrest cell death in order to extend the time window where treatment is efficient and also to protect photoreceptors during and after gene therapy treatment. In order to understand the signalling leading to cell death in Achromatopsia, the following questions were addressed in this thesis:

1.) Is there an imbalance of cGMP homeostasis in *Cnga3* KO mice?

cGMP is already shown to accumulate in retinal degeneration mouse models and has been suggested to have a crucial role in the process of photoreceptor loss (Xu et al., 2013, Paquet-Durand et al., 2009, Michalakis et al., 2010, Bowes et al., 1990). Therefore, in this study cGMP was detected at various time points of maturation and degeneration in the retina of *Cnga3* KO mice.

2.) Does cGMP influence the degeneration process or is it only a bystander effect?

To unravel the role of cGMP levels in the degeneration process, cGMP-production was decreased and the involvement of direct effectors of cGMP were further examined.

3.) Which proteins are involved in the signalling pathway leading to cell death?

Finally the study also aimed at identifying the signalling pathway downstream of cGMP that ultimately triggering a cell-death signal.

2 Materials and Methods

2.1 Animals

All mice used were on a mixed background. *cGKI/Cnga3* double and triple knockout mice (*cGKI/Cnga3*; *cGKII/Cnga3ko*; *cGKI/cGKII/Cnga3ko*) were generated by cross-breeding *Cnga3* KO mice on a C57BL/6 N background (Biel et al., 1999) with *cGKI* or *cGKII* KO mice on a 129/Sv genetic background (Weber et al., 2007, Pfeifer et al., 1996). The resulting offspring were identified by genotyping (PCR). Age matched *Cnga3* KO and wild type mice with the same mixed background were used for comparison. For in vivo tracing of cones after shRNA-application, *Cnga3* KO mice on a were also crossbred with RgeGFP mice (Ikawa et al., 2003).

Mice were given *ad libitum* access to food (Ssniff; regular feed: R/M-H, breeding feed: M-Z Extrudat) and water. Mice were maintained on a 12 h light/dark cycle. All procedures concerning animals were performed with permission of the local authority (Regierung von Oberbayern). Day of birth was considered as postnatal day 1 (P1).

2.2 Chemicals, solutions and buffers

All chemicals used were obtained by Bio-Rad, Fluka, Merck, Roth and Sigma-Aldrich if not mentioned otherwise. The quality was "pro analysis" or "for molecular biological use". For all solutions high pure and deionised water was used (Milli-Q Plus System, Milli-pore). In experiments that required a high purity all solutions were autoclaved (Sterlisator, Münchener Medizin Mechanik).

2.3 Genotyping

Genotyping was performed by polymerase chain reaction (PCR). The following genetic constitutions: knock out (ko), wild type (wt) and heterozygous (hz) were identified for the following gene-loci *Cnga3*, *Prkg1* (cGKI) and *Prkg2* (GKII). For the smooth muscle knockin of cGKI (SM1) and the RG-specific knock in of eGFP (RgeGFP knock in (ki) or wildtype was determined.

Mouse ear tissue samples were digested with 600µl of 50mM NaOH at 95°C for at least 15 Min. Samples were shock frozen in liquid nitrogen and again heated for ~5 Min. at 95°C. Subsequently probes were vortexed and 50µl 1mM Tris-HCl was added for neutralization. Tissue lysates were then used as DNA-templates for PCR reactions with the following primer-sets:

primer:

Table 2.1: Primer used for genotyping. All primers used were produced by Eurofins MWG.

Gene	Primer	Sequence
Cnga3	mCG76R (rev)	caa gtt ccc tat cct gaa cac g
Cnga3	mCG19F (for)	ctt agg ttt cct tga ggc aag g
Cnga3	NeoPR (rev)	gcc tgc tct tta ctg aag gct c
cGKII	AV3R (rev)	att aag ggc cag ctc att cc
cGKII	AV9R (rev)	ctg ctt aat gac gta gct gcc
cGKII	E2FB-AV (for)	ggt gaa gtt tta ggt gaa acc aag
Cngb1	PSHV6bR (rev)	gcc cag act aga aca caa gtc
Cngb1	PSHV9R (rev)	cac agc cat tac aca tag cag tg
Cngb1	PSHV8F (for)	cct cat gca tgc gac ctg aaa t
cGKI	RF53 (rev)	cct ggc tgt gat ttc act cca
cGKI	RF125 (for)	gtc aag tga cca cta tg
cGKI	RF118 (for)	aaa tta taa ctt gtc aaa ttc ttg

Table 2.2: Pipetting scheme of PCR for genotyping GoTaq G2 polymerase as well as 5× GoTag Buffer was purchased from Promega. 1 mM dNTP solution was made from 10mM dNTP Mix (Thermo Scientific) by diluting it in a ratio of 1:10.

Volume (µl)	Component
2	Tissue lysate
1,25	Primer forward (wt)
1,25	Primer Primer forward (ko/ki)
1,25	Primer reverse (common)

5	GoTaq Buffer (5x), Promega
4	dNTPs (1mM)
10,125	dl H ₂ O
0.125	Taq-Polymerase

Table 2.3: Cycle conditions for genotyping The Thermocycler ProFlex™ PCR System (Thermo Scientific) was utilized for PCR-amplification under the following cycle conditions.

	Time		<i>Cnga3l</i> eGFP		cGKI/SMI		cGKII		
Initial denaturation	5 min		95°C		95°C		95°C		
Denaturation	30 sec	30X	95°C	40X	95°C	11X	95°C	28X	95°C
Annealing	30-45 sec		57°C		55°C		57°C		57°C
Elongation	30 sec		72°C		72°C		72°C		72°C
Final elongation	7 min		72°C		72°C				72°C

2.4 Agarose gel electrophoresis

Gel-electrophoretic separations for the genotyping were performed on 2 % (w/v) agarose gels. To pour a gel, the corresponding amount of agarose (peqGOLD Universal-Agarose, Peqlab) was microwaved along with the appropriate volume of 1× TBE buffer until the agarose was completely dissolved. For visualization under ultraviolet light (Gel Doc 2000, Biorad) PeqGreen (peqlabs) solution (final concentration in the gel: 0,025µl/ml) was added. PeqGreen binds DNA and fluoresces at UV-light irradiation.

PCR samples were loaded into the sample wells. One additional well was loaded with the molecular weight ladder (GeneRuler 1 kb Plus DNA Ladder, Thermo Scientific). 1× TBE buffer was used as running buffer.

2.5 Retina dissection

Mice were euthanized with Isofloran and then sacrificed. Eyes were protruded out of the orbit (exophthalmus) and fixed with curved forceps. With a sharp blade, the cornea was incised and by pulling the forceps the retina, the lens and the vitreous body are smoothly removed from the eye. After rinsing in cold 0.1M PB and removing the lens and remaining RPE-cells, the tissue was transferred into a 1.5 ml reaction tube, shock frozen in liquid nitrogen and either directly processed for RNA or protein extraction or stored at -80°C until further use.

2.6 RNA extraction

Total RNA extraction was performed using the RNeasy-Mini Kit (Qiagen) according to the manufacturer's protocol. Briefly, 350 μ l RLT Buffer was added to two retina of one animal (approximately 20 mg tissue). The tissue was disrupted and homogenized using a 27G needle (Sterican) and a 1 ml syringe (Terumo). The supernatant was carefully transferred to a new microcentrifuge tube. 350 μ l of 70 % ethanol was added to the lysate, and mixed well by pipetting. The sample, including any precipitate, was transferred to an RNeasy MinElute spin column (Qiagen). The sample was centrifuged for 15 s at 10.000 rpm in a microcentrifuge (Fresco 17 microcentrifuge, Thermo Scientific). Next, 350 μ l Buffer RW1 was added to the RNeasy MinElute spin column. The sample was again centrifuged for 1 min at 10.000 rpm and 10 μ l DNase I stock solution was added to 70 μ l Buffer RDD. The DNase I incubation mix (80 μ l) was added to the RNeasy MinElute spin column membrane, and placed on the benchtop at room temperature for 15 min. Next 350 μ l Buffer RW1 was added to the RNeasy MinElute spin column and centrifuged for 15 s at 10.000 rpm. 500 μ l Buffer RPE was added to the spin column and centrifuged for 15 s at 10.000 rpm. Next, 500 μ l of 80 % ethanol was added. The RNA was eluted by adding 12 μ l RNase-free water directly on the centre of the spin column membrane and centrifuging for 1 min at full speed.

2.7 cDNA synthesis

Reverse Transcription (RT) was performed using the RevertAid First Strand cDNA Synthesis Kit (Thermo Scientific; cat.nr. K1691) according to the manufacturer's manual. In brief the following reagents were added into a sterile, nuclease-free tube on ice in the indicated order:

cDNA synthesis mixture (total volume: 20 μ l):

Template RNA/total RNA:	200 ng
primer: oligo (dT)	1 μ l
random hexamer primer	1 μ l
water, nuclease-free / add volume to	12 μ l
5 x Reaction buffer	4 μ l
10 mM dNTP Mix	2 μ l
RiboLock RNase Inhibitor (20 u/ μ l)	1 μ l
RevertAid Reverse Transcriptase (200 u/ μ l)	1 μ l

The sample was mixed gently, centrifuged and incubated for 5 min at 25 °C followed by 60 min at 42 °C. The reaction was terminated by heating at 70 °C for 5 min. The cDNA was used directly for qPCR or stored at - 80 °C for long-term storage.

2.8 Microarray analysis

Microarray experiments of retinal tissue were performed at two different ages (PW4 and PW8) comparing gene expression of Cnga3 KO and wild-type animals using an Affymetrix platform according to the manufacturer's instructions. Fragmented and labeled cRNA of the retinas of three wild-type and three Cnga3 KO mice were hybridized on Affymetrix Mouse Genome 430 2.0 Arrays. A probe-level summary was determined using the Affymetrix GeneChip Operating Software using the MAS5 algorithm. Normalization of raw data was performed by the Array Assist Software 4.0 (Stratagene, La Jolla, CA, USA), applying the GC-robust multichip average (RMA) algorithm. Significance was calculated using a *t*-test without multiple testing correction (Array Assist software), selecting all transcripts with a minimum change in expression level of 1.5-

fold together with a p value <0.05 . The heatmaps were generated using Multi Experiment Viewer Software (MeV v4.8.1.).

2.9 Gene regulation networks

Gene regulation networks were generated by Ingenuity Pathways Analysis (IPA) 8.8 (<http://www.ingenuity.com>). For that purpose, data sets containing gene identifiers and the corresponding expression and significance values were uploaded into the application. These genes, called Focus Genes, were overlaid onto a global molecular network developed from information contained in the Ingenuity Pathways Knowledge Base. Networks of these Focus Genes were then algorithmically generated based on their connectivity.

2.10 Functional analyses

Ingenuity functional analysis identified the biological functions and/or diseases that were most significant to the data set. Genes from the data set that met the negative logarithmic significance cut-off of five or higher, and were associated with biological functions and/or diseases in the Ingenuity Pathways knowledge base were considered for the analysis. Fisher's exact test was used to calculate a p value determining the probability that each biological function and/or disease assigned to that data set is due to chance alone

2.11 Real-time quantitative PCR (qPCR)

qPCR was performed on an Applied Biosystem LightCycler using SybrGreen QPCR Master mix (Applied Biosystem).

CT values were determined by the applied Biosystem BioOne Software using the following fast cycle protocol:

Table 2.4 Cycle conditions for real-time quantitative PCR (qPCR) measurements.

		°C	time
UDG activation		50	02:00
pre-incubation		95°C	00:05:00
40 cycles	Pre-incubation	95	00:00:05
	primer dependent annealing	55-60	00:00:05
	amplification	60	00:00:30
Melting curve		95	00:00:05
		65	00:01:00
	continuous	98	5-10

Expression levels of each sample were detected in duplicate reactions. Three different biological replicates were analysed in duplicates and normalized to the expression of the housekeeping gene aminolevulinic acid synthase (ALAS). Relative quantification was determined by the method described by Pfaffl delta delta Ct (2002). The data were presented as mean \pm SEM.

2.12 Retina dissection (IHC)

Mice were sacrificed and each eyeball was marked temporally by a glowing needle to remember the orientation. Eyes were protruded out of the orbit (exophthalmos) and removed with a scissor. For prefixation, eyes were pierced at the ora serrata using a cannula (21G, Sterican, B. Braun) and incubated in 4 % paraformaldehyde (PFA) on ice for 5 min. The cornea was removed by crosscutting along the *ora serrata* with a micro-eye spring scissor (Mini Vanas, blade 3 mm, Frohnhäuser) under a dissecting/stereo-scopic microscope (Stemi 2000, Zeiss). The temporal mark was preserved by placing a small incision into the eyecup. Subsequently, cornea, lens and vitreous body were dislodged and the remaining eyecup was fixed in 4 % PFA on ice for 45 min. Subsequently eyes were washed thrice in 0.1 M PB and dehydrated overnight in 30 % sucrose for cryopreservation. Finally, the eyecup was embedded in tissue freezing medium (Electron Microscopy Sciences) and frozen on dry ice. Tissue was kept at -80°C for at least 24 h before further processing or stored at -80°C until use.

Table 2.5 Composition of solutions used for retina dissociation.

0,1 M PB	$\text{Na}_2\text{HPO}_4 \times 2 \text{H}_2\text{O}$ 28.48 g $\text{NaH}_2\text{PO}_4 \times \text{H}_2\text{O}$ 5.52 g H_2O ad 2 l pH 7.4, stored at 4 °C.
4 % PFA (in PB)	Paraformaldehyd (Merck) 6 g 0.1 M PB ad 150 ml dissolved at 60 °C and sterile filtered using a 25mm syringe filter (VWR). Aliquots were stored at – 20 °C.
30 % sucrose solution (in PB)	sucrose 30 g 0.1 M PB ad 100 ml sterile filtered using a 25mm syringe filter (VWR) and stored at - 20 °C.

2.13 Retinal cryosections

For retinal cryosections embedded eyecups in tissue freezing medium were cut into 10 μm cryosections by a kryostat (Leica CM3050 S, Leica Biosystems) and mounted on glass object slides (Super Frost Plus, Menzel). Cryosections were dried at room temperature and stored at - 20 °C until further processing.

2.14 Immunohistochemistry

Retinal cryosections (10 μm) were thawed for at least 10 min at room temperature and then rehydrated with sterile 0.1 M phosphate buffered (PB) for 10 min. For post-fixation slides were incubated with 4 % para-formaldehyde (PFA) in 0.1 M PB, pH 7.4 for 10 min at room temperature (RT). After washing thrice with 0.1 M PB for 5 min, cryosections were incubated with the primary antibody-mixture containing 5 % chemiblocker (Millipore) and 0.3 % Triton X-100 in sterile 0.1 M PB for 3 h at RT or overnight at 4 °C. Subsequently they were washed thrice with 0.1 M PB for 5 min. and then incubated with the secondary antibody in sterile 0.1 M PB with 2 % CB for 1.5 h at RT.

Materials and Methods

The following secondary antibodies were used (catalogue number and working dilutions in brackets):

Alexa-Fluor 488 goat anti-mouse IgG (H+L) (1:800, Thermo Fisher Scientific, #A-11001)

Cy[™] (Cyanine) 3 donkey anti-rabbit IgG (1:400, Jackson ImmunoResearch Laboratories)

Cy[™] (Cyanine) 2 donkey anti-sheep IgG (1:200, Jackson ImmunoResearch Laboratories)

Cell nuclei were counterstained with Hoechst 33342 (5 µg/mL, Invitrogen) and sections were mounted with aqueous mounting medium (PermaFluor, Beckman-Coulter).

Table 2.6 Antibodies used for Immunohistochemical stainings.

Antibody	company	Dilution IHC
sheep anti-cGMP	Purchased from Prof Steinbusch, Maastricht University (Tanaka et al., 1997)	1:500
rabbit/guinea pig anti-glycogenphosphorylase (glypho)	Purchased from Prof Hamprecht, University of Tübingen.	1:1000
rabbit anti-cGKI alpha	kindly provided by F. Hoffmann	1:100
rabbit anti-cGKI beta	kindly provided by F. Hoffmann	1:100
rabbit anti- γ -H2AX	abcam	1:1000
goat anti-Atr	Santa Cruz	1:200
mouse anti-Npm1	Cell-Signalling	1:1000
Atr p428	Cell Signalling	1:1000

Retina morphology und number of cones were analysed using a Zeiss Axioscope epifluorescence microscope equipped with a HBO 100 mercury arc lamp, appropriate filters equipped with an MRc ccd camera (Zeiss). Laser scanning confocal micrographs were collected using a Leica SP8 microscope (Leica).

2.15 Terminal deoxynucleotidyl transferase dUTP nick end labeling (TUNEL)-assay

Retinal cryosections stored at -20°C were thawed and re-hydrated with sterile 0,1M PB for 5 minutes. Sections were fixed with 4 % PFA/PB for 10 minutes and then permeabilized with 0,25 % Triton X in PB for 20 min. For co-staining with *hmc* sections were permeabilized with 2N HCl instead. Slices were washed with deionized water and a positive control was prepared by DNase incubation for 30 minutes. Slices were washed again with deionized water and preincubated with TdT reaction buffer for 10 minutes at room temperature. The TdT reaction cocktail, containing EdUTP and TdT, was prepared and added on each sections. Coverslips were either incubated over night at room temperature or for one hour at 36°C.

After incubation cryosections were washed twice with 3 % BSA in PB for two minutes. The Click-it reaction cocktail, containing Alexa Fluor 647, was prepared, added on the slices and incubated for 30 minutes at room temperature protected from light. The mixture was removed and the slides were washed with 3 % BSA in PB once more for 5 minutes. Following TUNEL staining a costaining with *hmc* was performed as described in section 2.14 primary and secondary antibodies were incubated. Last coverslips were stained with Hoechst 33342 (5µg/ml) for 5 minutes protected from light and mounted as described in 2.14.

2.16 Cloning

For cloning techniques AAV-Vectors were used carrying an Ampicillin resistance (AmpR) for selection of recombinant bacterial cells. The expression cassette in these plasmids is framed by two inverted terminal repeats (ITR) encoding all cis-acting elements for efficient replication (rep)

and packaging (cap) of rAAVs in the presence of two helper plasmids described in the AAV-production. The packaging capacity of an AAV-Vector is approximately 5.1 kilobase pairs (kb).

For ubiquitous expression a pAAV2.1 *cis* plasmid was used with the cytomegalovirus (CMV) promoter, capable of driving heterologous gene expression in mammalian cells. Other promoters used in this study were the rod-specific mouse rhodopsin promoter (mRho) and the cone-specific short-wavelength opsin promoter (mSWS) making tissue-specific expression possible (Koch et al., 2012, Michalakis et al., 2010). Downstream of the gene of interest an enhanced green fluorescent protein (eGFP) was cloned as a report gene. eGFP and the gene of interest were separated by the “self-cleaving” 2A-region, ensuring equimolar levels of both genes (Robertson et al., 1985, Donnelly et al., 2001).. Finally a hepatitis virus posttranscriptional regulatory element (WPRE) was cloned into the vector to enhance gene expression.

For shRNA expression a modified pSub-Vector (Samulski et al., 1987) was used with a PolIII promoter, the so called U6-promoter was used. Additionally a mcherry was present as a reporter gene downstream of a phosphoglycerate kinase 1 (PKG) promoter. Again WPRE was cloned for enhanced expression. Cloning of constitutive active cGKI

2.16.1 Cloning of the catalytic domain of cGKI

The catalytic domain of cGKI was cloned into a recombinant Adeno-associated-virus (rAAV) vector for virus production (Ruth et al., 1997, Boerth and Lincoln, 1994, Deguchi et al., 2004).

By an overlap-PCR approach the insert for the pAAV2.1-sc-SWS-eGFP vector was generated. All primers used were synthesized and purchased at MWG Eurofins. The first educt for the overlap-PCR was amplified from pMT3-cGKIbeta (obtained from Hofmann, REF) using a forward primer binding at the beginning of the catalytic domain of cGKIbeta with a compatible restriction site (BamHI): 5'-TTGGATCCACCATGGCATATGAAGATGCAGAAGCTAAG-3'. The reverse primer on the other hand binding at the end of the catalytic domain containing the first fracture of the 2A-region (GGATCCGGAGCCACGAACTTCTCTGTAAAGCAAGCAGGAGACGTGGAAGAAAACCCCGGTCCT)

5'-**GTCTCCTGCTTGCTTTAACAGAGAGAAGTTCGTGGCTCCGGATCC**GAAGTCTATGT

CCCATCCTGAG-3'. The second educt was generated by a primer providing the other part of the 2A-peptide and

5'-**GCCACGAACTTCTCTCTGTTAAAGCAAGCAGGAGACGTGGAAGAAAACCCCGGTCCCTACTAGTATGGTGAGCAAGGGCGAGGA**-3' and a primer binding at the end of the eGFP-sequence 5'-TTACTTGTACAGCTCGTCCATG-3' of the pAAV2.1-sc-SWS-eGFP-vector. Finally the insert was generated out of these two overlapping PCR-products by combining both products and the PCR-primer 5'-TTGGATCCACCATGGCATATGAAGATGCAGAAGCTAAG-3' and 5'-TTACTTGTACAGCTCGTCCATG-3'. The final PCR-product was then restricted with the compatible restriction enzymes and ligated into the linearized vector (pAAV2.1-sc-SWS-eGFP) to obtain pAAV2.1-sc-SWS-cAcGKI-2A-eGFP

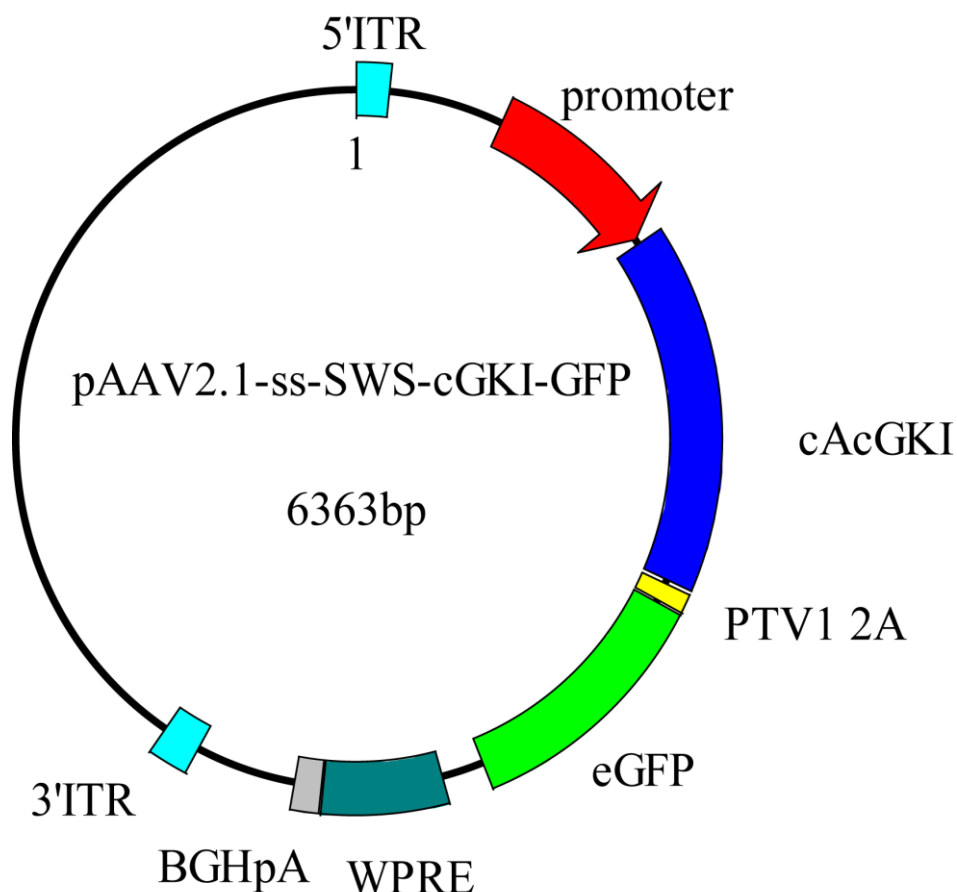


Figure 2.1 Recombinant Adeno-associated virus (rAAV) vector Between the ITR-regions of a vector for viral production the constitutive active cGMP-dependent kinase (cAcGK) was cloned behind the rod-specific promoter rhodopsin. An enhanced green fluorescent protein (eGFP) served as a report gene. The gene of interest and eGFP were separated by the “self-cleaving” 2A-region, ensuring equimolar levels of both genes. A hepatitis virus posttranscriptional regulatory element (WPRE) was cloned into the vector to enhance gene expression and the polyadenylation signal (pA) of the bovine growth hormone (BGH) was added for polyadenylation.

2.16.2 Cloning of shRNAs

For the generation of double stranded shRNAs 1 μ l of each single stranded oligo (both sense and anti-sense strands with compatible restriction site overhangs at 3 mg/ml) in 90 μ l dl water and 10 μ l of 10x-PCR-buffer. Oligo mix was heated to 95°C for 10 min, and slowly cooled to RT and immediately used for ligation.

Gucy shRNA:

Ccgggtgcccatgatgtctataatcaagagttatagacatcatgggcaccgtttt

Validated sequence adapted from (Tosi et al., 2011)

cGKII shRNA:

CCGAACCTATGACCTCAACAAAtcaagagTTTGTTGAGGTCATAGGTTTCGTTTTTGGAT

For validatin see section 2.19

cGKII shRNA

CCGCTTGGAAGTGGAATACTATCAAGAGTAGTATTCCACTTCCAAGCTTTTTTGAT

2.16.3 Restriction analysis

Restriction enzymes were purchased form the companies New England Biolabs (NEB) and Thermo Fisher Scientific (formerly Fermentas). The reaction conditions were conducted according to the respective manufacturer's protocols. The amount of DNA used for cloning was 3-5 μ g, whereas 0.5 μ g of DNA or 2 μ l of minipreparation of plasmid DNA (see 2.2.8) were used for restriction analysis.

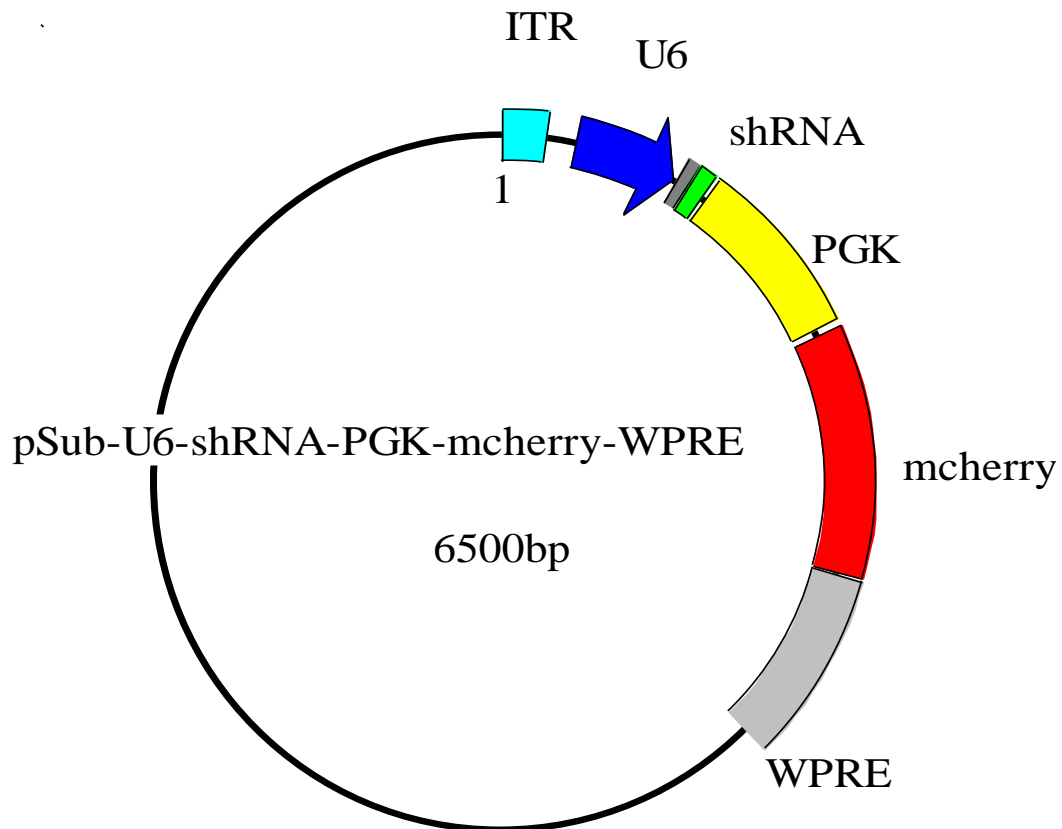


Figure 2.2 Recombinant Adeno-associated virus (rAAV) vector carrying a shRNA. Between the ITR-regions of a vector for viral production a shRNA was cloned behind the U6 promoter. A mcherry protein served as a reporter downstream of a phosphoglycerate kinase 1 (PGK) promoter. A hepatitis virus posttranscriptional regulatory element (WPRE) was cloned into the vector to enhance gene expression and the polyadenylation signal (pA) of the bovine growth hormone (BGH) was added for polyadenylation..

2.16.4 Ligation

Ligation was performed using T4 DNA ligase (NEB). The vector to insert ratio was between 1:3 to 1:5. Therefore, the amount of the vector and insert DNA fragments was calculated for each ligation reaction. Pipetting scheme and reaction conditions were applied according to the manufacturer's manual. The reaction was incubated overnight at 16 °C.

2.16.5 Transformation

100 μ l aliquots of chemically treated, competent β 10 *Escherichia coli* (*E. coli*) strain stored at -80 °C were thawed on ice and then transformed with 5-10 μ l ligation reactions. The bacteria suspension was gently mixed by tapping at the tube wall and was incubated on ice for 10-20 min. A subsequent heat shock was performed at 42 °C for 45 sec in a heat block and cells were chilled

on ice for another 10 min. The cell suspension was plated on the LB(+) selection agar plate containing 100 µg/ml ampicillin (resistance provided by the used plasmids) and was incubated overnight at 37 °C.

-LB(+) medium: peptone 10 g, NaCl 5 g, yeast extract 5 g, glucose 1, H₂O *ad* 1 l; adjust pH to 7.2-7.5 and autoclave

-LB(+) agar: agar 15 g, LB(+) medium *ad* 1 l, ampicillin 100 mg

2.16.6 Inoculation of bacterial cells and mini preparation of plasmid DNA

After overnight incubation bacterial clones were picked from the LB-plate and incubated in 3-6 ml LB(+) medium with 100 µg/ml ampicillin at 37 °C with 225 rpm for at least 16 hours. The suspension was centrifuged at 3500 rpm at room temperature (RT) for 10 min and the supernatant was removed. The pellet was re-suspended in 250 µl MP1 buffer and transferred into 2 ml Eppendorf tubes. For Lysis 250 µl MP2 buffer was added, the cell suspension was inverted 5 times and further incubated for at least 5 min at RT. With 250 µl MP3 buffer the lysis-mixture was neutralized over a time frame of 5 min and inverted 5 times. The suspension was then centrifuged at 13,000 rpm at 4 °C for 15 min. The supernatant containing the plasmid DNA was transferred into a fresh 1.5 ml Eppendorf tube. To precipitate the DNA, 525 µl isopropanol was added to the mix. After vortexing, the mixture was centrifuged at 13,000 rpm and 4 °C for 15 min. Subsequently, the pellet was washed with 70 % (v/v) ethanol by centrifugation at 13,000 rpm and 4 °C for 5 min. The supernatant was discarded and the pellet was air-dried before resuspension in 30 µl of H₂O. For large scale and high purity plasmid isolation, PureLink® HiPure Plasmid Midiprep or Megaprep Kit (Invitrogen) was used, following the instructions from the manufacturer's manual.

Subsequently every plasmid was sequenced by Eurofins MWG Operon to verify the cloning. Samples and corresponding primers were diluted to concentrations proposed by the company.

Buffers:

-MP1 Buffer (Resuspension buffer): Tris 6.06 g; EDTA 3.72 g; RNase A 100 mg; H₂O *ad* 1 l; adjust pH to 8.0 with 37 % HCl

-MP2 buffer (Lysis buffer): NaOH 8 g; 10 % (w/v) SDS solution 100 ml; H₂O *ad* 1 l

-MP3 buffer (Neutralization buffer): 3 M potassium acetate pH 5.5 500 ml; H₂O *ad* 1 l

2.17 AAV production

The two helper plasmids used for the generation rAAVs were pAD Helper plasmid and pAAV2/8-YF rep/cap plasmid which contains rep gene of serotype AAV2 and cap gene of serotype AAV8 for enhanced specific transduction of photoreceptors (Allocca *et al.*, 2007; Vandenberghe and Auricchio, 2012). The serotypes contain mutations (YF) substituting tyrosine (Y) with phenylalanine (F) residues at exposed sites of the capsid surface to allow for a high transduction efficiency in host retinal cells (Petr-Silva *et al.*, 2009; Petr-Silva *et al.*, 2011).

2.17.1 Transfection and harvest

HEK293T cell line was used for transfection of the pAAV2.1 vector plus the helper plasmids pAD Helper and pAAV 2/8 (YF) via calcium phosphate transfection method as described in chapter 2.3.2. In addition to the regular components of the transfection reagent, dextran 500 and polybrene were added to achieve higher transfection efficiencies (Wu and Lu, 2007). 24 h before transfection, confluent 15 cm dishes of HEK293T cells were split 1:6 into 15x 15 cm dishes for each construct. The following two equations were used to calculate the necessary amount of pAD Helper and pAAV2/8 for the transfection solution:

$$*\text{pAD Helper: } x\mu\text{g} = \frac{\text{DNA concentration of AAV plasmid}}{\text{MM of AAV plasmid} * \text{MM of pAD helper}}$$

$$**\text{pAAV2/8 (YF) } x\mu\text{g} = \frac{\text{DNA concentration of AAV plasmid}}{\text{MM of AAV plasmid} * \text{MM of pAAV 2/8 YF}}$$

MM = molar mass of double stranded plasmid

Materials and Methods

Transfection solution:

pAAV2.1 vector	270 μg
pAD Helper	calculated * μg
pAAV 2/8 (YF)	calculated ** μg
2.5 M CaCl_2	1.75 ml
8 mg/ml polybrene	17.5 μl
10 mg/ml dextran	1.75 ml
H_2O	<i>ad</i> 17.5 ml

The transfection solution was vortexed while adding 17.5 ml 2x BBS dropwise before adding to all 15 dishes with each 70-80 % cell confluence. Medium replacement was done 24 h post-transfection. After another 24 h, cells were harvested by scraping them with a cell scraper from each 15 cm dish and collecting cell suspensions from all dishes in a 500 ml centrifuge tube. The cell suspension was centrifuged at 2000x g and 4 °C for 15 min (4000 rpm in a J2-MC Beckman centrifuge using a JA-10 rotor). The medium was decanted from the cell pellet before resuspending in 7.5 ml lysis buffer and subsequent transferring into a 50 ml polystyrene tube.

Lysis buffer for AAVs: NaCl 150 mM, Tris-HCl pH 8.5 50 mM, sterile filtrate

2.17.2 Purification of rAAVs via iodixanol gradient centrifugation

The cell suspension was shock-frozen in liquid nitrogen and thawed at 37 °C in a water bath for three times. Benzonase was added to the thawed cell suspension to a final concentration of 50 U/ml and the suspension was incubated at 37 °C for 30 min. The cells were pelleted via centrifugation at 2000x g and 4 °C for 25 min and the virus-containing supernatant was transferred into a Beckman Quick-Seal polypropylene tube (Beckman). The virus-containing phase was underlain with 7 ml 15 % iodixanol, followed by 5 ml 25 %, 5 ml 40 %, and at last by 6 ml 60 % iodixanol. Using a sterile, long glass pipette and a Gilson MINIPULS3 pump the iodixanol underlayers were made without mixing of the layers. The polypropylene tubes were balanced with PBS-MK before sealing them with the Beckman Tube Topper. Gradient

centrifugation was carried out at 361,000x g and 18 °C for 1 h 45 min (70,000 rpm in an Optima LE-80K Beckman ultracentrifuge using a 70 Ti rotor). In the following step, the tube was pierced multiple times at the top near the seal for pressurization. To collect the 40 % phase containing the virus, a 21-gauge needle with a 5 ml syringe was used to pierce the tube through the side at the lower end of the 40-60 % interface. Approximately 5 ml of the 40 % phase were collected until the interface was close below the 25 % phase:

Table 2.7 Composition of solutions used for viral production

Tween/PBS-MK	10x PBS 50 ml 1 M MgCl ₂ 500 μl 2.5 M KCl 500 μl Tween 20 0.014 % (v/v) H ₂ O <i>ad</i> 500 ml, sterile filtrate
15 % iodixanol	10x PBS 5 ml 1 M MgCl ₂ 50 μl 2.5 M KCl 50 μl 5 M NaCl 10 ml Optiprep 12.5 ml 1 % (v/v) phenol red 37.5 μl H ₂ O <i>ad</i> 50 ml, sterile filtrate
25 % iodixanol	10x PBS 5 ml 1 M MgCl ₂ 50 μl 2.5 M KCl 50 μl Optiprep 20.9 ml 1 % (v/v) phenol red 50 μl H ₂ O <i>ad</i> 50 ml sterile filtrate
40 % iodixanol	10x PBS 5 ml 1 M MgCl ₂ 50 μl 2.5 M KCl 50 μl 5 M NaCl 10 ml

	Optiprep 33.3 ml H ₂ O <i>ad</i> 50 ml sterile filtrate
60 % iodixanol	1 M MgCl ₂ 50 µl 2.5 M KCl 50 µl Optiprep 50 ml 1 %(v/v) phenol red 37.5 µl sterile filtrate

2.17.3 Purification of rAAVs via anion exchange chromatography

For further virus purification, the ÄKTAprime plus chromatography system (GE Healthcare Life Sciences), HiTrap Q FF sepharose column (GE Healthcare Life Sciences), and PrimeView software (GE Healthcare Life Sciences) were used according to manufacturer's manual. The column was equilibrated with 25 ml of buffer A at 10 ml/min flow rate. The following manual run was selected with 1.0 ml/min flow rate and 1 ml fraction size. The virus phase was diluted 1:1 with buffer A prior to injection with a 10 ml syringe to the superloop. Injection of the virus dilution from the superloop into the system was started and 1 ml fractions were collected in 1.5 ml Eppendorf tubes. UV- and conductance curves were observed via the PrimeView software. When the conductance curve returned to base value, a switch to 100 % buffer B was performed at 10 ml/min flow rate and 0 ml fraction size to purge the sepharose column from remaining virus. It was then switched to sterile H₂O to wash remaining salt from the column and system at 10 ml/min flow rate. When the conductance curve reached zero, washing was continued for 20 min. All 1 ml fractions within the plateau phase of the conductance curve were combined and stored at -20 °C until virus concentration as described in chapter 2.6.4.

Buffer A: Tris 20 mM; NaCl 15 mM; H₂O ad 1 l

adjust pH to 8.5 and sterile filtrate

Buffer B: NaCl 2.5 M; H₂O ad 1 l

adjust pH to 8.5 and sterile filtrate

2.17.4 Concentration of rAAVs

4 ml of the purified virus fraction was applied to an Amicon ultra-4 centrifugal filter unit with a 100,000 molecular weight cutoff (Millipore) and centrifugation was done at 2000x *g* and 20 °C for 20 min (4000 rpm in a Beckman centrifuge using a JA-10 rotor). The flow-through was discarded and the residual virus fraction was applied to the Amicon filter. Centrifugation was continued until 500 μ l remained in the filter unit. Washing was done with 1 ml 0.014 % Tween/PBS-MK by pipetting up and down five times. Centrifugation in 10 min steps was continued until 100 μ l of concentrated virus suspension remained in the filter unit. It was then split into 10 μ l aliquots and stored in 1.5 ml tubes with screw cap. Virus suspensions were stored at -80 °C until determination of virus titer and subretinal injection.

2.17.5 rAAV titer determination via quantitative real-time PCR

To determine the genomic titer of the virus preparation by quantitative real-time PCR (QPCR), a standard curve was generated using a serial dilution of the WPRE fragment which was amplified from the pAAV2.1 vector with the following primers:

WPRE for: AGTTCCGCCGTGGCAATAGG

WPRE rev: CAAGGAGGAGAAAATGAAAGCC

After amplification, the amplified fragment was precipitated with the aid of 3 M sodium acetate buffer pH 5.2 and ethanol. The DNA concentration was measured by determining the absorption at 260 nm with a NanodropTM 2000c spectrophotometer (Thermo Scientific). The concentration of the standard for 1010 genomic copies per 5 μ l was calculated with the following equation:

$$c \text{ (pg}/\mu\text{l)} = \frac{10^{10} * 660 * 10^{12} \frac{\text{pg}}{\text{mol}} * \text{size of WPRE fragment}}{6.022 * \frac{10^{23}}{\text{mol}} * \mu\text{l}}$$

c = concentration of the standard for 1010 copies per 5 μ l

660 x 10¹² pg/mol = mean molar mass of a base pair (deoxyribosyladenosine with deoxyribosylthymidine or deoxyribosylcytidine with deoxyribosylguanosine)

6.022 x 10²³ /mol = Avogadro constant

Materials and Methods

Afterwards, a tenfold serial dilution was generated in which the first dilution contained 1×10^{10} copies/5 μl and the last dilution contained 1×10 copies/5 μl . 5 μl of H_2O was used for blank. Each dilution was amplified in two samples by qPCR using the Light Cycler LC480 (Roche). The SYBR green I (Roche) fluorescence intensity was analyzed for each cycle. The LightCycler software LC-Run (version 5.32, Roche) was used to generate a fluorescence curve and subsequently to calculate the crossing points (Cp) value which points out the cycle in which the fluorescence rises significantly above the background signal. The standard curve could then be formed from the logarithmized dilutions plotted against the Cp value. The purified and concentrated rAAV preparations were diluted 1:500 in H_2O before two of each sample were amplified via qPCR. Fluorescence was measured as described above and a fluorescence curve was generated. The software then calculated the genomic titers by correlating the Cp values of the rAAV samples to the standard curve.

Pipetting scheme for qPCR:

WPRES primer for (10 μM)	1 μl
WPRES primer rev (10 μM)	1 μl
SYBR green I master mix	10 μl
template	5 μl
H_2O	<i>ad</i> 20 μl

qPCR conditions:

Initial denaturation 95 °C	10 min	
Denaturation 95 °C	10 sec	} x 40
Annealing 60 °C	5 sec	
Elongation 72 °C	20 sec	
Final elongation 72 °C	5 min	

2.18 Cell culture and plasmid transfection

Human embryonic kidney (HEK) 293T cells were transfected with plasmid DNA containing the protein of interest. All cell culture work was performed under a laminar flow (Hera Safe, Thermo Scientific) under aseptic conditions.

The following plasmids were used in this study:

pSub_U6_shRNAGucy_PKG_mcherry_SV40_WPRE

pSub_U6_shRNAcGKII_PKG_mcherry_SV40_WPRE

pCDNA3_CMV_cGKIImyc

HEK293T cells were cultivated in DMEM + GlutaMAX medium (+ 4.5 g/l glu-cose, - pyruvate + 10 % FBS) + 1 % penicillin/streptomycin (Blochrom) at 37 °C with 10 % CO₂ in an incubator (Heraeus Cells, Thermo Scientific). Transient transfections of HEK293T cells were performed using the calcium phosphate technique.

The calcium phosphate based transfection was performed by adding following solutions to a 15 ml falcon tube (Sarstedt):

DNA 20 µg
2.5 M CaCl₂ 100 µl
ddH₂O ad 1 ml

While vortexing this mixture, 1 ml 2 x BBS solution was added in a drop-wise manner. Then, the mixture was incubated for max. 5 min. at room temperature. This mixture was added drop-wise to the 50-70 % confluent cells and the cells were incubated at 37 °C with 5 % CO₂ in an incubator (Hera Cell, Thermo Scientific). 24 h after transfection, the medium was replaced and the cells were incubated at 37 °C for 24 h with 10 % CO₂ in an incubator (Hera Cell, Thermo Scientific).

2 x BBS Solution
BES 10.65g
NaCl 16.35g
Na₂HPO₄ 0.21g
H₂O ad 950 ml
adjust to pH 6.95 with NaOH and sterile filtrate using a 25mm syringe filter (VWR).

2.19 shRNA validation

HEK293T-cells were co-transfected with myc-tagged cGKII and shRNA. As a control HEK-cells were co-transfected with cGKII-myc and a scrambled sh-RNA. Two days after transfection HEK-

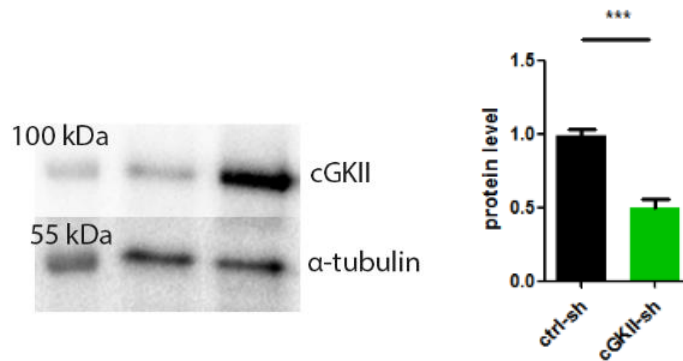


Figure 2-3: shRNA validation. HEK293T-cells were cotransfected with cGKII-myc and either cGKII-shRNA (cGKII-sh) or scrambled shRNA (ctrl-sh) as a control. By western blotting myc-tagged cGKII was detected and efficiency of the shRNA was determined by quantification (b) Summary data are mean ± SEM. *** $p < 0.001$ (Student's t -test)

cells were harvested and protein (see section 2.23) was analysed by western blotting (see section 2.24). HEK-cells transfected with cGKII shRNA display a significant reduction (49 %) of myc-tagged cGKII.

2.20 Subretinal injection

Two week old mice (P14) were intraperitoneally injected with ketamine (0.05 mg/g) and xylazine (0.01 mg/g). For older mice 0.1 mg/g ketamine and 0.02 mg/g xylazine was used. As soon as the mice were anesthetized Tropicamide eye drops were applied to the eyes for pupil dilation (Mydriadicum Stulln, Pharma Stulln GmbH, Stulln, Germany) and the mice were placed on a 37 °C heat plate. A NanoFil 34-gauge beveled needle (World Precision Instruments) was placed into a glass syringe and loaded with the virus particles in PBS-MK. The different titer of charges of e.g. gene of interest and control were fitted by according dilution titer-matched rAAV copies. Using a stereomicroscope the eye fundus was visible and at a roughly 60 ° angle the eye was penetrated by the needle until it was visible beneath the retina. After slow injection of 1 µl of virus suspension, the formation of a clear subretinal bleb confirmed the correct application into

the subretinal space. For verification of subretinal application an OCT- scanning laser ophthalmoscopy (Spectralis, Heidelberg Eye Instruments) was used.

The needle was carefully withdrawn and the injected eye was treated with gentamicin 5 mg/g and dexamethasone 0.3 mg/g eye salve. The anaesthetized mouse was placed under a heat lamp and was kept under supervision until it awakened from the narcosis. Minimum 10 days were required for sufficient protein expression in the retina. Two weeks post injection, retinas were analyzed for the fluorescence using scanning laser ophthalmoscopy (Spectralis, Heidelberg Eye Instruments).

2.21 Ophthalmological examinations

For ophthalmological examinations, adult mice received intraperitoneal injections of ketamine (0.1 mg/g) and xylazine (0.02 mg/g). Before the scanning procedure, Tropicamide eye drops were applied to the mice eyes for pupil dilation (Mydriadicum Stulln, Pharma Stulln GmbH, Stulln, Germany). Subsequently, hydroxylpropyl methylcellulose (Methocel 2 %; OmniVision, Puchheim, Germany) was applied to keep the eyes moist. The examination was performed with an adapted Spectralis HRA + OCT system from Heidelberg Engineering (Dossenheim, Germany) in combination with optic lenses described previously (Schon et al., 2012). The system allowed for imaging of the eye fundus by confocal laser scanning ophthalmoscopy (cSLO) and examination of the retinal morphology by optical coherence tomography (OCT). OCT scans were conducted with a 12° circular scan mode centered at the optic nerve head. This procedure

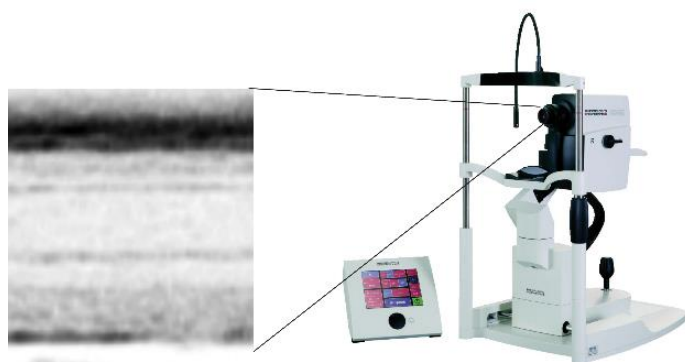


Figure 2-4 Ophthalmological examination. Optical coherence tomography (OCT) and confocal laser scanning ophthalmoscopy (cSLO) was performed with a Spectralis HRA and OCT system from Heidelberg Engineering (Dossenheim, Germany).

enabled measurements of the photoreceptor layer thickness at a comparable distance from the optic nerve head and allowed for comparison of values in longitudinal examinations of the same eye and between individuals. In detail, photoreceptor layer thickness was measured between the clearly visible outer plexiform layer and the border of neuronal retina and the RPE. The photoreceptor layer thickness is equivalent to the term ‘photoreceptor plus’ occasionally used in other studies for quantification of OCT data. For statistical analysis, the mean photoreceptor layer thickness was calculated from single values measured in the dorsal, temporal, nasal and ventral region around the optic nerve. cSLO images of the eye fundus were obtained using the infrared laser (820 nm) and the scanner set to a 30° field of view at high resolution mode.

2.22 SDS-polyacrylamide electrophoresis (SDS-PAGE)

A gradient SDS-polyacrylamide gel (SDS-gel) was used to separate isolated proteins according to their molecular weight. 6-12 % separation gels were prepared using the Mini Protean 3 gel system (BioRad). PageRuler Prestained Protein Ladder (Thermo Scientific) was loaded together with the protein samples to determine the protein sizes. Electrophoresis was run at 60 mA until the protein ladder bands were clearly separated.

10x electrophoresis buffer

Tris	30 g
glycin	144 g
SDS	10 g
H ₂ O	ad 1 l

4x Tris-HCl/SDS pH 6.8 buffer

Tris-HCl	0.5 M
SDS	0.4 %

adjust pH to 6.8

4x Tris-HCl/SDS pH 8.8 buffer

Tris-HCl	1.5 M
SDS	0.4 %

adjust pH to 8.8

Stacking gel (for 2 gels)

30 % acrylamide/bis-acrylamide	1 ml
4x Tris-HCl/SDS pH 6.8 buffer	1.9 ml
H ₂ O	4.6 ml
APS	37.5 μ l
TEMED	7.5 μ l

Separation gel (for 2 gels)

	<u>6 % gel</u>	<u>12 % gel</u>
30 % acrylamide/bis-acrylamide	2.3 ml	4.6 ml
4x Tris-HCl/SDS pH 8.8 buffer	2.8 ml	2.8 ml
H ₂ O	6.2 ml	3.9 ml
APS	22.5 μ l	22.5 μ l
TEMED	7.5 μ l	7.5 μ l

Pipet 4 ml 6 % gel solution and then 5 ml of 12 % gel solution into a 10 ml pipette. Gently mix by aspirating one air bubble before pouring the gradient gel solution into the gel system.

2.23 Whole cell protein lysates

The tissue was rinsed twice in 0.1 M PB buffer and then lysed in 500 μ l RIPA lysis buffer (5 M NaCl, 0.5 M EDTA (pH 8.0), 1 M Tris, pH 8.0, NP-40 (IGEPAL CA-630), 10% sodium deoxycholate, 10% SDS, add 100ml dH₂O) containing protease inhibitor and phosphatase inhibitor (Mass Spectrometry Safe Protease and Phosphatase Inhibitor Cocktail, Sigma). The tissue was homogenized by a mortar and pestle. Subsequently samples were centrifuged with maximum rpm and supernatant was retained. Samples were either further processed or stored at –80 °C for long-term storage.

2.24 Western blotting

Western blotting was performed at 90 V for 1-2 hours in a mini trans-blot cell (BioRad) according to standard procedure. After the protein transfer to the PVDF membrane, the latter was shortly blocked in 5 % milk powder for 10 min at room temperature with shaking. Then, the incubation of the membrane with the appropriate primary antibody was performed. The optimal incubation time and the optimal antibody concentration were determined empirically. Hereafter, the membrane was washed three times in TBST for 5 min followed by a 1-2 h incubation with the secondary antibody at room temperature with rotation. The membrane was washed 3-4 times with TBST for 5 min and once in ddH₂O. After the incubation with the western blotting luminol reagent (Santa Cruz) according to manufacturer's protocol the chemiluminescence was detected using the Chemidoc MP Imaging system (BioRad) and ImageLab software. The optimal exposure time was determined empirically.

Transfer buffer

Tris 3 g
glycin 14.4 g
H₂O ad 1 l

10x TBS

Tris 12.1 g
NaCl 80.2 g
H₂O ad 1 l

TBST

10x TBS 100 ml
Tween 20 1 ml
H₂O ad 1 l

Blocking solution

TBST 15 ml
milk powder 0.75 g
H₂O ad 1 l

Table 2.8 Antibodies used for western blotting

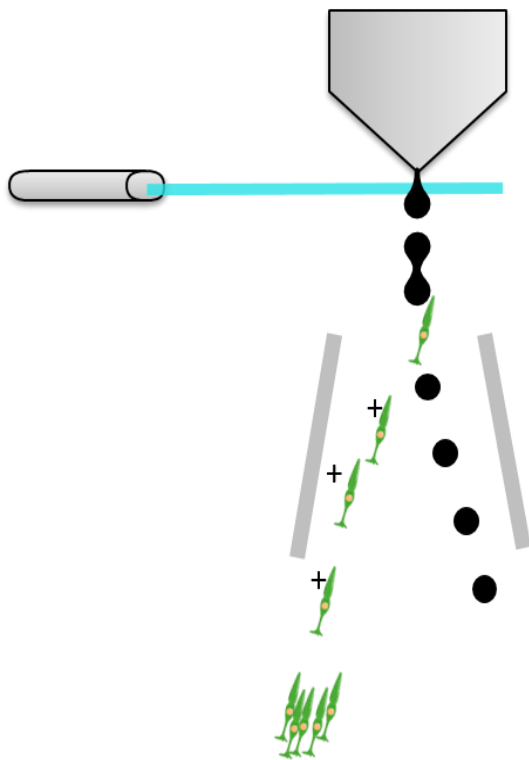
Antibody	company	Dilution IHC
mouse anti-myc	Purchased from Cell Signaling	1:2000
mouse anti-alpha-tubulin	Dianova, Hamburg	1:2000
goat anti-Atr	Santa Cruz	1:200
mouse anti-NPM1	abcam	1:100
anti-mouse HRP	Santa Cruz	1:2000
anti-goat HRP	Santa Cruz	1:2000

2.25 Co-Immunoprecipitation (Co-IP)

Immunoprecipitation was performed using Protein G Dynabeads (Invitrogen) according to manufacturer's instructions. Briefly, protein extracts were prepared without the use of detergents 100 μ l beads were added in a 1.5 ml Eppendorf tube together with 1-2 μ g primary antibody. Next, the volume was adjusted to 500 μ l using 0.1 M PBS and incubated for 30 min at 4 °C under rotation. Tubes were placed on a magnet rack for precipitation and the supernatant was discarded. The beads were washed twice with 300 μ l PBS solution. Subsequently, 500 μ g protein lysate was added to the beads and incubated for 30-60 min at 4 °C under rotation. The supernatant was discarded and the beads were washed 3 times with 300 μ l PBS solution. After the last wash, the suspension was transferred into fresh 1.5 mL Eppendorf tubes and the supernatant was removed completely. Beads were resuspended in 6 x Lämmli buffer (with or without DTT, depending on the application) and incubated at 70°C for 15 min. Finally, the supernatant was loaded on the appropriate SDS PAGE gel.

In some cases, the antibody and IgG's of protein G were crosslinked to the beads by means of irreversible, non-cleavable crosslinker BS3 (Thermo Scientific). For this purpose, after the coupling of the antibody to the beads, BS3 was added to the reaction in a final concentration of 5

mM. Then, the suspension was incubated for 30 min at room temperature and was quenched subsequently by adding Tris-HCl pH 7.5 (final concentration 50 mM) and incubating the reaction for 15 min at room temperature. Then, protein lysate was added and the reaction was processed as described above.



2.26 Retina dissociation

RG-eGFP positive mice or RG-eGFP x *Cnga3* KO mice were euthanized with Isofloran and then sacrificed. Eyes were protruded out of the orbit (exophthalmus) and fixed with curved forceps. With a sharp blade, the cornea was cut and by pulling the forceps the retina was smoothly extracted from the eye. After rinsing in cold PB (0.1M) and removing the lense as well as remaining RPE the tissue was transferred into a 1.5 ml reaction tube containing 250µl papain solution (provided by the papain dissociation kit). Retinas were incubated in the papain

Figure 2-5: Fluorescence-activated cell sorting (FACS). Dissociated retina with eGFP-expressing cones have been sorted by FACS to obtain pure cone-lysates.

solution for 20-30 min in a shaker (400 rpm) at 37 °C. After papain incubation the papain solution containing the partially digested retina were transferred into an EBBS-solution

containing 60 µl of DNase I (10 mg/ml) + 60 µl of ovomucoid solution (provided by the kit). Using a fire polished pipette, mechanical dissociation was performed (10x up and down). Single cell suspension was pipetted gently on top of 1 ml of ovomucoid solution, to generate two layers. Suspension was centrifuged for 5 min at 300 g (approximately 1,300 rpm). The supernatant was discarded and cells were resuspended in 500 µl of cell medium for sorting by Fluorescence-activated cell sorting (FACS).

2.27 Fluorescence-activated cell sorting (FACS)

Cells were analyzed with a FACS Aria II instrument (Becton Dickinson) and data analysis was performed using FlowJo version 7.2.5. eGFP positive cells were sorted into EBBS medium (provided by the papain dissociation kit) and cell pellets were stored at -80°C for protein purification and mass spectrometry.

FACS-sorting was performed with the help of Dr. Daniela Meilinger (Group of Prof Heinrich Leonhardt, Faculty of Biology at the LMU, Munich)

2.28 Phospho-enrichment of Proteins

50 μl (1 mg) of MagReSyn[®] Ti-IMAC were washed twice in 200 μl of 70 % ethanol on a magnetic separator with gentle agitation (e.g. vortex mixing) for 5 min. Then microparticles were washed in 100 μl of 1 % NH_4OH on a magnetic separator with gentle agitation (e.g. vortex mixing) for 10 min. Last particles were equilibrated thrice in 50 μl loading buffer (1M glycolic acid in 80 % ACN, 5 % TFA) for 60 s. The loading buffer was removed and microparticles were ready for phospho-enrichment.

Protein digest was adjusted (containing ~ 455 μg total protein) with one equivalent volume of loading buffer (100 μl) and added to the equilibrated MagReSyn[®] Ti-IMAC microparticle pellet. Microparticles were resuspended in the peptide sample by vortexing or pipette aspiration. After incubation for 20 min at room temperature with end-over-top mixing, the tubes were placed on a magnetic separator and microparticles were allowed to clear. Coupling supernatant was removed and discarded. Unbound sample was removed by washing with 100 μl of loading buffer for 30 s with gentle agitation. The tube was placed on a magnetic separator and the supernatant was removed and discarded. Non-specifically bound peptides were removed by resuspending the microparticles in 100 μl wash buffer (aqueous solution of 80 % ACN and 1 % TFA) for 2 min with gentle agitation. The supernatant was removed and discarded on a magnetic separator. Washing was repeated with 100 μl of wash buffer and again discarded on a magnetic separator. Bound phosphopeptides were then eluted from microparticles by adding 80 μl elution buffer (1 % NH_4OH) for 15 min under constant gentle agitation. Elution was repeated twice to obtain a final elution volume of 240 μl . On a magnetic separator the eluate containing the

phosphopeptides was removed and transferred to a new tube. 60 μl of 10 % Formic Acid was added to the 240 μl eluate to acidify the solution. Samples were analysed the by mass spectrometry.

2.29 Mass-spectrometry

Whole cell protein lysates were incubated with 1 μL Benzonase for 1 h at 0 °C. Then, 250 μL of MS-grade water was added and 4 retinas (2 animals) were pooled together. To precipitate the proteins, 7 mL of ice-cold acetone was added to each sample and they were incubated at -20 °C overnight. After centrifugation at 10000g for 10 minutes, the supernatant was removed and the pellet was washed two times with 1 mL of 80% acetone_(aq) each.

To the resulting pellets 2 mL of digestion-buffer (50 mM TEAB, 1 mM MgCl_2 in MS-grade water) and 2 mL of MS-grade water were added and the samples were sonicated (5 cycles @ 50% power output, 5 min) on ice to resuspend the samples. The protein concentration of the samples was determined by conducting a Bradford assay.

For full proteome analysis, from each triplicate of the samples 2.25 μg of protein content were diluted with digestion-buffer to give a total volume of 100 μL . The proteins were reduced with TCEP_(aq) (5 μL , 1M) for 45 min at 60 °C and thereafter neutralized with TEAB_(aq) (30 μL , 1M) and alkylated with iodoacetamide_(aq) (6 μL , 1M) for 30 min at room temperature in the dark. Finally, trypsin (2 μL , 0.1 $\mu\text{g}/\mu\text{L}$ in 50 mM AcOH_(aq)) was added and the samples were incubated at 37 °C and 350 rpm with interval mixing on a thermomixer overnight.

For phosphoenrichment samples, a volume equivalent of 445 μg protein content was taken for the knock-out, the wild type and the IIA-samples. Since not enough protein could be recovered from the biological replicates of IA-samples, only a volume containing 283.5 μg protein amount was used. For digestion, samples were processed in the same way as for the full-proteome analysis with the following amounts: TCEP_(aq) (1M) was added to a final concentration of 41.8 mM, 255 μL of TEAB_(aq) (1M) were added to neutralize the solution, iodoacetamide_(aq) (1M) was added to a final concentration of 41.1 mM and 210 μL of TEAB_(aq) (1M) were added to adjust the pH-value for digestion. Finally, 5 μg trypsin were added per sample (3 μg in case of the IA-triplicate samples).

After digestion, peptides were desalted by stage-tip purification (SDB-RPS material, see Kulak et al., 2014) and concentrated to dryness on a speed-vac. Full proteome samples were solved in 12 μ L MS-solvent (MS-grade water, 0.1% formic acid, 2% MeCN) each and analysed by mass spectrometry.

The phosphoenrichment samples were processed as described in 2.28. After elution, phosphopeptide-containing samples were acidified with FA_(aq) and desalted by stage-tip purification (SDB-RPS material, see Kulak et al., 2014) and concentrated to dryness on a speed-vac. The phosphopeptide-samples were solved in 12 μ L MS-solvent and analysed by mass spectrometry.

Mass spectrometry and MaxQuant Analysis was performed by Andrea Künzel and Michael Stadlmeier (Carell group, LMU Munich).

2.30 Statistics

All values are given as mean \pm standard error of the mean (S.E.M) or mean \pm standard deviation (SD) and n is the number of experiments. An unpaired Student's t-test was performed for the comparison between two groups. Values of $p < 0.05$ were considered as significant. Fisher's exact-test was applied to analyse significance of contingency tables.

3 Results

3.1 Transcriptional changes in the retina of *Cnga3* KO mice

Gene expression changes in the retina of *Cnga3* KO mice, were investigated by a Microarray approach. The overall up- and down-regulation of gene-transcripts is visualized in a heatmap shown in Figure 3.1A. At four weeks after birth (PW4) 561 genes have a changed expression-pattern while at eight weeks after birth (PW8) only 257 genes are detected to be misregulated. Taking a closer look at the transcriptional changes, it is apparent that a considerably higher number of genes are down-regulated at PW4 (498) compared to genes being down-regulated at PW8 (129). The number of genes up-regulated on the other hand is twice as much at PW8 (128) compared to PW4 (63). Gene Ontology analysis uncovered the gene groups being misregulated in the *Cnga3* KO mouse model showing a high representation of enzymes and a relatively high number of transcription factors (Fig3.1B). By pathway analysis with the computer program Ingenuity IPA the significance of regulated genes can be evaluated in the context of biological systems. The analysis divides the data into cellular functions termed as biological processes and metabolic processes termed as canonical pathways. Over represented pathways, associated to the dis-regulated genes, can then be detected.

At PW4 “cell death and survival” mechanisms, the “nervous system”, “development and functions” and “gene expression” are profoundly affected, while at PW8 “cell morphology”, “tissue development”, “molecular transport” and “phototransduction” are affected.

3.2 cGMP accumulation in cones of *Cnga3* KO mice

In the outer nuclear layer (ONL) of *Cnga3* KO mice an increase of cGMP could be detected by immunohistochemistry. cGMP could be detected by an antibody raised against a **cGMP-formaldehyde-thyroglobulin conjugate** (de Vente et al., 1987, Ikawa et al., 2003)).

As displayed in Figure 3.2, *Cnga3* KO mice show an enhanced level of the second messenger cGMP compared to age-matched wild type mice with the same background. Most importantly this increase is cone specific and present throughout the degeneration process.

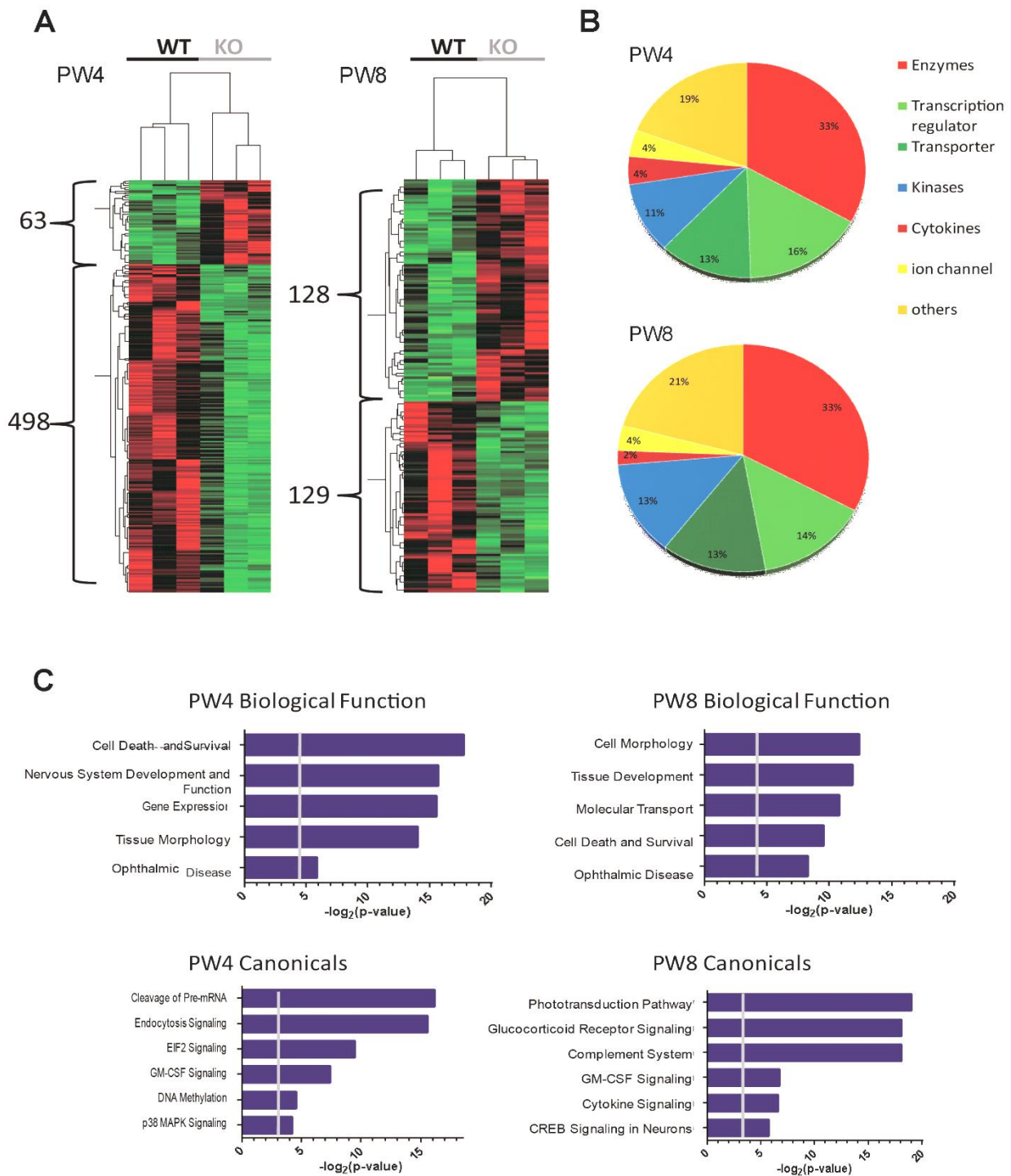


Fig3.1: Gene expression analysis during cone photoreceptor degeneration. (A) A heat map visualizes the up- and downregulation of genes in *Cnga3* KO compared to wild type mice at four and eight weeks after birth (PW4/PW8). While 561 genes are detected to be deregulated at PW4 only 257 genes show a different expression at PW8 (B) Gene ontology analysis on genes being deregulated during the degeneration of *Cnga3* KO mice reveals the function of the gene groups being deregulated. (C) By pathway analysis, biological processes and canonical pathways can be determined which are associated to a significant number of dysregulated genes. The p-value shows if this association is due to random chance or significant. (All displayed Pathways have a p-value ≤ 0.05)

Results

The accumulation could be detected several days before eye opening (P6) and before full maturation of the retina. Interestingly, cGMP accumulation persisted in the few residual surviving cones in the dorsal part of the twelve-month-old *Cnga3* KO mouse retina (PM12, Fig3.2 C). The earliest time point of detection was four days after birth (P4, Figure 3.2A). At this time point only a few cones show a faint and spotty cGMP-positive staining. At P6 however the cGMP signal further broadened and is present in all cones of the mouse retina (Figure 3.2 A). Taken together the data shows an accumulation of cGMP at remarkably early time points until very late stages of degeneration in the adult mouse (Fig 3.1).

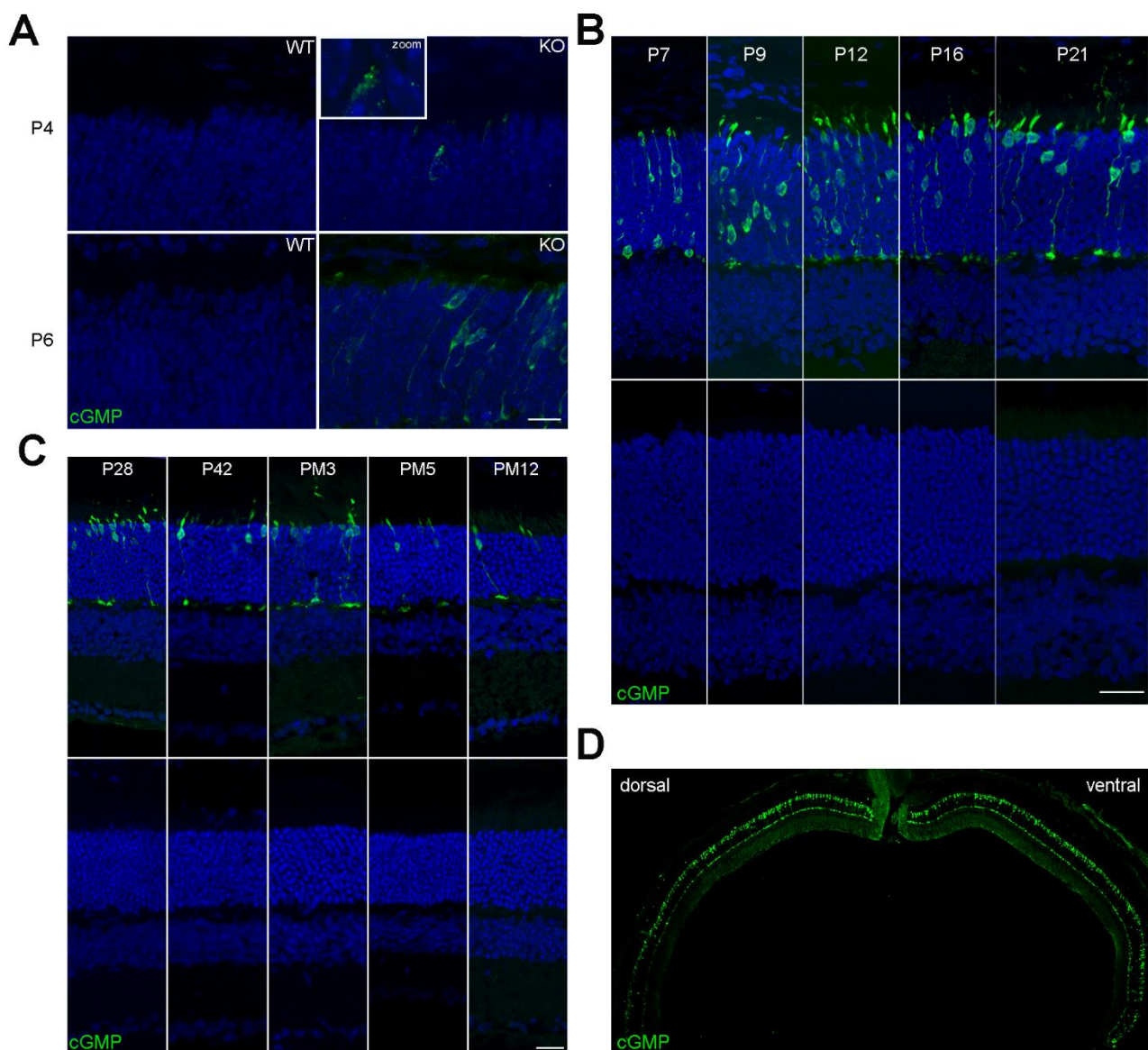


Fig: 3.2: cGMP accumulation in cones of *Cnga3* KO mice. At postnatal day four (P4) a weak signal for cGMP is detected in the retina of *Cnga3* KO mice. This signal increased at P6 (A; scale bar marks 10 μ m). Throughout maturation (P7-P21) an accumulation of cGMP is present in cones (B, scale bar marks 25 μ m) and sustained throughout the degeneration process (C, scale bar marks 25 μ m). Even at very late stages of the degeneration process (PM12) when only a few cones are residual, cGMP accumulation is still detected (C). This accumulation can be detected in dorsal as well as ventral cones at all given time points as seen in D (PW4).

3.3 Knock-down of guanylyl cyclase during degeneration

Guanylate cyclase 2E (encoded by *Gucy2e*) is the only known cGMP-producing enzyme present in cones (Sokal et al., 2003, Takemoto et al., 2009, Yang et al., 1999). To test if the observed cGMP accumulation (Figure 3.2) is critically involved in photoreceptor cell death or just represents a bystander effect of the degeneration, *Gucy2e* in *Cnga3* KO retina was down-regulated using specific shRNA.

For the purpose of in-vivo cone tracing *Cnga3* KO mice were first cross-bred with mice expressing eGFP under the control of the cone specific human red/green opsin (RG)-promoter (Ikawa et al., 2003). An adeno associated virus (AAV)-vector expressing a *Gucy2e*-specific shRNA and the fluorescent marker protein mCherry was then delivered into the subretinal space of RgeGFP x A3ko-mice (Figure 3.3). To interfere with *Gucy2e* expression before the peak of apoptosis at PW3 and before the degeneration sets in, the *Gucy2e*-specific shRNA was applied right after eye opening at P14. Only one eye (OD, right) was injected, while the second eye (OS, left) served as a control to monitor the degeneration process in direct comparison. After two weeks of recovery the density of eGFP-positive cone photoreceptors and the range of shRNA-expression could be determined by measuring the fluorescence of the reporter genes (eGFP and mCherry) by *in vivo* confocal laser scanning ophthalmoscopy (cSLO, Heidelberg spectralis) (Figure 3.4 A-D).

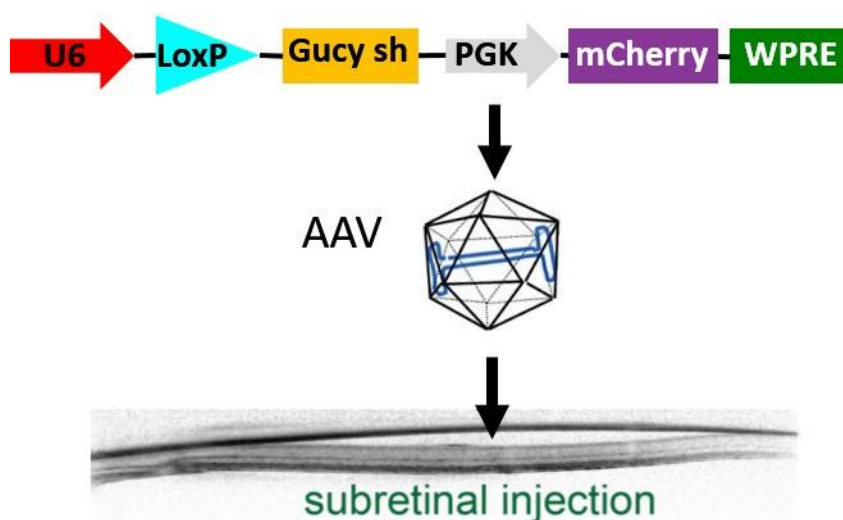


Figure 3.3: Subretinal application of a shRNA directed against the cGMP-producing guanylyl cyclase. The sh-RNA was cloned into a recombinant Adeno associated virus (rAAV)-vector downstream of an U6-promoter with mcherry as a report gene. After AAV-production the virus was injected subretinally in close proximity to the photoreceptors of *Cnga3* ko and wild type mice.

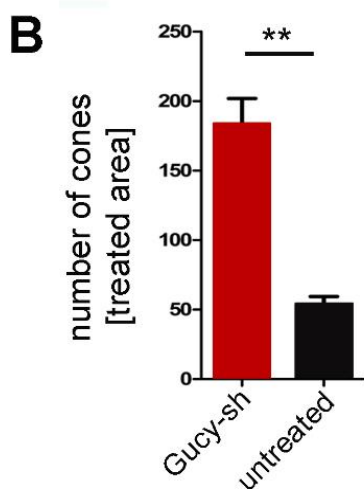
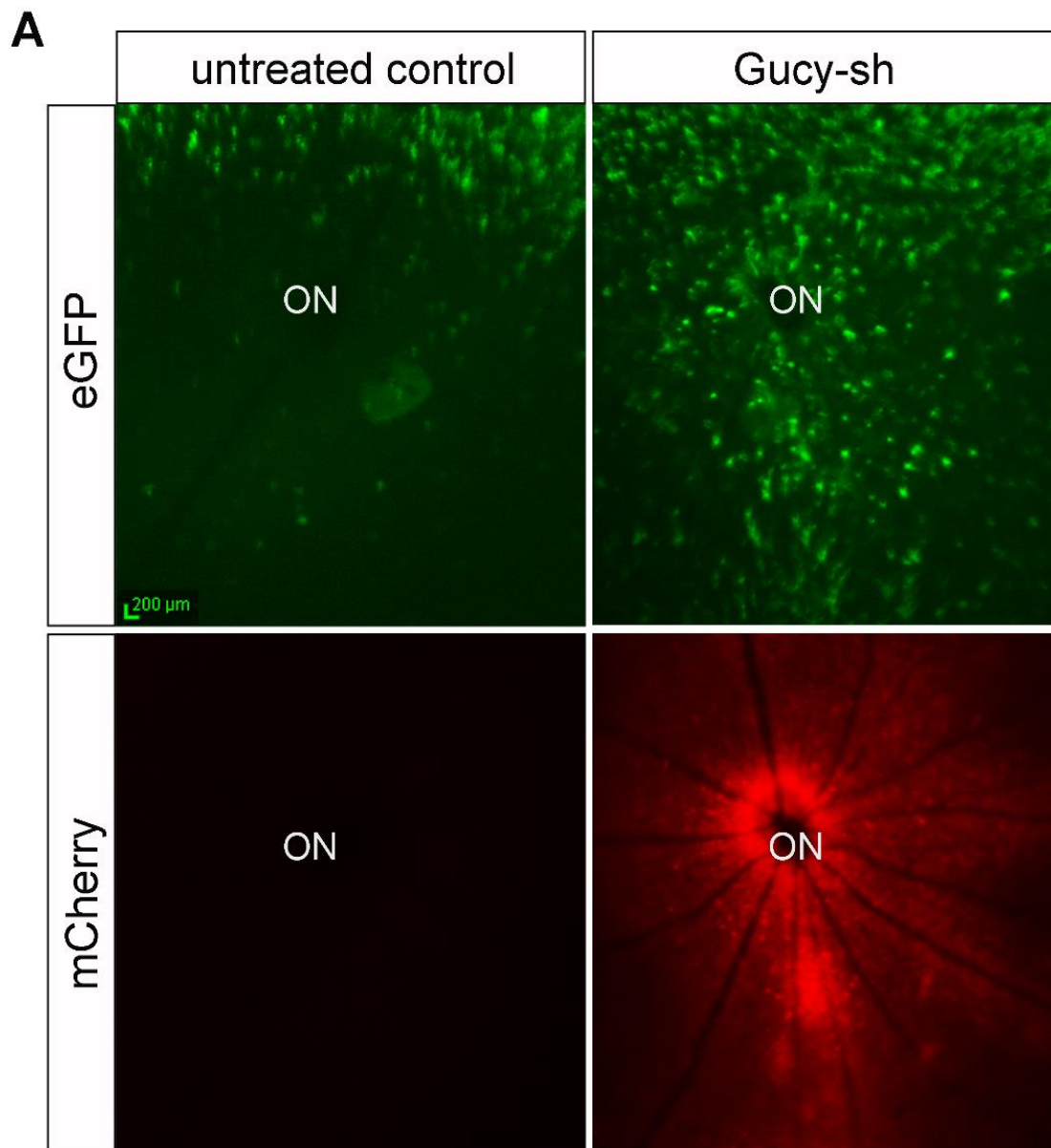


Figure 3.4: Prolonged survival of cone photoreceptors in *Cnga3* KO mice after down regulation of cGMP-production during degeneration process. A shRNA-directed against the Guanylyl cyclase 2e, expressed with mCherry as a report gene was applied to the retina of *Cnga3* KO mice. This knock down delayed the degeneration of eGFP-positive cones in the ventral part of a treated compared to an untreated retina 11 weeks after injection at PM3 (A). Quantification of eGFP-positive cones in the treated (mcherry-positive) area displays a significant decline of cone degeneration (B).

Summary data are mean \pm SEM. ** $p < 0.01$ (Student's t-test)

Cone survival was then ascertained by counting the number of eGFP-positive cells in the designated area.

Measurements of eGFP and mcherry fluorescence were repeated at an interval of one week. Already 11 weeks after the injection (at 13 weeks of age/PM3) a significant difference of the number of cones could be detected between the treated and untreated eye of *Cnga3* KO mice (Fig3.4 E). Cones were quantified in an area of $\sim 6020 \mu\text{m}^2$ of the retina of treated and untreated eye.

3.4 cGMP dependent kinases (cGKs) in the retina

To further understand how a dysregulation of cGMP-levels can lead to cell-death, it was most essential to investigate the signalling downstream of cGMP in the retina. Alongside the CNG channel other targets known to be regulated by cGMP are the cGMP-dependent kinases (cGK) I and II. To clarify whether these alternative cGMP effectors influence the cone degeneration in the disease of Achromatopsia, the expression level and pattern of cGKI (*Prkg1*) as well as cGKII (*Prkg2*) was further examined. qRT-PCR measurements showed that both kinases are present in the adult mouse retina. Figure 3.5 shows the expression of these cGMP-targets at three different postnatal developmental stages. While cGKI is relatively low expressed before eye opening (P6), the expression level gradually increases during retinal maturation. There was no apparent difference in cGKI mRNA levels between wt and *Cnga3* ko retina. cGKII expression was rather constant with during this period of time with only a minor increase at two weeks after birth. At p6 cGKII mRNA levels were similar in wt and *Cnga3* ko retina. However, around eye opening (p14) there was a transient and significant increase in the expression level of cGKII in the *Cnga3* KO retina when compared to the wt (Fig 3.5).

Sorting retina lysates by a fluorescence-activated cell sorter (FACS) resulted in pure rods or cones. RNA extracted from these pure fractions were then used for expression analysis of cGKI and cGKII by qRT-PCR. Both kinases show an enrichment in cones compared to rod photoreceptors (Figure3.5CB). The localisation of cGKI in the retina was further determined by immunohistochemistry and showed that cGKI is mainly expressed in Müller glia cells (Figure 3.5 C). A suitable cGKII-specific antibody was not available.

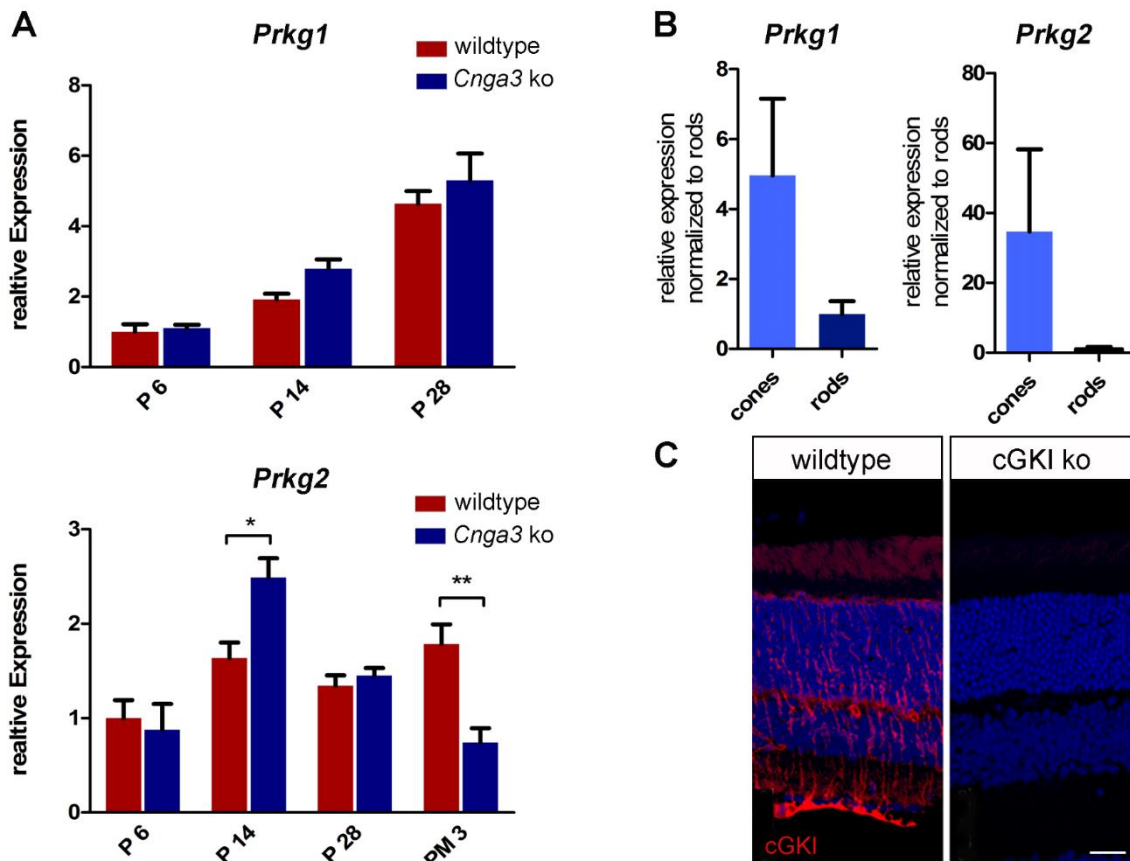


Figure 3.5: Expression pattern of the cGMP dependent kinases (cGKs) in the retina of *Cnga3* KO mice: Expression of *Prkg1*(cGKI) gradually increases during development from postnatal day 6 (P6) until P28 with no apparent difference between *Cnga3* ko and wildtype (wt) mice. *Prkg2* (cGKII) shows more constant expression levels in the wt. However, in the *Cnga3* ko cGKII shows a transient and significant increase at P14. (A). Both, cGKI and cGKII, mRNA is enriched in cone photoreceptors compared to rod photoreceptors (B). Immunohistochemical staining of four weeks old wt and cGKIko mouse retinal cross-sections using a cGKI-specific antibody. cGKI immunosignal (red) is found in all retinal layers with a strong signal in Müller glia cells (C, scale bar marks 25 μ m). * $p < 0.05$, *** $p < 0.001$ (Student's t -test).

3.5 Overexpression of cGK in wild type mice

Based on the finding that cGMP accumulates in diseased photoreceptors, it is likely that the respective effectors of cGMP are more active. To evaluate whether increased cGK-activity can influence the photoreceptor viability, AAV vectors expressing a constitutively active cGK variant were delivered into the subretinal space of wild type mice.

cGKs are known to be regulated by an N-terminal regulatory domain which changes the conformation upon binding of cGMP (see Figure1.9). Without its regulatory domain cGK is independent of an activation by cGMP and can phosphorylate its targets in the absence of the

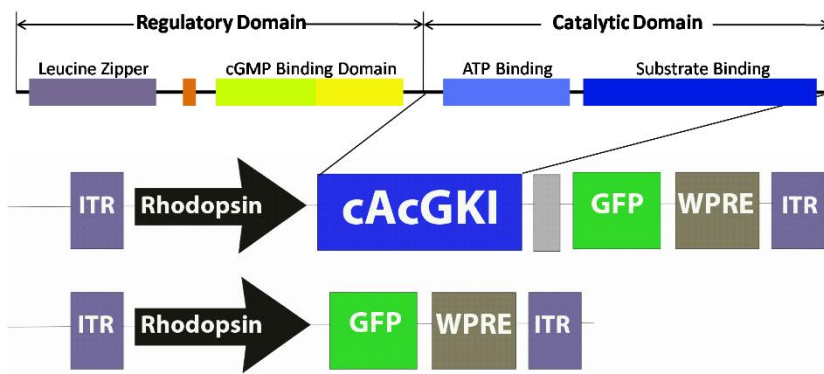


Figure 3.6: Expression of a constitutively active cGMP-dependent kinase (cGK) in mouse photoreceptors. The catalytic domain of the cGMP-dependent kinase (cAcGKI) was cloned behind the rod-specific rhodopsin-promoter with eGFP as a reporter gene for Adeno-associated-virus (AAV) production to achieve cell-specific gene-delivery. eGFP cloned behind the rhodopsin-promoter served as a control.

ligand, it is so called “constitutively active” (CAcGK) (Ruth et al., 1997, Boerth and Lincoln, 1994, Deguchi et al., 2004). The regulatory domain of cGKI lacking the N-terminal regulatory domain part was cloned with a Rhodopsin-promoter for rod photoreceptor-specific expression and a 2A-eGFP cassette into an AAV vector plasmid (Figure 3.6 and section 2.16 and Figure 2.1, Materials and Methods). From this vector CACGK was coexpressed with the reporter gene eGFP separated by the “self-cleaving” 2A-region, ensuring equimolar levels of both genes (Robertson et al., 1985, Donnelly et al., 2001). A vector expressing solely eGFP under the same promoter was used in the control experiment (Figure 3.6). Both constructs were packed as AAV8 (Y733F mutant) particles and delivered into the retina by subretinal injection. After one week of recovery the fundus and thickness of the retina of these mice were monitored each week. eGFP fluorescence, marking the treated region of the injected retina, could be determined by confocal laser scanning ophthalmoscopy (cSLO)-imaging (not shown). Expression of eGFP alone had no effect on the outer nuclear layer (ONL) thickness. However, treatment with the constitutive active cGK (cA-cGK)-expressing vector resulted in a continuous time-dependent decrease in the outer nuclear layer (ONL) thickness over a time-frame of five weeks (Figure 3.7A). After five weeks a tremendous effect could be observed and the photoreceptor layer of the cA-cGK-injected eye was completely lost (Figure 3.7 B). Quantification of this difference is highly significant (Figure 3.7 C).

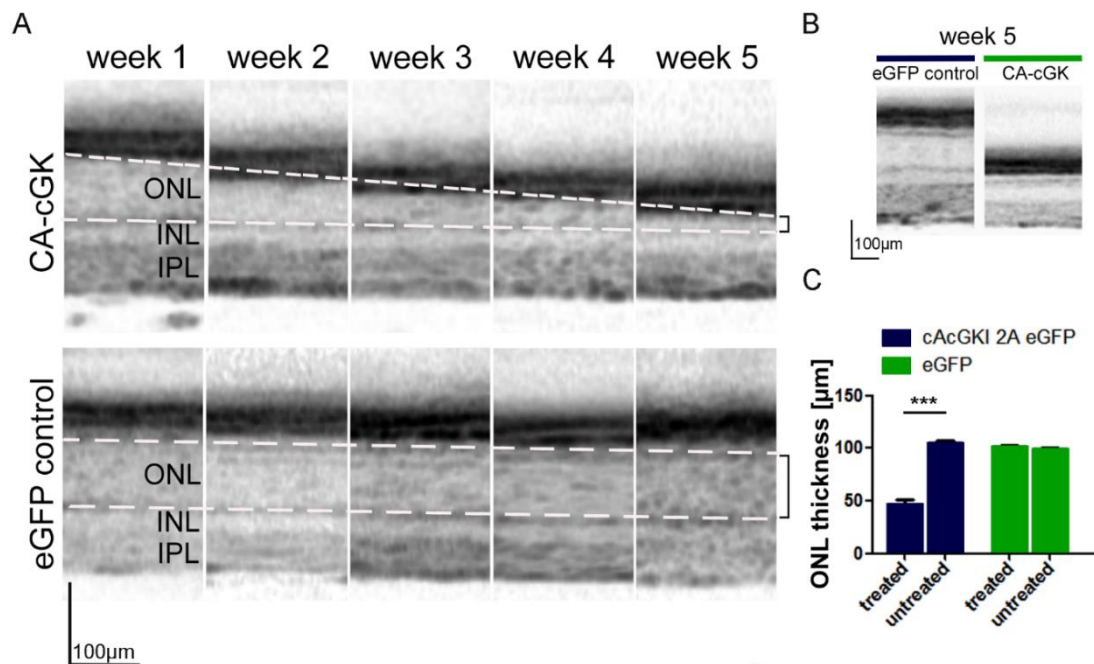


Figure 3.7: High activity of cGMP-dependent kinase (cGK) leads to photoreceptor death in wild type mice. Constitutively active cGK (cA-cGK) was expressed in wildtype retina and thickness of the outer nuclear layer (ONL) was monitored *in vivo* during a five weeks post injection observation period. Optical coherence tomography (OCT)-analysis showed a progressive loss of the ONL in animals treated with cA-cGK, while eGFP treated control animals showed a stable retina thickness over the same time frame (A). Panel B shows the retina thickness of treated Quantification of the ONL thickness showed a significant difference between cAcGKI-treated retina compared to either untreated or eGFP-treated retina (C). N=3 *** $p < 0.001$ (Student's t-test)

3.6 Knockout of cGK during degeneration delays cone degeneration in *Cnga3* KO mice

Providing that a high activity of cGMP-dependent kinase can induce cell death in photoreceptors, the next step was to determine whether the activity of this kinase is involved in the cell death of photoreceptors in Achromatopsia. To assess the influence cGMP dependent kinases might have on the degeneration process, mice carrying a *Cnga3* disruption (A3 KO mice) were crossbred with either cGKI KO or cGKII KO mice. Since a complete knock-out of cGKI in mice leads to premature lethality at approximately 6 weeks due to smooth muscle dysfunction. Therefore, cGKI mice were used with a smooth muscle (SM)-specific knock-in (ki) of cGKI to rescue this phenotype while all other cell types lack cGKI expression (Weber et al., 2007). The cGKI KO / SM-cGKI ki “rescue” mice are hereafter abbreviated as cGKI KO mice.

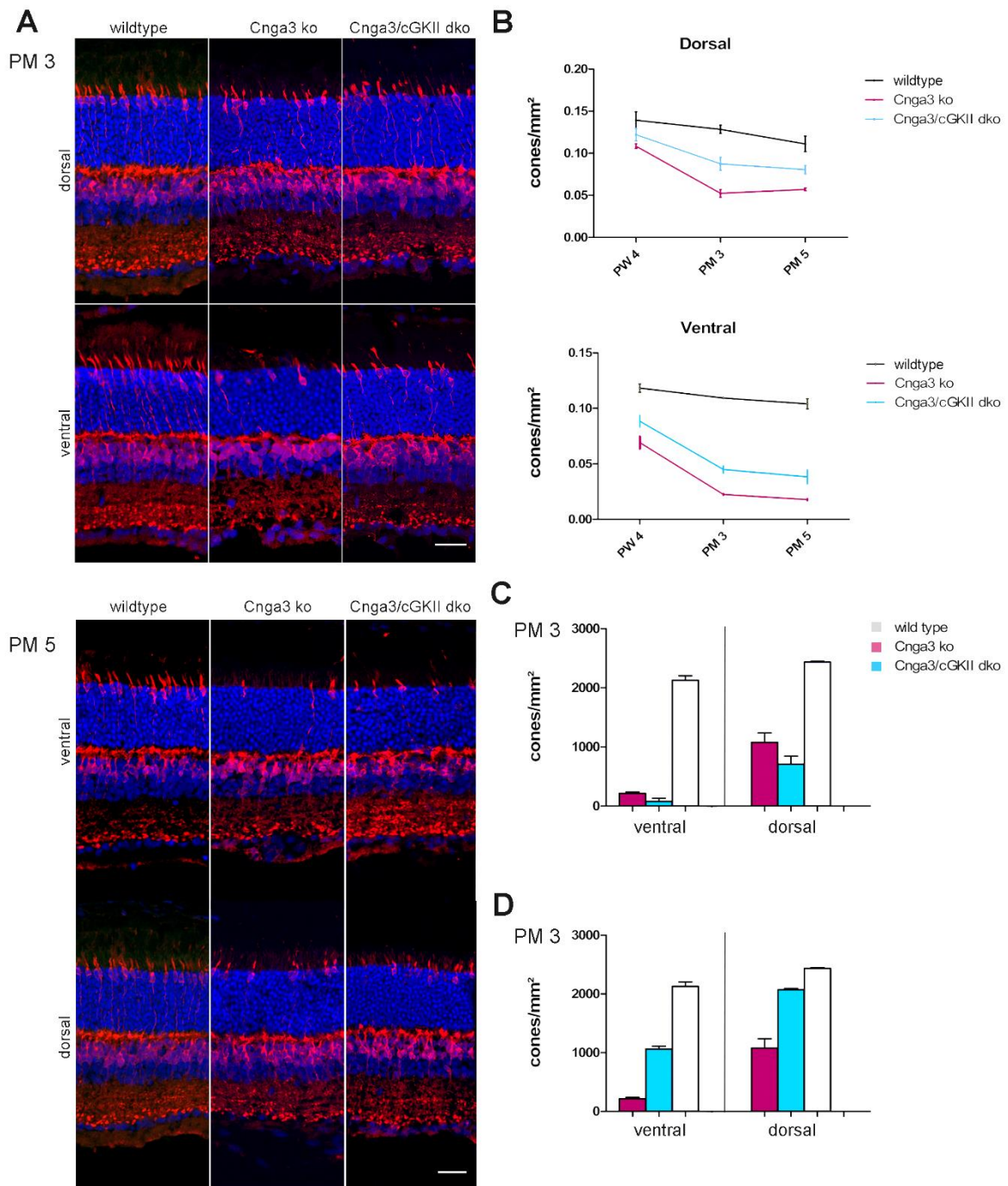


Figure 3.8: Cone survival in *Cnga3* KO mice upon knock out of cGMP dependent kinases (cGKs). (A/B) 3 and 5 months after birth (PM3/5) *cGKII/Cnga3* dko mice show a higher density of cones in the ventral and dorsal part of the retina compared to *Cnga3* ko mice. A quantification (C) shows that the difference in cone survival is significant at PM3 and PM5. A knock out of cGKI had no influence of cone survival (D) but interestingly knocking out both kinases in the *Cnga3* KO model has an even stronger effect on the viability of cones. $N \geq 3$, * $p < 0.05$ ** $p < 0.01$ *** $p < 0.001$ (Student's *t*-test); Scale bar marks 25 μm .

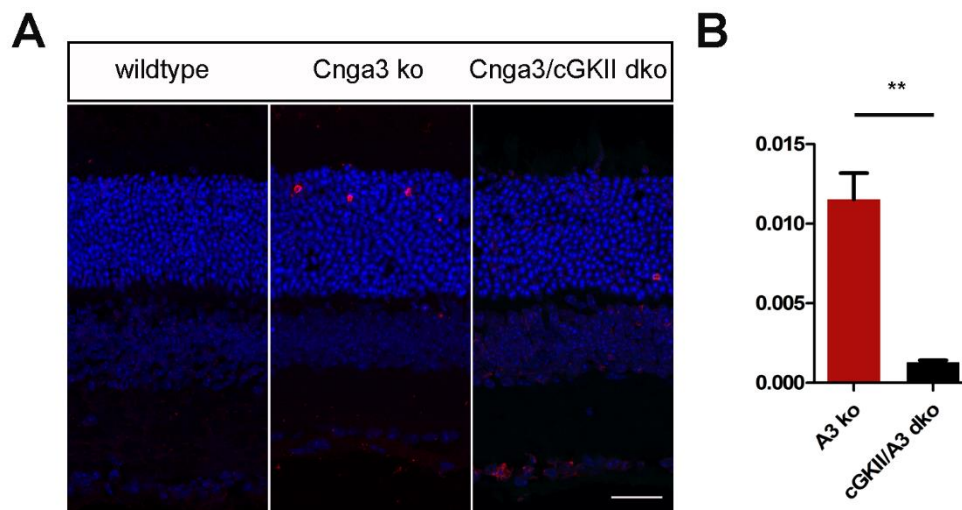


Fig 3.9 Reduced photoreceptor cell death in *Cnga3/cGKII* dko mice. (A) TUNEL staining display a decrease of cells undergoing cell death in *cGKII/Cnga3* DKO mice compared to *Cnga3* KO mice four weeks after birth (PW4)(B) Quantification of TUNEL-positive cells shows the decrease of cell-death is significant. N=3, ** $p < 0.01$ (Student's t-test); Scale bar marks 25 μ m

The generated *cGKI/Cnga3* and *cGKII/Cnga3* double KO (DKO) mice were born in normal Mendelian ratio and had a life span similar to the single knockout mice. Next, these mouse lines were used for comparative quantification of the number of surviving cones in the dorsal and ventral part of the retina. Retinal tissue was collected at the age of PW4, right after the peak of photoreceptor death, but also at PM3 and PM5 mice and cone survival was evaluated.

Loss of *cGKI* showed no positive effect on the cone survival in *Cnga3* KO mice. A significant difference could be detected at PM3 and PM5 between *cGKII/Cnga3* DKO and *Cnga3* KO retina. *cGKI/cGKII/Cnga3* triple knock out (tko) SM ki mice were also generated and showed an even more pronounced rescue of cones at PM3 (Figure 3.8).

In order to further support the finding that less photoreceptors are dying in *cGKII/Cnga3* DKO mice, a TUNEL assay was performed. By TUNEL assay DNA fragmentation, a programmed hallmark of cell death (Negoescu et al., 1998, Gavrieli et al., 1992), is visualized by incorporation of fluorescent dUTPs at the 3'-OH ends of DNA fragments. At PW4 the retina of *cGKII/Cnga3* DKO mice displayed a significantly lower number of cells undergoing cell death compared to *Cnga3* KO mice (Figure 3.9).

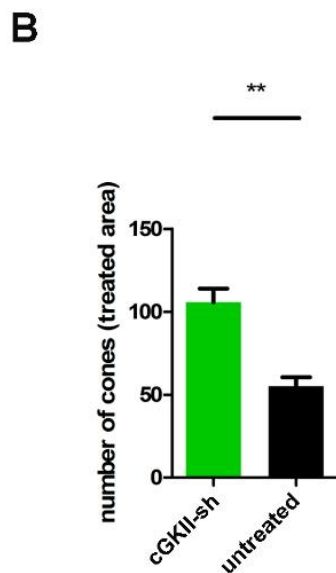
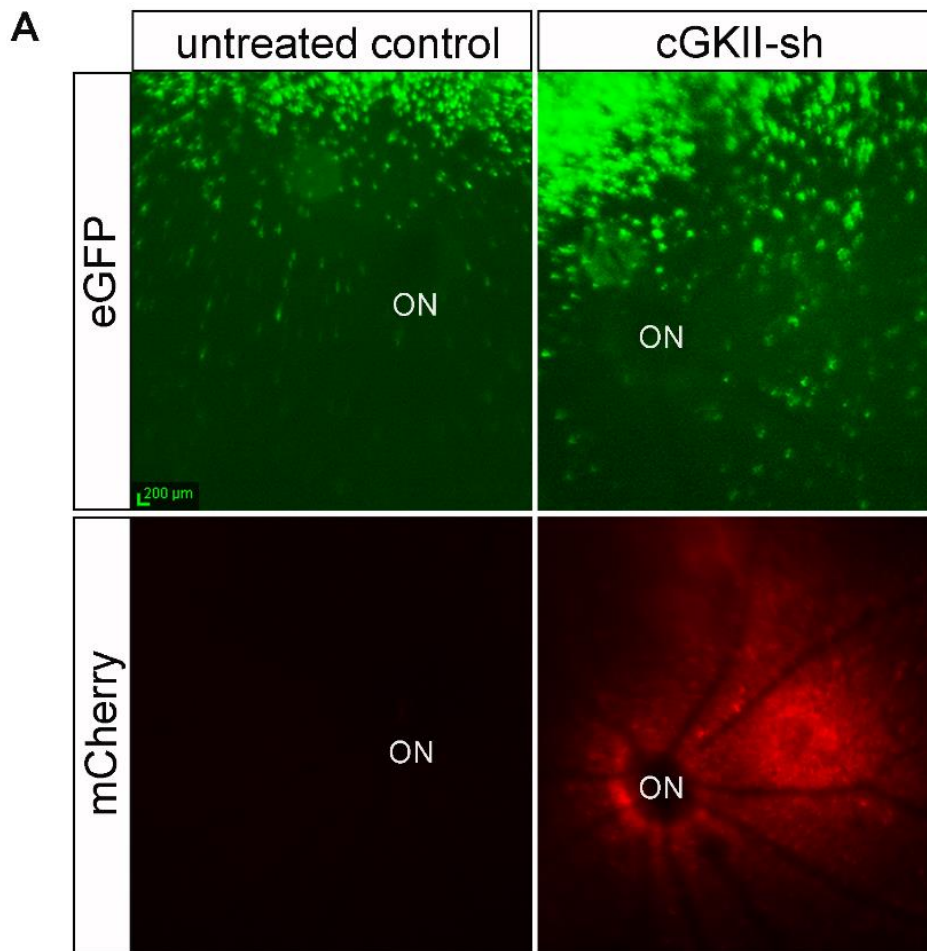


Figure 3.8: Delayed degeneration in *Cnga3* KO mice after down regulation of cGMP-dependent kinase II (cGKII). An AAV vector expressing a specific shRNA directed against the cGKII with mCherry as a report gene was applied to the retina of *Cnga3* KO mice (C/D). This knock down delayed the degeneration of eGFP-positive cones in the ventral part of a treated (B) compared to an untreated (A) retina 3 months after injection. Quantification of eGFP-positive cones in the treated (mcherry-positive) area displays a significant decline of cone degeneration (E). N=3, ** p< 0.01 (Student's test)

3.7 Knock-down of cGK II

To evaluate possible therapeutic options and to potentially increase the window of opportunity for gene replacement therapy, a AAV-vector was generated expressing a cGKII-specific shRNA under control of an U6-promoter and used for packaging AAV8 (Y733F mutant) vector particles for delivery *in vivo* experiments. After subretinal injections in *Cnga3* KO mice at the age of two weeks, the shRNA-expression was monitored indirectly by imaging the mCherry reporter gene encoded by the same AAV vector genome using SLO. The cone density was also monitored by SLO-imaging each week. Again *Cnga3* KO mice were used with eGFP tagged cones (*Cnga3* KO x RgeGFP-mice) for *in vivo*-detection. At about 10 weeks after delivery (PM3) quantification of surviving cones in the shRNA-treated area of *Cnga3* KO mice revealed a significantly higher cone density compared to the untreated eye (Fig 3.10).

3.8 cGKII signalling in the retina

Various substrates of cGKI and cGKII have already been identified but for the central nervous system (CNS) and the retina in particular their targets are still largely unknown. In order to further understand the degeneration and the role of cGMP in the process it is indispensable to determine which proteins get phosphorylated by the cGMP regulated kinases.

3.8.1 Mass spectrometry based analysis of proteins expressed in cone photoreceptors.

A mass spectrometry based approach was chosen to identify proteins enriched in degenerating *Cnga3* KO cone photoreceptors. In order to obtain pure cone preparations, RgeGFP-expressing wildtype and *Cnga3* KO mouse retinas were dissociated and single-cell solutions were used for fluorescence-activated cell sorting (FACS). Protein-lysates of the retained eGFP-positive cones were then analysed by label free quantification (LFQ) liquid chromatography coupled to mass-spectrometry (LC-MS). Evaluation with the *Perseus* software (version 1.5.0.9) identified the protein Nucleophosmin (Npm1) enriched in *Cnga3* KO cones with a highly significant ratio compared to wildtype cones as visualized in the volcano plot of Figure 3.11 A.

Npm1 also known as nucleolar phosphoprotein, B23, numatrin or NO38, is a protein involved in a variety of cellular functions ranging from ribosome biogenesis, cell cycle regulation, centrosome duplication, genomic stability, apoptosis and protein folding (Pfister and D'Mello,

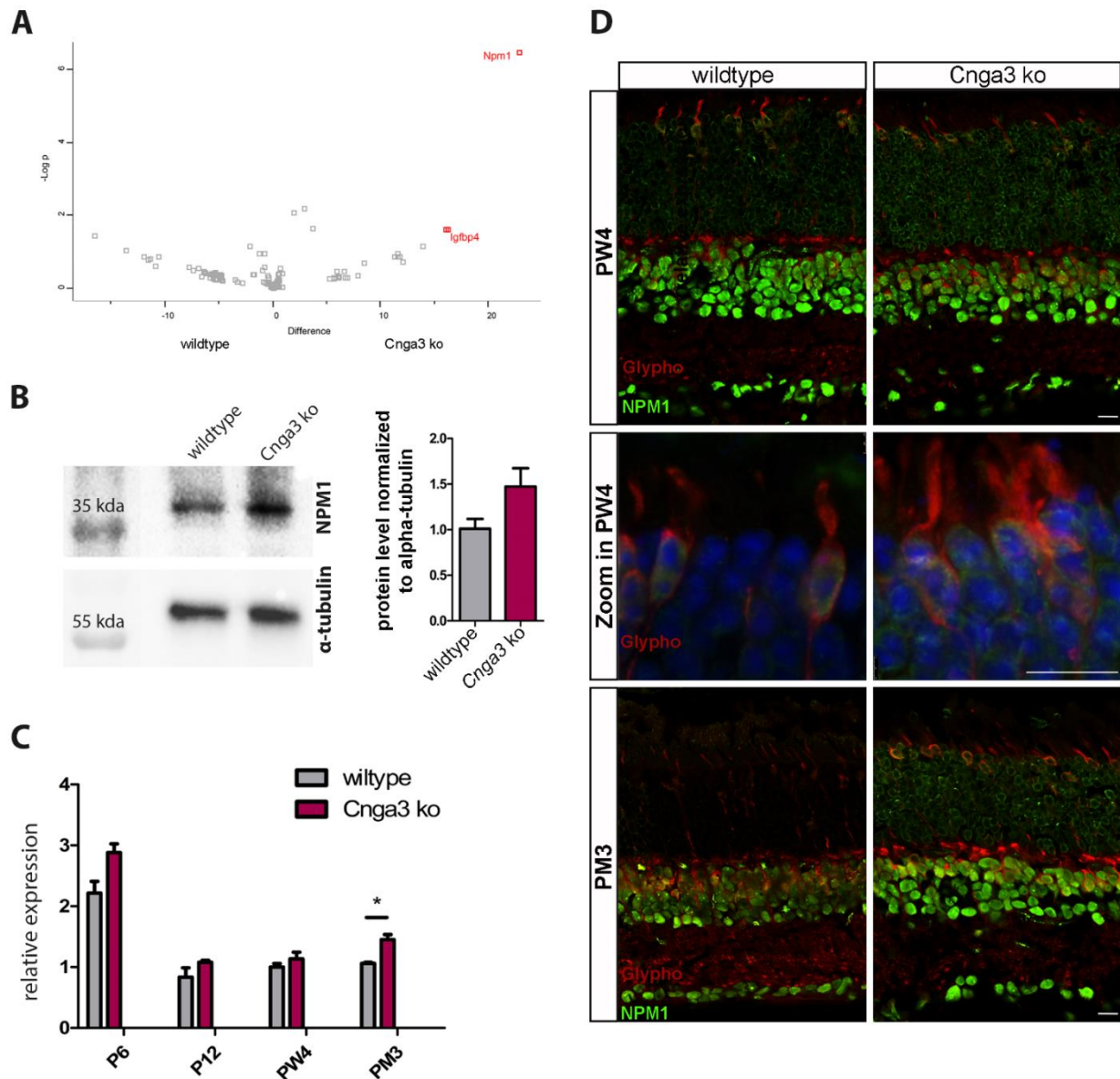


Fig 3.11 Mass spectrometry based analysis of proteins expressed in cone photoreceptors. (A) Volcano plot shows the ratios of proteins between FAC-sorted wildtype cones and *Cnga3* KO cones as a function of statistical significance (Student t-test $-\log p$ value). Proteins with no detectable signal in one of the subsets were assigned a value of zero. Nucleophosmin (Npm1) was detected to be enriched in *Cnga3* KO cones. (B) On protein level of whole retina lysates the increased level of Npm1 could be verified. (C) mRNA expression analysis by QPCR show a significant increase of Npm1 expression at PM3 (N=3, * $p < 0.05$, student's t-test). (D) Immunohistochemistry verifies an increase of Npm1 in the outer nuclear layer of *Cnga3* KO mice. The stainings with the cone marker glypho further show an enrichment of Npm1 in cones compared to rods in both genotypes. (scale bar marks 5 μ m).

Results

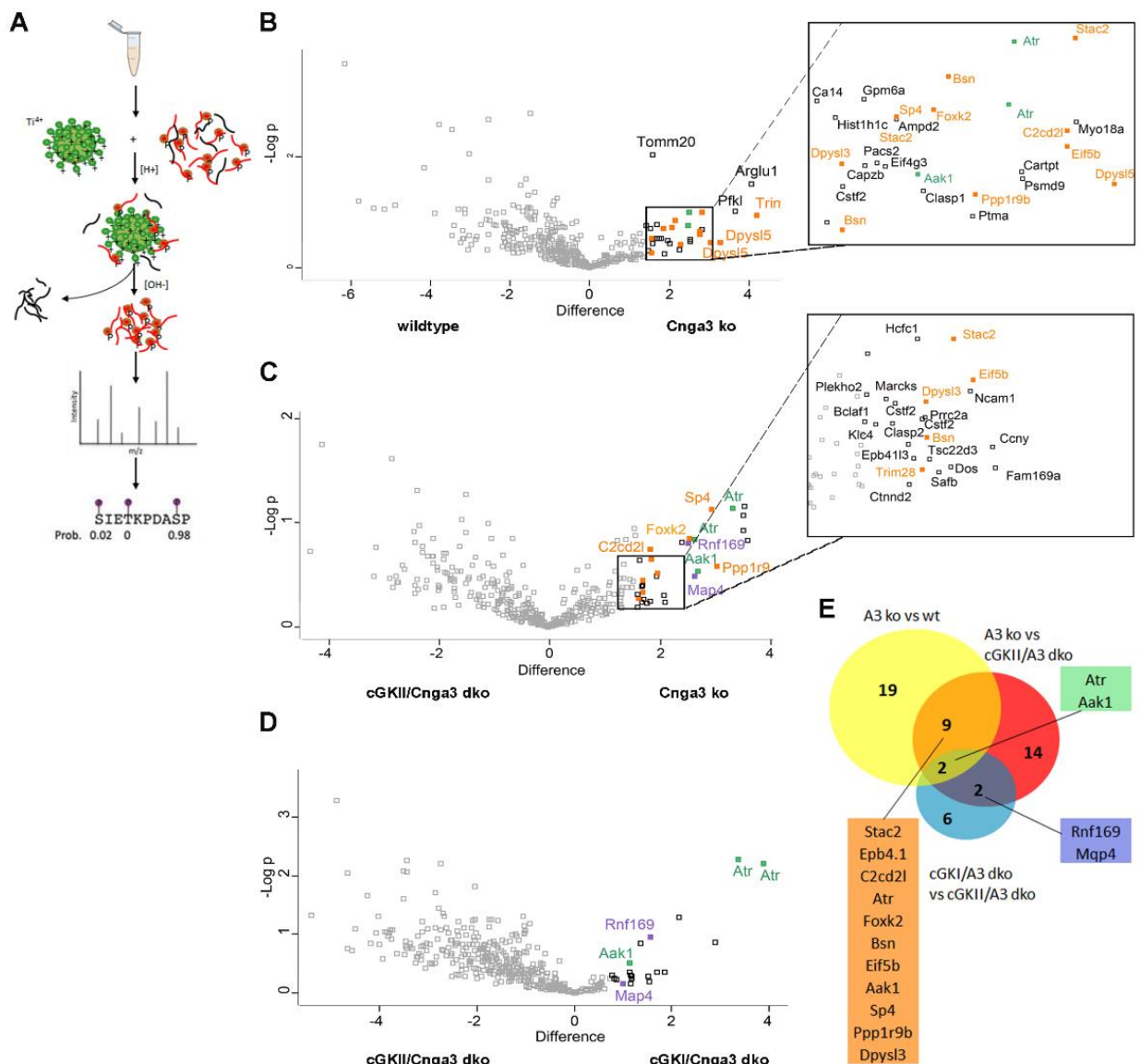


Fig 3.12 Phospho-proteomics of retina with different genetic modifications. (A) For phospho-enrichment Ti^{4+} -magnetic beads were used. Obtained proteins were identified by label free quantification (LFO) mass spectrometry. (B-D) Volcano plots show the ratios of detected phosphorylation sites of the given proteins between wildtype mice and *Cnga3* KO mice or *Cnga3* KO and *cGKII/Cnga3* DKO mice or *cGKII/Cnga3* DKO and *cGKI/Cnga3* DKO mice as a function of statistical significance (Student t-test p value ≤ 0.01). (E) Venn Diagram visualizes overlaps of enriched proteins identified in the volcano plots of B-D.

2015). Npm1 shuttles between cytoplasm and nucleus but is mainly located in the nucleolus (Szebeni et al., 1995, Borer et al., 1989)-

In the wildtype retina Npm1 is mainly detected in nuclei of the ganglion cell layer and inner nuclear layer but is also present in the outer nuclear layer (Fig 3.11 D). In the ONL the staining clearly shows an enrichment in cone nuclei, while in rods NPM1 is rather detected in the cytoplasm (Figure 3.11 D). Immunohistochemistry and western blot both indicate a slight increase of Npm1 in *Cnga3* KO retina (Figure 3.11 B/D). qRT-PCR gene expression analysis also revealed higher *Npm1* transcript levels in the *Cnga3* KO retina, however, the increase does not reach significance until three months after birth (Fig3.11 C).

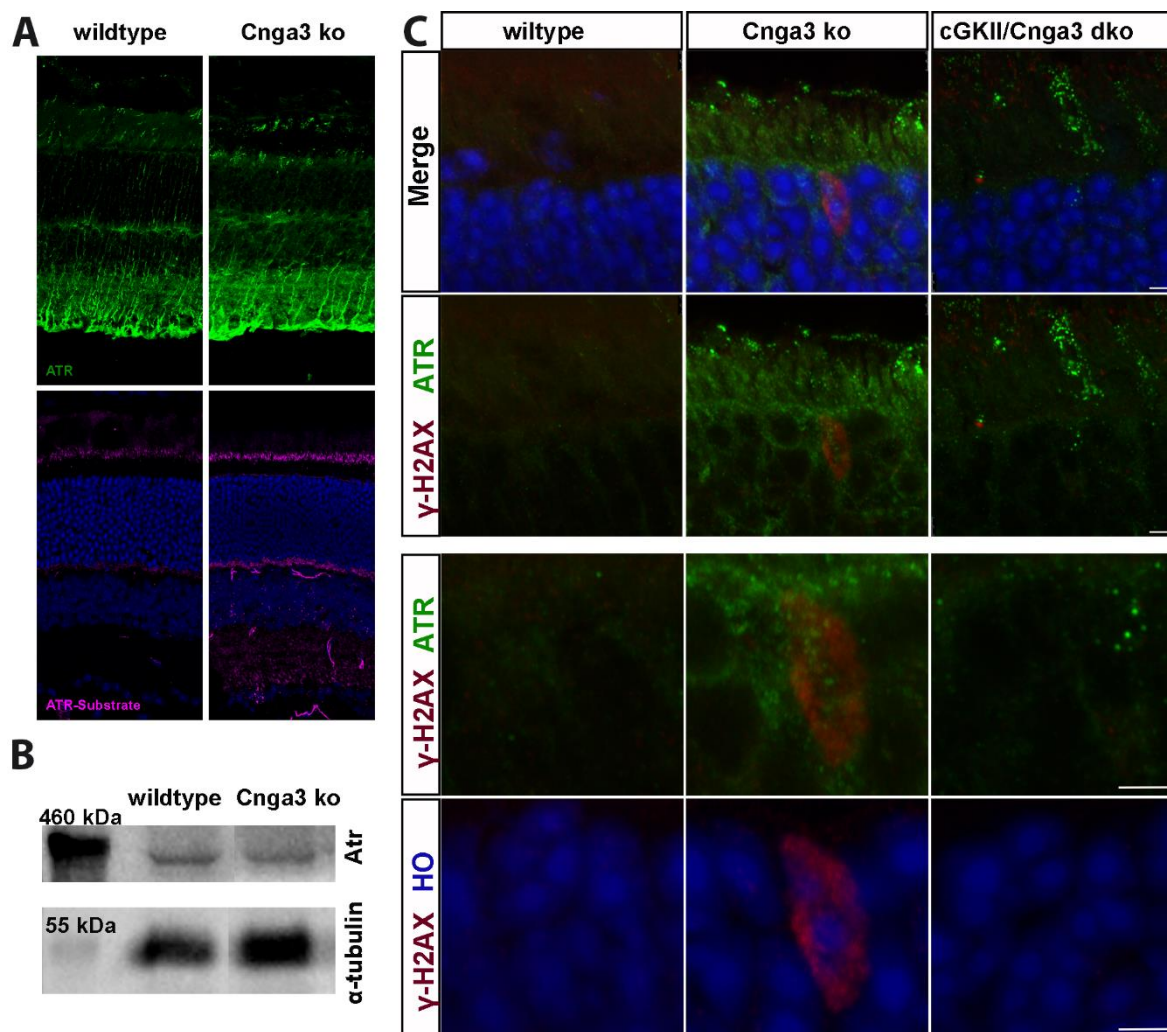


Fig 3.13 Activation of Atr. (A) By immunohistochemistry the distribution of the serine/threonine-kinase ATR can be detected in the retina. An antibody specifically detecting proteins carrying the recognition sequence of Atr displays the localisation of possible substrates. (B) Western blotting shows no difference in the protein level of Atr (N=3, PW4) (C) H2AX gets phosphorylated by ATR (γ -H2AX) and is a marker for DNA-damage High levels of γ -H2AX can be detected in several *Cnga3* KO cone nuclei but not in cones of cGKII/*Cnga3* DKO or wildtype animals. N=3; scale bar marks 5 μ m.

3.8.2 cGK-dependent phosphoprotein analysis

Genomic deletion and knockdown of cGKII had a neuroprotective effect on for *Cnga3* KO cones. This effect is most likely attributable to altered phosphorylation of cellular proteins due to the lack of cGKII. Therefore an experiment was designed to identify cGK-dependent phosphoproteins that are enriched in *Cnga3* KO retina. Using titanium ion (Ti^{4+}) chelated magnetic particles phosphorylated proteins were enriched out of full retina protein lysates wild type, *Cnga3* KO, *cGKI/A3* DKO, *cGKII/A3* DKO mice and further analysed by label free quantification (LFQ) mass spectrometry (Fig 3.12 A).

Proteins detected in the phospho-enriched lysates of *Cnga3* KO mice but not in DKO lysates were classified as potential targets of the respective cGMP kinase. As visualized by the volcano plots in Figure 3.12 B-D, several proteins could be detected rather enriched in phospho-lysates of *Cnga3* KO tissue compared to wildtype or *cGKI/A3* DKO tissue. A plot visualizing the ratio between *cGKI/Cnga3* DKO and *cGKII/Cnga3* DKO further emphasizes that the kinases have different targets in the mouse retina. A potential protein not found in either wildtype or *cGKII/Cnga3* KO but highly phosphorylated on two phosphorylation sites in *Cnga3* KO and *cGKI/Cnga3* DKO retina was ATM-Rad3-related protein (Atr) a serine/threonine-specific protein kinase (Figure 3.12 B-E). Atr belongs to the phosphatidylinositol 3-kinase-related kinase family and is known to be a sensor for DNA damage, activating DNA damage checkpoint and cell-cycle arrest by phosphorylating downstream effector proteins (Sancar et al., 2004).

Atr is essential for replication (Brown and Baltimore, 2003, Murga et al., 2009) and therefore an important target in tumour biology. During double strand breaks (DSBs) the histone H2A histone family member X (H2AX) accumulates in close proximity to the DNA breakage site and gets phosphorylated by the phosphatidylinositol-3-kinase-related kinases family, including Atr. Accordingly the phosphorylated H2AX termed as γ -H2AX is a widely used marker for DNA damage and for the activity of Atr (Harper and Elledge, 2007). γ -H2AX is also found during apoptotic DNA-fragmentation (Rogakou et al., 2000) and senescing cells (Sedelnikova et al., 2004).

Atr seems to be mainly localized in Müller glia cells (Figure 3.13A). Atr can also be detected in the outer and inner segments of photoreceptors. Possible substrates of Atr that are carrying the recognition site are also mainly found in the outer segments of photoreceptors (Figure 3.13A).

The protein level of Atr in whole retina lysates of *Cnga3* KO mice are unchanged in comparison to wildtype tissue (Figure 3.13 B), but increase of Atr activity might be concluded from γ -H2AX staining, showing an accumulation of phosphorylated H2AX in cone nuclei of *Cnga3* KO mice but not in those of *Cnga3* ko/*cGvKII* DKO mice (Figure 3.13 C). Furthermore H2AX-positive nuclei show a signal for Atr in the cell nucleus (Figure 3.12 C).

4 Discussion

4.1 Pathway analysis

The pathophysiological events leading to cell death in cones of Achromatopsia patients are still not fully understood. Analysis of a microarray approach highlight the substantial transcriptional changes in the retina of *Cnga3 KO* mice during the degeneration process and might shed light into the unknown molecular mechanisms leading to cell death. Looking at the time point of four weeks after birth (PW4), more than double the amount of genes are misregulated compared to the genes detected eight weeks after birth (PW8). In total 561 genes were detected to have a changed expression pattern at PW4. Taking into account that cone cell death in *Cnga3 KO* mice has its peak at around PW4 (Arango-Gonzalez et al., 2014)), it is reasonable to assume that genes associated to 'cell death and cell survival' are changed in their expression pattern in the *Cnga3* model as confirmed by the pathway analysis. This analysis further predicted a disruption of genes involved in the pathway 'development and function'. During development, a delay of postnatal migration of cone somata has been detected and described in *Cnga3 KO* mice (Michalakis et al., 2005). This delay might be a result of the disruption of the pathway 'development and function'. However the delay did not abolish the migration and cones in the adult *Cnga3 KO* retina show wildtype-like somata with a normal morphology and localization (Michalakis et al., 2005). Furthermore alterations in the pathway 'gene expression' were identified. This can be explained by the high percentage of transcription factors with a changed expression pattern, detected by gene ontology analysis. Pathway analyses at PW8 rather display the consequences of gene disruptions happening at PW4. Pathways like 'cell morphology', 'ophthalmic disease' and 'photo-transduction' are affected, implying substantial alteration in the cell morphology and might already imply a loss of photoreceptors.

This microarray approach emphasizes that major gene expression alterations happen early in the degeneration process (PW4). Accordingly, to further understand cell death mechanisms in cones gene changes and pathway changes should be further examined at the time point of PW4.

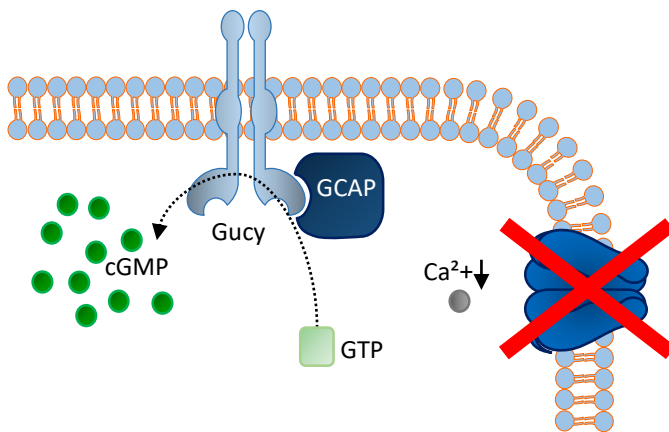


Figure 4.1: cGMP accumulation in cones of *Cnga3* ko mice. Loss of the cyclic nucleotide gated (CNG) cation channel leads to a decline of intracellular calcium levels. Thus Ca^{2+} -free GCAP can activate the cGMP-producing guanylate cyclase (Gucy) and cGMP gets produced continuously.

4.2 cGMP accumulation and cell death

Accumulation of cGMP was shown in *Cnga3* KO mice throughout the degeneration process. Remarkably, cGMP accumulation was already observed before eye opening and persisted as long as the cone cells survived.

The detected cGMP-accumulation was cone specific and probably caused by a low calcium level (Figure 4.1). Due to the loss of the CNG channel, calcium-influx is disrupted and the intracellular calcium level decreases. The guanylate cyclase activating protein (GCAP) is calcium-free and can, thus, directly bind and activate the membrane bound guanylate cyclase E (Gucy-E). Guicy-E gets activated upon binding and continuously produces cGMP regardless of a light stimulus.

By knocking down Guicy-E, the only cGMP-producing enzyme in cones, a clear rescue of cone degeneration was detected. In the regions of shRNA expression in the retina, a higher percentage of cones survived compared to the uninjected control eye. This supports the hypothesis that the balance of the second messenger cGMP has a strong influence on the vitality of cones. A previous paper could already show that a knock-out of the guanylate cyclase has a protective effect on the survival of cones (Xu et al., 2013). The presented results of this study further support the previous published data and further shows that viral interference two weeks after birth is sufficient to prolong cone survival.

Discussion

Deficiency as well as sustained overload of the second messenger has both major consequences for the viability of photoreceptors. According to literature, knocking out the guanylyl cyclase and a loss of GCAPs leads to cone degeneration (Yang et al., 1999, Payne et al., 1998). Overload of cGMP in rods by knocking out the phosphodiesterase (PDE) as seen in the rd1 mouse leads to severe photoreceptor loss (McLaughlin et al., 1993, Drager and Hubel, 1978, Pittler and Baehr, 1991).

Surprisingly, high cGMP concentrations were detected at very early time points, long before eye opening and before the maturation of photoreceptors was fully accomplished. These results imply that Gucy-E, the CNG channel and the other visual cascade proteins are already active in cones around postnatal day four (P4). Most importantly these results show that cGMP accumulation has no influence on cone development and maturation. Apart from the delay of postnatal cone somata migration which has not been linked to cGMP so far, no deficits have been described in the cone development of *Cnga3* KO mice (Michalakis et al., 2005).

Contradictory to this early detection of cGMP, cell death is not detected in *Cnga3* KO mice before week two and has its peak around 30 to 35 days after birth (Michalakis et al., 2005, Arango-Gonzalez et al., 2014). Since cGMP is detected from day four onwards, these results indicate that cGMP accumulation does not induce photoreceptor death before two weeks after birth. At this time point eye opening occurs. Thus cGMP-overload itself does not seem to be toxic for photoreceptors but as soon as light enters the eye and when the visual cascade is functional, cell death seems to set in. Looking closely at the targets regulated by cGMP, it is worth mentioning that in the *Cnga3* KO retina cGKII shows an expression peak at P14 that matches the onset of degeneration. At this age cGKII is even significantly higher expressed in knockout mice compared to wildtype mice. The activation of the vision cascade by light might induce an up-regulation of cGKII due to an unknown cGMP-regulated transcription feed-back mechanism. The expression of cGKI on the other hand is relatively low at P6 and constantly rises until PW4 and shows no expression-difference between knockout and wildtype tissue.

The progression of cell death in the *Cnga3* KO mouse model is surprising compared to other mouse models. While most mouse models have a constantly ascending increase in the number of photoreceptors undergoing cell death, *Cnga3* KO mice have a small number of TUNEL positive cells onward from the week two until 27 days after birth, when a sudden rise in cell death is

observed with a peak between 30-35 days after birth (Arango-Gonzalez et al., 2014). This indicates that a sudden mechanism sets in at about four weeks after birth. This hypothesis is further supported by the high number of genes detected in the microarray at the four week time point. An explanation would be that the high expression level of cGKII at P14 induces a downstream mechanism which first leads to cell death 2 weeks after induction. The expression level of cGKII drops back after the two week time point which would also explain the temporary peak of cell death.

4.3 Role of cGMP-dependent kinases in cone degeneration

In this study, it was shown that high activity of the cGMP-kinase has vital consequences for photoreceptor survival. Conversely, photoreceptor-specific expression of the constitutively active cGK (CAcGK) induced a rapid degeneration and complete loss of the photoreceptor layer of wildtype mice. These results show that an enhanced activity of cGK induces cell death in photoreceptors. Nevertheless, the question remains which of the cGMP-dependent kinases might trigger the cell death signal. In a previous study the activity of cGK was measured in the retina of *Nrl/Cnga3* DKO mice (Xu et al., 2013). *Nrl* KO mice are devoid of the neural retina leucine zipper (*Nrl*) and thus photoreceptor progenitor cells differentiate into S-cones instead of rods during development. This cone-dominant mouse model showed an enhanced activity of cGK. These findings are in line with the hypothesis that in the absence of *CNGA3* increased cGMP levels trigger the activation of cGKs in affected cone photoreceptors.

Evaluation of cone survival in *cGKI/Cnga3* DKO or *cGKII/Cnga3* DKO showed that lack of cGKII but not cGKI can distinctively delay cone cell death. Interestingly, genomic deletion of cGKI alone was not sufficient to rescue cone cell death and rather accelerated the degeneration process. This further emphasizes that cGKI and cGKII clearly have different targets and different functions in the retina. Surprisingly a triple knockout of cGKI, cGKII and *Cnga3* led to a more pronounced rescue of cone degeneration. This might indicate that the downstream signalling of cGKI, *e.g.* in cones, might also trigger a cell death signal. *cGKI/Cnga3* DKO mice might not show a rescue of cone cell death, due to the high expression of cGKI in Müller glia cells. The maintenance of Müller glia is essential for a healthy retina (Reichenbach and Bringmann, 2013, Bringmann et al., 2006). A global loss of cGKI expression might have major consequences for

Müller glia cells or might induce an immune response which might further promote cell death. Accordingly, a cone specific deletion or inhibition of cGKI is needed to clarify whether high activity of cGKI mediates cell death signalling in cones while it is indispensable for other cells like Müller glia. This would further explain why cGKII knockout is not sufficient to fully rescue the degeneration. Account should also be taken of a possible function of cGKII in other cell types of the retina or a role of cGKII during development. All these open questions emphasize the need for a cell-specific manipulation of these kinases.

4.4 Cell death signalling in photoreceptors

The molecular mechanisms leading to cell death in retinal degenerations remain an open question. Several processes have been so far implicated in photoreceptor cell death (Pierce, 2001). Already a continuous activation of the visual transduction cascade leads to a degeneration of photoreceptors. High light exposure activates the transduction cascade and has been shown to lead to photoreceptor death in mice (Fain and Lisman, 1999). Furthermore, mutations in the alpha subunit of PDE or the guanylate cyclase are both causing a chronic activation of transduction and cause photoreceptor degeneration (Dryja et al., 1995, Perrault et al., 1996).

Another important factor for photoreceptor survival are the retinal pigment epithelial (RPE) cells. It is well established that photoreceptor function and survival strongly depends on RPE cells (Marmorstein et al., 1998, Rizzolo, 1997, Bok, 1993) and that a dysfunction of the latter can lead to photoreceptor degeneration (Weng et al., 1999, Redmond et al., 1998). RPE cells are crucial for retinal homeostasis. They are not only important for nutrient supply to photoreceptors but also for recycling of the chromophore needed for phototransduction (Steinberg, 1985, Saari, 2000).

Disruptions in the photoreceptor outer segment morphogenesis have been identified to cause retinal cell death (Hagstrom et al., 1999, Molday, 1998, Hawkins et al., 1985). Unfortunately, the mechanisms are largely unknown but photoreceptors start to die secondary to a dysfunction observed in the morphogenesis of outer segments.

A more recent hypothesis for retinal degeneration is the activation of calpain (Doonan et al., 2003, Paquet-Durand et al., 2006, Donovan and Cotter, 2002, Azuma et al., 2004). High levels

of calcium have been detected in the *rd1* mouse as a result of continuous activation of the CNG channel, by cGMP (Fox et al., 1999). At that time the calcium overload has been hypothesized to trigger apoptotic cell death in rods (Fox et al., 1999). Other studies gave indirect proof that high levels of calcium have toxic effects on photoreceptors, by applying calcium-blockers (Ozaki et al., 2013, Bush et al., 2000). However, more recent studies could show that the high content of calcium triggers non-apoptotic pathways through calpain activation in the *rd1* mouse (Doonan et al., 2003, Paquet-Durand et al., 2006) but also in light-induced retinal degeneration (Donovan and Cotter, 2002).

A unique feature of photoreceptors is their ability to obtain energy from aerobic glycolysis (Winkler 1995). Photoreceptors drain vast amounts of energy to maintain their outer segments (Ames et al., 1992, Demontis et al., 1997). Thus they consume high amounts of oxygen, for their metabolism of glucose, and high amounts of glucose for glycolysis. Their oxygen consumption is three to four times higher compared to other retinal cells and to neuronal cells of the central nervous system (Alder et al., 1990, Braun et al., 1995). It has been shown that photoreceptors are vulnerable to inhibition of glycolysis and display a selective degeneration (Noell, 1951). They are further also susceptible to energy exhaustion and degenerate upon metabolic overload (Travis, 1998, Tsang et al., 1996).

Since the cGMP-directed pathway through cGKII activation does not completely rescue the phenotype, other mechanisms have to be taken into account as a possible explanation for cell death events in Achromatopsia. A continuous activation of the phototransduction cascade as well as a calcium-overload followed by calpain activation can be ruled out due to the lack of CNG channel in *Cnga3* KO mice. RPE cells also seem to be unaffected in Achromatopsia patients and only start to degenerate in the fovea of humans at very late stages secondary to the observed cone loss (Thiadens et al., 2010b, Genead et al., 2011). However disruptions in the outer segments of *Cnga3* KO mice have been described in the literature (Michalakis et al., 2005). The opsins seem to fail to be routed into the cone outer segments of *Cnga3* KO mice. This impairment has already been suggested as a cause for cone loss (Michalakis et al., 2005). However, no mechanism has been found so far to further support this hypothesis.

Another reasonable explanation is metabolic overload. Since cGMP metabolism is a main energy drain, a possible explanation for photoreceptor degeneration in *Cnga3* KO mice could be energy

exhaustion by the intense production of cGMP. Only recently a study could proof that cone survival could be maintained by the stimulation of aerobic glycolysis (Ait-Ali et al., 2015). A factor called rod-derived cone viability factor (RdCVF), an inactive thioredoxin, is secreted by rods and binds in cones the transmembrane protein basigin-1 (BSG1) important for aerobic glycolysis. BSG1 directly binds the glucose transporter (GLUT1) and increases the entry of glucose which further stimulates aerobic glycolysis und leads to cone survival in rd1 mice (Ait-Ali et al., 2015). Since rods are unaffected by a *Cnga3* mutation, RdCVF is not the limiting factor in *Cnga3* KO mice but the study further supports the hypothesis that cones die upon a disruption of glycolysis.

4.5 cGKII signalling

In order to gain a better understanding of the cGK dependent delay of photoreceptor death a phospho-specific mass-spectrometry approach was performed. With the phospho-proteom of the *Cnga3* KO mouse line, potential substrates of cGKII were identified. The data reveal an important role for ataxia telangiectasia and Rad-3-related (Atr) in the *Cnga3* KO mediated degeneration. Two specific Atr-phosphorylation-sites were enriched in *Cnga3* KO and cGKII/*Cnga3* DKO retina lysates compared to wildtype and cGKII/*Cnga3* DKO retina lysates. These phosphorylation sites of Atr have not been reported before. Therefore no antibody was available specifically recognizing these phosphorylation-sites.

Looking at the detected AA sequence, the consensus sequence (R/K(2-3)-X-S/T-X) of cGKII can be recognized at the enriched phosphorylation-site. Thus Atr might be a direct target of cGKII. Atr is a serine-threonine protein kinase and its activation is a hallmark of homologous recombination. Atr is activated upon double strand breaks (DSB) to initiate repair-mechanisms and cell survival (Cliby et al., 1998, Nghiem et al., 2001, Hurley and Bunz, 2007, Wilsker and Bunz, 2007, Nishida et al., 2009). Activation of Atr could be confirmed by γ -H2AX staining. *Cnga3* KO nuclei showed several γ -H2AX-positive nuclei at PW4. The protein level of Atr is not changed in *Cnga3* KO tissue indicating that the phosphorylation either influences the activation state or the localisation of the kinase. Immunohistochemical staining show that γ -H2AX-positive cones also show a signal for Atr in the cell nucleus. This indicates that Atr translocates into the

cell nucleus of *Cnga3* KO cones. This translocation might be caused by cGKII-specific phosphorylation.

Another proteomic approach on cone-nuclear extracts identified Npm1 as a highly enriched protein in cone-nuclei of *Cnga3* KO mice. The role of NPM1 has been mainly investigated in proliferative cells but its function in post-mitotic neurons or retinal cells is largely unknown. An enrichment of Npm1 in cones compared to rods could be shown by immunohistochemistry. Immunohistochemical stainings also indicated a higher level of Npm1 in the ONL of *Cnga3* KO mice compared to wildtype mice. Both Atr and Npm1 are mainly localised nucleolar but can translocate to the nucleoplasm and cytoplasm. Interestingly, Npm1 is a target of Atr and can act

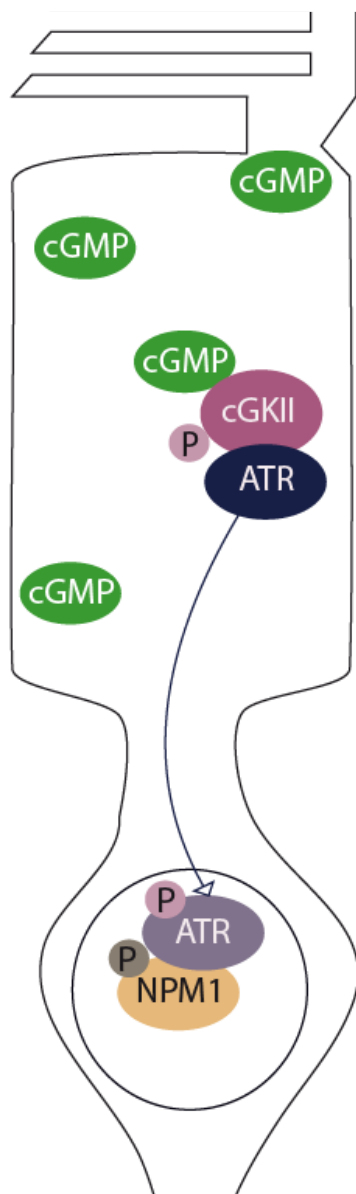


Figure 4.2: Model for possible cGMP-signalling in Achromatopsia. By the accumulation of cGMP in cones cGMP-dependent kinase (cGK) II is activated and phosphorylates ataxia telangiectasia and Rad-3-related (Atr). The phosphorylation enables Atr to translocate into the nucleus. In the nucleus it can then phosphorylate Nucleophosmin (Npm1) a protein mainly localized in the nucleus and an important player involved in survival and cell-death mechanisms.

towards cell survival and cell death (Pfister and D'Mello, 2015). It can act pro-survival through PI3-K/Akt and MAPK/ERK signaling pathways (Ahn et al., 2005, Pfister and D'Mello, 2015). Furthermore, it can act protective against apoptotic events by either inhibiting p53 activation (Dhar and St Clair, 2009, Li et al., 1998a) or by preventing caspase-3-cleavage (Haindl et al., 2008, Liu et al., 2007). Nevertheless Npm1 can also act apoptotic through Bax protein, a co-factor of p53 (Dhar and St Clair, 2009, Geng et al., 2010, Li et al., 1998a). Thus Npm1 seems to set a threshold of induction of cell death events.

Our hypothesis is that cGKII gets activated by the elevated cGMP level and phosphorylates the kinase Atr. Activated Atr in turn translocates into the nucleus of cones and phosphorylates Npm1 and other targets. Npm1 might first activate cell survival mechanisms, but eventually triggers cell death due to a continuous activation (Pfister and D'Mello, 2015).

4.6 Therapeutic applications

The findings of this study unravel an important function of cGMP signalling in cone degeneration in the *Cnga3* KO mouse model of Achromatopsia (Michalakis et al., 2013, Xu et al., 2013). The main focus of this study was to decrease the cell death signalling leading to cone loss in Achromatopsia; in particular, for enlarging the window of opportunity for gene-based therapies and for providing additional neuroprotection in support of gene therapies. Treatment with cGKII shRNAs significantly slows down the degeneration mechanism. Thus the time window for treatment can be extended and cell death can be decreased during therapy.

Further the data of this thesis might also help treating patients suffering from cone degeneration due to mutation not directly associated with the visual transduction cascade, e.g. in the recently discovered novel Achromatopsia gene *ATF6* (Kohl 2015).

A dysregulation of the cGMP production has already been identified as a trigger for rod degeneration and cell death in *rd1* mice (Paquet-Durand et al., 2011, Paquet-Durand et al., 2009). The *rd1* mutation renders the PDE non-functional leading to cGMP overload due to the inability of the rod photoreceptor to cleave and metabolize this second messenger. However, due to elevated Ca^{2+} level, the current hypothesis for rod cell death in *rd1* mice is activation of calpain (Paquet-Durand et al., 2011). However, in RP patients non-affected cones also degenerate secondary to rods. Thus in RP patients a cGK-inhibition might rescue the degeneration of cones which might be caused by an increase of cGMP and the effects of cGKII activation in cones since cGKII is hardly expressed in rods.

5 Conclusion and Outlook

It has previously been suggested that cGMP might contribute to the degeneration process in retinal degeneration (Farber and Lolley, 1974). More recent studies also suggested an important function of cGMP-signalling in cell death mechanisms of cones (Michalakis et al., 2013, Xu et al., 2013) but until today the importance of cGMP homeostasis in cone viability has not been understood. The data of this thesis helps clarifying this issue. It has been shown that the onset of cone degeneration is indeed influenced by cGMP and its downstream signalling. The proper control of the cellular levels of this crucial second messenger seems to be vital for the survival of cones (Figure 3.2).

The main effector of cGMP signalling leading to cell death in cone degeneration appears to be the cGMP-dependent kinase II. Loss of cGKII signalling by knockout or knockdown of the kinase could significantly delay cone photoreceptor degeneration in *Cnga3* KO mice. Since therapeutic fine-tuning of cGMP-levels is rather difficult, cGKII might be a novel target for neuroprotection in cone degeneration. However, loss of cGKII was not able to fully rescue the cone cell death suggesting that additional mechanisms might contribute to cone degeneration. One explanation for this phenomenon could be that cGKI also triggers cell death through an unknown mechanism, and that both kinases must be targeted in a cell type-specific manner to fully rescue the degeneration process. cGMP-cGK signalling might have additional important functions in the retina and a global loss of the kinases might trigger a negative feedback. Thus a cell-specific knockout or knock-down would be advantageous. Other mechanisms possibly contributing to cell death are impaired opsin-targeting or metabolic overload caused by the intense cGMP production.

Finally potential downstream targets of the cGKII were identified and cell death of cones might be triggered in *Cnga3* KO mice by Npm1 through the serine/threonine kinase Atr.

6 Summary

Achromatopsia (ACHM) is a currently untreatable inherited eye disease that severely impairs daylight vision. The clinical manifestation results from cone photoreceptor dysfunction and is characterized by poor visual acuity, lack of colour discrimination and photophobia. In addition, a progressive degeneration and loss of macular cone photoreceptors is observed. In total six disease genes are known, but the majority of patients carries mutations in *CNGA3* (29% of cases) or *CNGB3* (48% of cases); the two genes encoding the cone cyclic nucleotide-gated (CNG) channel. This ion channel is directly gated by the second messenger cyclic GMP (cGMP) and is an integral part of the so called phototransduction cascade that translates light signals into electrical stimuli. Interestingly, genetic deletion of the CNG channel subunit CNGA3 in mice leads to high cellular levels of cGMP in affected cone photoreceptors. The aim of this thesis was to characterize the role of impaired cGMP signalling during cone photoreceptor degeneration in the *Cnga3* knockout (KO) mouse model for ACHM.

First, the developmental time course of cGMP accumulation was investigated using a cGMP-specific antibody. One point worthy of note is that elevated cGMP levels could be observed as early as four days after birth. Using a virus-mediated *in vivo* gene knockdown (KD) approach it was possible to identify guanylate cyclase 2E (*Gucy2e*) as the main source of cGMP. Moreover, *Gucy2e* KD resulted in prolonged survival of cones in *Cnga3* KO mice suggesting a toxic role of sustained cGMP overload in affected photoreceptors. Given the absence of CNG channels in *Cnga3* KO cones this toxic effect has to be mediated by other cGMP targets. Promising candidates that were further investigated were the cGMP-dependent kinases (cGKs). To investigate the impact of elevated cGK signalling for photoreceptor viability a constitutively active cGK was overexpressed in wildtype mouse photoreceptors using viral vectors. This induced a dramatic decrease of the photoreceptor layer and demonstrated that these kinases can induce cell death. To verify this and to define the effect of the two kinase types, *Cnga3* KO mice were cross-bred with cGKI and cGKII KO mice and further examined morphologically. Global loss of cGKII but not cGKI significantly protected cone photoreceptors resulting in lower levels of degeneration and cell death. This finding was confirmed using viral vector-mediated delivery of a cGKII specific shRNA into cone photoreceptors of *Cnga3* KO mice. Expression of cGKII-

shRNA in adult *Cnga3* KO mice again showed a decrease of degeneration suggesting cGKII as a novel target for neuroprotection in cone degeneration.

Finally, to further unravel the cGMP signalling triggering cell death in cones two proteomic approaches were performed to identify potential downstream targets of cGKII. These screens could identify a link between a cGMP-cGK-signalling pathway and the serine/threonine kinase Atr.

In conclusion this thesis presents strong evidence that cGMP-signalling accelerates retinal degeneration and identifies cGMP/cGKII signalling as a novel target for neuroprotective therapies to prolong cone survival in ACHM and other cone degenerations.

7 Zusammenfassung

Achromatopsie (ACHM) ist eine bis heute nicht heilbare erblich bedingte Augenkrankheit, die das Sehvermögen bei Tageslicht erheblich beeinträchtigt. Die Symptome entstehen durch eine Dysfunktion der Zapfen und sind geprägt von einem vollständigen Ausfall des Farbsinns, einer geringen Sehschärfe und einer extremen Blendungsempfindlichkeit der Betroffenen. Außerdem ist eine schnell fortschreitende Degeneration der Zapfen in der Makula zu beobachten. Mutationen in sechs Genen werden mit ACHM assoziiert, die meisten Patienten tragen jedoch eine Mutation in den Genen, die den in den Zapfen exprimierten zyklisch-Nukleotid gesteuerten (CNG) Kanal kodieren: *CNGA3* (29 % der Fälle) und *CNGB3* (48 % der Fälle). Dieser Ionenkanal wird durch Bindung des zellulären Botenstoffes - dem zyklischen GMP (cGMP) - geöffnet und ist zudem ein wichtiger Bestandteil der „Sehkaskade“ (sog. Phototransduktionskaskade), die Lichtsignale in elektrische Impulse umwandelt. Interessanterweise führt eine genetische Deletion der Untereinheit CNGA3 bei Mäusen zu einem erhöhten zellulären Level von cGMP in betroffenen Zapfen. Ziel dieser Arbeit war es, die Rolle der beeinträchtigten cGMP-Signalwege während der Zapfendegeneration des *Cnga3* Knockout (KO) Mausmodelles zu charakterisieren.

Zunächst wurde der entwicklungspezifische Verlauf der cGMP Akkumulation untersucht. Überraschenderweise war bereits vier Tage nach der Geburt ein erhöhtes cGMP Level festzustellen. Mit Hilfe eines Virus-vermittelten Gen-Knockdowns (KD) war es möglich die Guanylatzyklase 2E (Gucy2E) als die Hauptquelle des cGMP in Zapfen zu identifizieren. Therapierte Augen zeigten eine erhöhte Zapfendichte, was darauf hinweist, dass eine cGMP-Überlastung toxische Auswirkungen auf die betroffenen Zapfen hat. Ohne den CNG-Kanal in *Cnga3* KO Zapfen kann die toxische Wirkung nur durch andere cGMP-Targets herbeigeführt werden. Vielversprechend für weitere Experimente erschienen dabei die cGMP-abhängigen Kinasen (cGKs), die weiter untersucht wurden. Um die Auswirkungen von erhöhten cGK-Signalwegen zu untersuchen, wurde in Wildtypmäusen durch virale Vektoren eine konstitutiv aktive cGK überexprimiert. Dies hatte einen drastischen Verlust der Photorezeptorschicht zur Folge und zeigte, dass diese Kinasen Zelltod auslösen können. Um dies zu verifizieren wurden *Cnga3* KO Mäuse mit cGKI und cGKII KO Mäusen gekreuzt und morphologisch untersucht. Ein globaler Verlust der cGKII nicht aber der cGKI schützte die Zapfen vor Zelltod und führte

zu einer signifikant verminderten Degeneration. Dieses Ergebnis wurde durch die Applikation einer cGKII-shRNA in *Cnga3* KO Mäusen bestätigt, die ebenfalls einen signifikanten Rückgang des Zellsterbens zeigte. Diese Anwendung zeigt, dass cGKII ein möglicher neuer Anknüpfungspunkt für neuroprotektive Mechanismen in Zapfendegenerationen sein kann.

Um letztendlich den cGMP Signalweg, der zum Zelltod führt, besser verstehen zu können, wurden mögliche Targets der cGKII durch zwei Massenspektrometrie-Ansätze identifiziert. Die Ergebnisse dieser Experimente weisen auf einen Zusammenhang zwischen dem cGMP-cGK-Signalweg und der Serin/threonine Kinase Atr hin.

Zusammenfassend liefert diese Arbeit aussagekräftige Nachweise, dass cGMP-Signalwege die retinale Degeneration beschleunigen und identifiziert einen cGMP-cGK Signalweg als neuen Anknüpfungspunkt für neuroprotektive Therapien um die Lebensdauer der Zapfen in ACHM und anderen Zapfendegenerationen zu verlängern.

8 Appendix

8.1 Sequences

SEQ pAAV2.1-ss-Rho-cGKI-2A-GFP: 6692 bp;

Vector from pAAV2.1-Rho-WPRE-MCS 4345bp AgeI+SacII

Insert from pAAV2.1-ss-SWS-cGKI-GFP 2347bp; AgeI+SacII

Insert position from 1306

Composition 1620 A; 1776 C; 1701 G; 1595 T; 0 OTHER

Percentage: 24.2% A; 26.5% C; 25.4% G; 23.8% T; 0.0%OTHER

Molecular Weight (kDa): ssDNA: 2064.83 dsDNA: 4125.75

KEYWORD CIRCULAR

ORIGIN

```

1      AGCGCCCAAT  ACGCAAACCG  CCTCTCCCCG  CGCGTTGGCC  GATTCATTAA  TGCAGCTGGC
61     ACGACAGGTT  TCCCAGACTGG  AAAGCGGGCA  GTGAGCGCAA  CGCAATTAAT  GTGAGTTAGC
121    TCACTCATTAA  GGCACCCCAG  GCTTTACTACT  TTATGCTTCC  GGCTCGTATG  TTGTGTGGAA
181    TTGTGAGCGG  ATAACAATTT  CACACAGGAA  ACAGCTATGA  CCATGATTAC  GCCAGATTTA
241    ATTAAGGCTG  CGCGCTCGCT  CGCTCACTGA  GGCCGCCCCG  GCAAAGCCCC  GGCGTCGGGC
301    GACCTTTGGT  CGCCCGGCCT  CAGTGAGCGA  GCGAGCGCGC  AGAGAGGGAG  TGGCCAACTC
361    CATCACTAGG  GGTTCCTTGT  AGTTAATGAT  TAACCCGCCA  TGCTACTTAT  CTACGTAGCC
421    ATGCTCTAGG  AAGATCGGAA  TTCGCCCTTA  AGCTAGCAGA  TCTTCCCCAC  CTAGCCACCT
481    GGCAAAGTGC  TCCTTCTCTC  AAAGGCCCAA  ACATGGCCTC  CCAGACTGCA  ACCCCCAGGC
541    AGTCAGGCC  TGTCTCCACA  ACCTCACAGC  CACCCTGGAC  GGAATCTGCT  TCTTCCACA
601    TTTGAGTCCT  CCTCAGCCCC  TGAGCTCCTC  TGGGCAGGGC  TGTTTCTTTC  CATCTTTGTA
661    TTCCCAGGGG  CCTGCAAATA  AATGTTTAAT  GAACGAACAA  GAGAGTGAAT  TCCAATTCCA
721    TGCAACAAGG  ATTGGGCTCC  TGGGCCCTAG  GCTATGTGTC  TGGCACCAGA  AACGGAAGCT
781    GCAGGTTGCA  GCCCCTGCCC  TCATGGAGCT  CCTCCTGTCA  GAGGAGTGTG  GGGACTGGAT
841    GACTCCAGAG  GTAACCTGTG  GGGGAACGAA  CAGGTAAGGG  GCTGTGTGAC  GAGATGAGAG
901    ACTGGGAGAA  TAAACCAGAA  AGTCTCTAGC  TGTCCAGAGG  ACATAGCACA  GAGGCCCATG
961    GTCCCTATTT  CAAACCCAGG  CCACCAGACT  GAGCTGGGAC  CTTGGGACAG  ACAAGTCATG
1021   CAGAAGTTAG  GGGACCTTCT  CCTCCCTTTT  CCTGGATGGA  TCCTGAGTAC  CTCTCCTCC
1081   CTGACCTCAG  GCTTCCTCCT  AGTGTACCT  TGGCCCCTCT  TAGAAGCCAA  TTAGGCCCTC
1141   AGTTTCTGCA  GCGGGGATTA  ATATGATTAT  GAACACCCCC  AATCTCCCAG  ATGCTGATTC
1201   AGCCAGGAGC  TTAGGAGGGG  GAGGTCACCT  TATAAGGGTC  TGGGGGGGTC  AGAACCCAGA
1261   GTCATCCCCT  GAATTCTGCA  GATATCCATC  AACTGGCCGG  CCGCACCGGT  CGACTAGAGG
1321   ATCCACCATG  GCATATGAAG  ATGCAGAAGC  TAAGGCAAAA  TATGAAGCTG  AAGCTGCTTT
1381   CTTCGCCAAC  CTGAAGCTGT  CTGATTTCAA  CATCATTGAC  ACCCTTGGAG  TTGGAGGTTT
1441   CGGACGCGTA  GAACTGGTCC  AGTTAAAAAG  TGAAGAATCC  AAAACCTTTG  CAATGAAGAT
1501   TCTCAAGAAA  CGCCACATCG  TGGATACAAG  ACAGCAGGAA  CACATCCGCT  CGGAGAAGCA
1561   GATCATGCAG  GGGGCCCAT  CGGACTTCAT  AGTGAGATTA  TACAGAACAT  TTAAGGACAG
1621   CAAATATTTG  TATATGTTGA  TGGAAAGCTG  CCTAGGTGGA  GAGCTCTGGA  CCATTCTCAG
1681   GGATCGGGGG  TCATTTGAAG  ATTCTACAAC  CAGATTTTAT  ACAGCATGTG  TGGTAGAAGC
1741   TTTTGCCTAT  CTGCATTCCA  AAGGAATCAT  TTACAGGGAC  CTCAAGCCTG  AAAATCTCAT
1801   CCTAGATCAC  CGAGGTTATG  CCAAAGTGGT  TGATTTTGGC  TTTGCAAAGA  AAATAGGATT
1861   TGGAAAGAAA  ACATGGACTT  TTTGTGGGAC  TCCAGAATAT  GTAGCCCCAG  AGATCATCCT
1921   GAACAAAGGC  CATGACATTT  CAGCCGACTA  TTGGTCACTG  GGAATCCTCA  TGTATGAGCT
1981   TCTGACTGGC  AGCCACCTT  TCTCAGGCC  AGATCCTATG  AAAACCTATA  ACATCATATT
2041   GAGGGGGATT  GACATGATAG  AGTTTCCAAA  GAAGATTGCC  AAAAATGCTG  CTAATTTAAT
2101   TAAAAACTA  TGCAGGGATA  ATCCATCAGA  AAGATTAGGG  AATTTGAAAA  ACGGAGTGAA
2161   AGACATTCAA  AAGCACAAAT  GGTTTGAGGG  CTTTAATTGG  GAAGGCTTAA  GAAAAGGCAC
2221   CTTGACACCT  CCTATAATAC  CAAGTGTGTC  ATCACCCACA  GACACAAGCA  ATTTTGACAG
2281   TTTCCCTGAG  GACAATGACG  AACCGCCACC  TGATGACAAC  TCAGGATGGG  ACATAGACTT
2341   CGGTACCGGA  GCCACGAACT  TCTCTCTGTT  AAAGCAAGCA  GGAGACGTGG  AAGAAAACCC
2401   CGGTCCCTACT  AGTATGGTGA  GCAAGGGCGA  GGAGCTGTTC  ACCGGGGTGG  TGCCCATCCT
2461   GGTCGAGCTG  GACGGCGACG  TAAACGGCCA  CAAGTTCAGC  GTGTCCGGCG  AGGGCGAGGG
2521   CGATGCCACC  TACGGCAAGC  TGACCCTGAA  GTTCATCTGC  ACCACCGGCA  AGCTGCCCGT

```

2581 GCCCTGGCCC ACCCTCGTGA CCACCCTGAC CTACGGCGTG CAGTGCTTCA GCCGCTACCC
 2641 CGACCACATG AAGCAGCACG ACTTCTTCAA GTCCGCCATG CCCGAAGGCT ACGTCCAGGA
 2701 GCGCACCATC TTCTTCAAGG ACGACGGCAA CTACAAGACC CGCGCCGAGG TGAAGTTCGA
 2761 GGGCGACACC CTGGTGAACC GCATCGAGCT GAAGGGCATC GACTTCAAGG AGGACGGCAA
 2821 CATCCTGGGG CACAAGCTGG AGTACAATA CAACAGCCAC AACGTCTATA TCATGGCCGA
 2881 CAAGCAGAAG AACGGCATCA AGGTGAACTT CAAGATCCGC CACAACATCG AGGACGGCAG
 2941 CGTGCAGCTC GCCGACCACT ACCAGCAGAA CACCCCATC GGCACGGCC CCGTGCTGCT
 3001 GCCCGACAAC CACTACCTGA GCACCCAGTC CGCCCTGAGC AAAGACCCCA ACGAGAAGCG
 3061 CGATCACATG GTCCTGCTGG AGTTCGTGAC TCAACCTCTG CCGCCCGGG ATCACTCTCG GCATGGACGA
 3121 GCTGTACAAG TAAAGCGGCC GCGTCGACAA TCAACCTCTG GATTACAAA TTTGTGAAAG
 3181 ATTGACTGGT ATTCTTAACT ATGTTGCTCC TTTTACGCTA TGTGGATACG CTGCTTAAAT
 3241 GCCTTTGTAT CATGCTATTG CTTCCCGTAT GGCTTTTCATT TTCTCCTCCT TGTATAAATC
 3301 CTGGTTGCTG TCTCTTTATG AGGAGTTGTG GCCCGTTGTC AGGCAACGTG GCGTGGTGTG
 3361 CACTGTGTTT GCTGACGCAA CCCCCACTGG TTGGGGCATT GCCACCACCT GTCAGCTCCT
 3421 TTCCGGGACT TTCGCTTTCC CCCTCCCTAT TGCCACGGCG GAACTCATCG CCGCCTGCCT
 3481 TGCCCGCTGC TGGACAGGGG CTCGGCTGTT GGGCACTGAC AATTCCGTGG TGTGTGCGGG
 3541 GAAGCTGACG TCCTTTCCAT GGCTGCTCGC CTGTGTTGCC ACCTGGATTG TCGCGGGAC
 3601 GTCCTTCTGC TACGTCCCTT CGGCCCTCAA TCCAGCGGAC CTTCTTCCC GCGCCTGCT
 3661 GCCGGCTCTG CGGCCTCTTC CGCGTCTTCG AGATCTGCCT CGACTGTGCC TTCTAGTTGC
 3721 CAGCCATCTG TTGTTTGCCC CTCCCCCGTG CCTTCTTGA CCCTGGAAGG TGCCACTCCC
 3781 ACTGTCCTTT CCTAATAAAA TGAGGAAATT GCATCGCATT GTCTGAGTAG GTGTCATTCT
 3841 ATTCTGGGGG GTGGGGTGGG GCAGGACAGC AAGGGGGAGG ATTGGGAAGA CAATAGCAGG
 3901 CATGCTGGGG ACTCGAGTTA AGGGCGAATT CCCGATTAGG ATCTTCTTAG AGCATGGCTA
 3961 CGTAGATAAG TAGCATGGCG GGTTAATCAT TAACTACAAG GAACCCCTAG TGATGGAGTT
 4021 GGCCACTCCC TCTCTGCGCG CTCGCTCGCT CACTGAGGCC GGGCGACCA AGGTCGCCCG
 4081 ACGCCCGGGC TTTGCCCGGG CGGCCCTCAGT GAGCGAGCGA GCGCGAGCC TTAATTAACC
 4141 TAATTCCTG GCCGTCGTTT TACAACGTCG TGACTGGGAA AACCCGTGCG TTAACCAACT
 4201 TAATCGCCTT GCAGCACATC CCCCTTTCGC CAGCTGGCGT AATAGCGAAG AGGCCCGCAC
 4261 CGATCGCCCT TCCCAACAGT TGCGCAGCCT GAATGGCGAA TGGGACGCGC CCTGTAGCGG
 4321 CGCATTAAAG GCGGCGGGTG TGGTGGTTAC GCGCAGCGTG ACCGCTACAC TTGCCAGCGC
 4381 CCTAGCGCCC GCTCCTTTTC CTTTCTTCCC TTCCTTTCTC GCCACGTTTC CCGGCTTTCC
 4441 CCGTCAAGCT CTAAATCGGG GGCTCCCTTT AGGGTTCCGA TTTAGTGCTT TACGGCACCT
 4501 CGACCCCAA AAACCTTGATT AGGGTGATGG TTCACGTAGT GGGCCATCGC CCCGATAGAC
 4561 GGTTTTTCGC CCTTTGACGC TGGAGTTCAC GTTCTCAAT AGTGGACTCT TGTTCAAAC
 4621 TGGAACAACA CTCAACCCTA TCTCGGTCTA TTCCTTTGAT TTATAAGGA TTTTCCGAT
 4681 TTCGGCCTAT TGGTTAAAA ATGAGCTGAT TTAACAAAA TTTAACGCGA ATTTTAACAA
 4741 AATATTAACG TTTATAATTT CAGGTGGCAT CTTTCGGGGA AATGTGCGCG GAACCCCTAT
 4801 TTGTTTATTT TTCTAAATAC ATTCAAATAT GTATCCGCTC ATGAGACAAT AACCCGTGATA
 4861 AATGCTTCAA TAATATTGAA AAAGGAAGAG TATGAGTATT CAACATTTCC GTGTCGCCCT
 4921 TATTCCCTTT TTTGCGGCAT TTTGCCTTCC TGTTTTTGCT CACCCAGAAA CGCTGGTGAA
 4981 AGTAAAAGAT GCTGAAGATC AGTTGGGTGC ACGAGTGGGT TACATCGAAC TGGATCTCAA
 5041 TAGTGGTAAG ATCCTTGAGA GTTTTCGCCC CGAAGAACGT TTTCCAATGA TGAGCACTTT
 5101 TAAAGTTCTG CTATGTGGCG CGGTATTATC CCGTATTGAC GCCGGGCAAG AGCAACTCGG
 5161 TCCGCGCATA CACTATTCTC AGAATTACTT GGTGAGTAC TCACCAGTCA CAGAAAAGCA
 5221 TCTTACGGAT GGCATGACAG TAAGAGAATT ATGCAGTGCT GCCATAACCA TGAGTGATAA
 5281 CACTGCGGCC AACTTACTTC TGACAACGAT CGGAGGACCG AAGGAGCTAA CCGCTTTTTT
 5341 GCACAACATG GGGGATCATG TAACTCGCCT TGATCGTTGG GAACCGGAGC TGAATGAAGC
 5401 CATAACAAAC GACGAGCGTG ACACCACGAT GCCTGTAGTA ATGGTAACAA CGTTGCGCAA
 5461 ACTATTAAC TGGCGAACTAC TTACTCTAGC TTCCCGCAA CAATTAATAG ACTGGATGGA
 5521 GGCGGATAAA GTTGACAGG CACTTCTGCG CTCGGCCCTT CCGGCTGGCT GGTTTATTGC
 5581 TGATAAATCT GGAGCCGGTG AGCGTGGGTC TCGCGGTATC ATTGCAGCAC TGGGGCCAGA
 5641 TGGTAAGCCC TCCCGTATCG TAGTTATCTA CACGACGGGG AGTCAGGCAA CTATGGATGA
 5701 ACGAAATAGA CAGATCGCTG AGATAGGTGC CTCACTGATT AAGCATTGGT AACTGTCAGA
 5761 CCAAGTTTAC TCATATATAC TTTAGATTGA TTTAAAACCT CATTTTAAAT TTAAGAGGAT
 5821 CTAGGTGAAG ATCCTTTTTG ATAATCTCAT GACCAAAAAT CCTTAACGTG AGTTTTCGTT
 5881 CCACTGAGCG TCAGACCCCG TAGAAAAGAT CAAAGGATCT TCTTGAGATC CTTTTTTTCT
 5941 GCGCGTAATC TGCTGCTTGC AAACAAAAAA ACCACCGCTA CCAGCGGTGG TTTGTTTGCC
 6001 GGATCAAGAG CTACCAACTC TTTTCCGAA GGTAACGGC TTCAGCAGAG CGCAGATACC
 6061 AAATACTGTC CTTCTAGTGT AGCCGTAGTT AGGCCACCAC TTCAAGAACT CTGTAGCACC
 6121 GCCTACATC CTCGCTCTGC TAATCCTGTT ACCAGTGGCT GCTGCCAGTG GCGATAAGTC
 6181 GTGTCTTACC GGGTTGGACT CAAGACGATA GTTACCAGGAT AAGGCGCAGC GGTGCGGCTG
 6241 AACGGGGGGT TCGTGCACAC AGCCAGCTT GGAGCGAACG ACCTACACCG AACTGAGATA
 6301 CCTACAGCGT GAGCTATGAG AAAGCGCCAC GCTTCCCGAA GGGAGAAAGG CGGACAGGTA

Appendix

```
6361 TCCGGTAAGC GGCAGGGTTCG GAACAGGAGA GCGCACGAGG GAGCTTCCAG GGGGAAACGC
6421 CTGGTATCTT TATAGTCCTG TCGGGTTTCG CCACCTCTGA CTTGAGCGTC GATTTTGTG
6481 ATGCTCGTCA GGGGGGCGGA GCCTATGGAA AAACGCCAGC AACCGGCCCT TTTTACGGTT
6541 CCTGGCCTTT TGCTGCGGTT TTGCTCACAT GTTCTTTTCT GCGTTATCCC CTGATTCTGT
6601 GGATAACCGT ATTACCGCCT TTGAGTGAGC TGATAACCGCT CGCCGCAGCC GAACGACCGA
6661 GCGCAGCGAG TCAGTGAGCG AGGAAGCGGA AG
```

SEQ pSub-U6-LoxP-sh Gucy-PGK-mcherry-WPRE: 6501 bp; Plasmid Construction:
Composition 1575 A; 1700 C; 1715 G; 1511 T; 0 OTHER
Percentage: 24.2% A; 26.1% C; 26.4% G; 23.2% T; 0.0% OTHER
Molecular Weight (kDa): ssDNA: 2007.85 dsDNA: 4008.03
KEYWORD CIRCULAR

ORIGIN

```
1 CAGCTGCGCG CTCGCTCGCT CACTGAGGCC GCCCGGGCAA AGCCCGGGCG TCGGGCGACC
61 TTTGGTCGCC CGGCCTCAGT GAGCGAGCGA GCGCGCAGAG AGGGAGTGGC CAACTCCATC
121 ACTAGGGGTT CTTGTAGTAT AATGATTAAC CCGCCATGCT ACTTATCTAC GTAGCCATGC
181 TCTAGGAAGA TCGGAATTCG CCCTTAAGCT AGCTTAATTA AATCCGACGC CGCCATCTCT
241 AGGCCCCGCG CGGCCCCCTC GCACAGACTT GTGGGAGAAG CTCGGCTACT CCCCTGCCCC
301 GGTTAATTTG CATATAATAT TTCCTAGTAA CTATAGAGGC TTAATGTGCG ATAAAAGACA
361 GATAATCTGT TCTTTTTAAT ACTAGCTACA TTTTACATGA TAGGCTTGGA TTTCTATAAG
421 AGATACAAAT ACTAAATTAT TATTTTAAAA AACAGCACAA AAGGAAACTC ACCCTAACTG
481 TAAAGTAATT GTGTGTTTTG AGACTATAAA TATCCCTTGG AGAAAAGCCT TGTATCGGT
541 ACCATAACTT CGTATAGCAT ACATTATACG AAGTTATGAG CTCCGGTGCC CATGATGTCT
601 ATAATCAAGA GTTATAGACA TCATGGGCAC CGTTTTTGAT ATCGAATTC CACGGGGTTG
661 GGGTTGCGCC TTTTCCAAGG CAGCCCTGGG TTTGCGCAGG GACGCGGCTG CTCTGGGCGT
721 GGTTCGGGA AACGCAGCGG CGCCGACCCT GGGTCTCGCA CATTCTTCAC GTCCGTTTCG
781 AGCGTCACCC GGATCTTCGC CGCTACCCTT GTGGGCCCCC CGGCGACGCT TCCTGCTCCG
841 CCCCTAAGTC GGAAGGTTTC CTTGCGGTTTC GCGGCGTGCC GGACGTGACA AACGGAAGCC
901 GCACGTCTCA CTAGTACCCT CGCAGACGGA CAGCGCCAGG GAGCAATGGC AGCGCGCCGA
961 CCGCGATGGG CTGTGGCCAA TAGCGGCTGC TCAGCGGGG GCGCCGAGAG CAGCGGCCCG
1021 GAAGGGGCGG TCGGGGAGGC GGGGTGTGGG GCGGTAGTGT GGGCCCTGTT CCTGCCCGCG
1081 CGGTGTTCGG CATTCTGCAA GCCTCCGGAG CGCACGTCGG CAGTCGGCTC CCTCGTTGAC
1141 CGAATCACCG ACCTCTCTCC CCAGGGGGAT CCACCGGTAT GGTGAGCAAG GCGGAGGAG
1201 ATAACATGGC CATCATCAAG GAGTTCATGC GCTTCAAGGT GCACATGGAG GGCTCCGTGA
1261 ACGGCCACGA GTTCGAGATC GAGGGCGAGG GCGAGGGCCG CCCCTACGAG GGCACCCAGA
1321 CCGCCAAGCT GAAGGTGACC AAGGGTGGCC CCCTGCCCTT CGCCTGGGAC ATCCTGTCCC
1381 CTCAGTTCAT GTACGGCTCC AAGGCCTACG TGAAGCACCC CGCCGACATC CCCGACTACT
1441 TGAAGCTGTC CTTCCCCGAG GGCTTCAAGT GGGAGCGCGT GATGAACTTC GAGGACGGCG
1501 GCGTGGTGAC CGTGACCCAG GACTCCTCCC TGCAGGACGG CGAGTTCATC TACAAGGTGA
1561 AGCTGCGCGG CACCAACTTC CCCTCCGACG GCCCCGTAAT GCAGAAGAAG ACCATGGGCT
1621 GGGAGGCCTC CTCCGAGCGG ATGTACCCCG AGGACGGCGC CCTGAAGGGC GAGATCAAGC
1681 AGAGGTGAA GCTGAAGGAC GGCGCCACT ACGACGCTGA GGTCAAGACC ACCTACAAGG
1741 CCAAGAAGCC CGTGCAGCTG CCCGGCCCTT ACAACGTCAA CATCAAGTTG GACATCACCT
1801 CCCACAACGA GGACTACACC ATCGTGGAAC AGTACGAACG CGCCGAGGGC CGCCACTCCA
1861 CCGGCGGCAT GGACGAGCTG TACAAGTAAG TTTAAACGTC GACAATCAAC CTCTGGATTA
1921 CAAAATTTGT GAAAGATTGA CTGGTATTCT TAACTATGTT GCTCCTTTTA CGCTATGTGG
1981 ATACGCTGCT TTAATGCCTT TGTATCATGC TATTGCTTCC CGTATGGCTT TCATTTTCTC
2041 CTCCTTGTAT AAATCCTGGT TGCTGTCTCT TTATGAGGAG TTGTGGCCCG TTGTCAGGCA
2101 ACGTGGCGTG GTGTGCACTG TGTTTGTCTG CGCAACCCCC ACTGGTTGGG GCATTGCCAC
2161 CACCTGTCAG CTCCTTTCCG GGACTTTCGC TTTCCCCCTC CCTATTGCCA CGGCGAACT
2221 CATCGCCGCC TGCCTTGCCC GCTGCTGGAC AGGGGCTCGG CTGTTGGGCA CTGACAATTC
2281 CGTGGTGTG TCGGGGAAGC TGACGTCCCT TCCATGGCTG CTCGCCTGTG TTGCCACCTG
2341 GATTCTGCGC GGGACGTCC TCTGCTACGT CCCTTCGGCC CTCAATCCAG CGGACCTTCC
2401 TTCCC GCGGC CTGCTGCCGG CTCTGCGGCC TCTTCCGCGT CTTGAGATC TGCTCGACT
2461 GTGCCTTCTA GTTGCCAGCC ATCTGTTGTT TGCCCTCCC CCGTGCCTTC CTTGACCTG
2521 GAAGGTGCCA CTCCCCTGT CTTTCTCTAA TAAAATGAGG AAATTCATC GCATTGTCTG
2581 AGTAGGTGTC ATTCTATTCT GGGGGGTGGG GTGGGGCAGG ACAGCAAGGG GGAGGATTGG
2641 GAAGACAATA GCAGGCATGC TGGGGACTCG AGTTAAGGGC GAATTCCTCGA TTAGGATCTT
2701 CCTAGAGCAT GGCTACGTAG ATAAGTAGCA TGGCGGGTTA ATCATTAAC ACAAGGAACC
```

2761 CCTAGTGATG GAGTTGGCCA CTCCCTCTCT GCGCGCTCGC TCGCTCACTG AGGCCGGGCG
 2821 ACCAAAGGTC GCCCGACGCC CGGGCTTTGC CCGGGCGGCC TCAGTGAGCG AGCGAGCGCG
 2881 CAGCTGGGCC TCAGTGAGCG AGCGAGCGCG CAGCTGCATT AATGAATCGG CCAACGCGCG
 2941 GGGAGAGGCG GTTTGCCTAT TGGGCGCTCT TCCGCTTCCT CGCTCACTGA CTCGCTGCGC
 3001 TCGGTCGTTT GGCTGCGGCG AGCGGTATCA GCTCACTCAA AGGCGGTAAT ACGGTTATCC
 3061 ACAGAATCAG GGGATAACGC AGGAAAGAAC ATGTGAGCAA AAGGCCAGCA AAAGGCCAGG
 3121 AACCGTAAAA AGGCCGCGTT GCTGGCGTTT TTCCATAGGC TCCGCCCCCC TGACGAGCAT
 3181 CACAAAAATC GACGCTCAAG TCAGAGGTGG CGAAACCCGA CAGGACTATA AAGATACCAG
 3241 GCGTTTCCCC CTGGAAGTCC CCTCGTGCGC TCTCCTGTTT CGACCCCTGCC GCTTACCGGA
 3301 TACCTGTCCG CCTTTCTCCC TTCGGGAAGC GTGGCGCTTT CTCATAGCTC ACGTGTAGG
 3361 TATCTCAGTT CGGTGTAGGT CGTTTCGCTCC AAGCTGGGCT GTGTGCACGA ACCCCCGTT
 3421 CAGCCCGACC GCTGCGCCTT ATCCGGTAAC TATCGTCTTG AGTCCAACCC GGTAAGACAC
 3481 GACTTATCGC CACTGGCAGC AGCCACTGGT AACAGGATTA GCAGAGCGAG GTATGTAGGC
 3541 GGTGCTACAG AGTTCTTGAA GTGGTGGCCT AACTACGGCT ACACTAGAAG AACAGTATTT
 3601 GGTATCTGCG CTCTGCTGAA GCCAGTTACC TTCGAAAAA GAGTTGGTAG CTCTTGATCC
 3661 GGCAAACAAA CCACCGCTGG TAGCGGTGGT TTTTTTGTTC GCAAGCAGCA GATTACGCGC
 3721 AGAAAAAAG GATCTCAAGA AGATCCTTTG ATCTTTTCTA CGGGGTCTGA CGCTCAGTGG
 3781 AACGAAAAT CACGTTAAGG GATTTTGGTC ATGAGATTAT CAAAAAGGAT CTTACCTAG
 3841 ATCCTTTTAA ATTAATAATG AAGTTTAAA TCAATCTAAA GTATATATGA GTAAACTTGG
 3901 TCTGACAGTT ACCAATGCTT AATCAGTGAG GCACCTATCT CAGCGATCTG TCTATTTCTG
 3961 TCATCCATAG TTGCCTGACT CCCCCTCGTG TAGATAACTA CGATACGGGA GGGCTTACCA
 4021 TCTGGCCCCA GTGCTGCAAT GATACCGCGA GACCCACGCT CACCGGCTCC AGATTTATCA
 4081 GCAATAAACC AGCCAGCCGG AAGGGCCGAG CGCAGAAGTG GTCTTGC AAC TTTATCCGCC
 4141 TCCATCCAGT CTATTAATTG TTGCCGGGAA GCTAGAGTAA GTAGTTCGCC AGTTAATAGT
 4201 TTGCGCAACG TTGTTGCCAT TGCTACAGGC ATCGTGGTGT CACGCTCGTC GTTTGGTATG
 4261 GCTTCAATCA GCTCCGGTTC CCAACGATCA AGGCGAGTTA CATGATCCCC CATGTTGTGC
 4321 AAAAAAGCGG TTAGTCTCCTT CGGTCTCCG ATCGTTGTCA GAAGTAAGTT GCGCCAGATG
 4381 TTATCACTCA TGGTTATGGC AGCACTGCAT AATTCTCTTA CTGTCATGCC ATCCCTAAGA
 4441 TGCTTTTCTG TGACTGGTGA GTACTCAACC AAGTCATTCT GAGAATAGTG TATGCGCGCA
 4501 CCGAGTTGCT CTTGCCCGGC GTCAATACGG GATAATACCG CGCCACATAG CAGAACTTTA
 4561 AAAGTGCTCA TCATTGGA AAAACGTTCTTCG GGGCGAAAAAC TCTCAAGGAT CTTACCGCTG
 4621 TTGAGATCCA GTTCGATGTA ACCCACTCGT GCACCCAACT GATCTTCAGC ATCTTTTACT
 4681 TTCACCAGCG TTTCTGGGTG AGCAAAAACA GGAAGGCAAAA ATGCCGCAAAA AAAGGGAATA
 4741 AGGGCGACAC GGAAATGTTG AATACTCATA CTCTTCCTTT TTCAATATTA TTGAAGCATT
 4801 TATCAGGGTT ATTGTCTCAT GAGCGGATAC ATATTTGAAT GTATTTAGAA AAATAAACAA
 4861 ATAGGGGTTT CGCGCACATT TCCCCGAAAA GTGCCACCTG ACGTCTAAGA AACCATPATT
 4921 ATCATGACAT TAACCTATAA AAATAGGCGT ATCACGAGGC CCTTTCGCTC CGCGCGTTTC
 4981 GGTGATGACG GTGAAAACCT CTGACACATG CAGCTCCCCG AGACGGTCCAC AGCTTGTCTG
 5041 TAAGCGGATG CCGGGAGCAG ACAAGCCCGT CAGGGCGCGT CAGCGGGTGT TGGCGGGTGT
 5101 CGGGGCTGGC TTAACCTATGC GGCATCAGAG CAGATTGTAC TGAGAGTGCA CCATATGCGG
 5161 TGTGAAATAC CGCACAGATG CGTAAGGAGA AAATACCGCA TCAGGCGATT CCAACATCCA
 5221 ATAAATCATA CAGGCAAGGC AAAGAATTAG CAAAATTAAG CAATAAAGCC TCAGAGCATA
 5281 AAGTAAATC GGTGTACCA AAAAATTTAG GACCCTGTAA TACTTTTGGC GGAGAAGCCT
 5341 TTATTTCAAC GCAAGGATAA AAATTTTAG AACCTCATA TATTTTAAAT GCAATGCCTG
 5401 AGTAATGTGT AGGTAAAGAT TCAAACGGGT GAGAAAGGCC GGAGACATC AAAATCCCAT
 5461 CAATATGATA TTCAACCGTT CTAGCTGATA AATTCATGCC GGAGAGGGTA GCTATTTTTG
 5521 AGAGGTCTCT ACAAAGGCTA TCAGGTCAAT GCCTGAGAGT CTGGAGCAAAA CAAGAGAATC
 5581 GATGAACGGT AATCGTAAAA CTAGCATGTC AATCATATGT ACCCCGGTTG ATAATCAGAA
 5641 AAGCCCCAAA AACAGGAAGA TTGTATAAGC AAATATTTAA ATTGTAAGCG TTAATATTTT
 5701 GTTAAATTC GCGTTAAAT TTTGTTAAAT CAGCTCATTT TTTAACCAAT AGGCCGAAAT
 5761 CGGCAAAATC CTTATAAAT CAAAAGAATA GACCAGATA GGGTTGAGTG TTGTTCCAGT
 5821 TTGGAACAAG AGTCCACTAT TAAAGAACGT GGACTCCAAC GTCAAAGGGC GAAAAACCGT
 5881 CTATCAGGGC GATGGCCCAC TACGTGAACC ATCACCTAA TCAAGTTTTT TGGGTCGAG
 5941 GTGCCGTAAA GCACTAAATC GGAACCTAA AGGGAGCCCC CGATTTAGAG CTTGACGGGG
 6001 AAAGCCGGCG AACGTGGCGA GAAAGGAAGG GAAGAAAGCG AAAGGAGCGG GCGCTAGGGC
 6061 GCTGGCAAGT GTAGCGGTCA CGCTGCGCGT AACCACCACA CCCGCCGCGC TTAATGCGCC
 6121 GCTACAGGGC GCGTACTATG GTTGCTTTGA CGAGCACGTA TAACGTGCTT TCCTCGTTAG
 6181 AATCAGAGCG GGAGCTAAAC AGGAGGCCGA TTAAAGGGAT TTTAGACAGG AACGGTACGC
 6241 CAGAATCCTG AGAAGTGTTC TTATAATCAG TGAGGCCACC GAGTAAAAGA GTCTGTCCAT
 6301 CAGCAAAT AACC GTTGTGTC GCAATACTTC TTTGATTAGT AATAACATCA CTTGCCCTGAG
 6361 TAGAAGAAT CAAACTATCG GCCTTGCTGG TAATATCCAG AACAATATTA CCGCCAGCCA
 6421 TTGCAACGGA ATCGCCATTC GCCATTACAG CTGCGCAACT GTTGGGAAGG GCGATCGGTG
 6481 CGGGCCTCTT CGCTATTACG C

SEQ pSub-U6-LoxP-sh cGKII-PGK-mcherry-WPRE: 6501 bp;

Composition 1576 A; 1699 C; 1714 G; 1512 T; 0 OTHER

Percentage: 24.2% A; 26.1% C; 26.4% G; 23.3% T; 0.0%OTHER

Molecular Weight (kDa): ssDNA: 2007.85 dsDNA: 4008.03

ORIGIN

```

1      CAGCTGCGCG CTCGCTCGCT CACTGAGGCC GCCCGGGCAA AGCCCGGGCG TCGGGCGACC
61     TTTGGTTCGCC CGGCCTCAGT GAGCGAGCGA GCGCGCAGAG AGGGAGTGGC CAACTCCATC
121    ACTAGGGGTT CTTGTAGT AATGATTAAC CCGCCATGCT ACTTATCTAC GTAGCCATGC
181    TCTAGGAAGA TCGGAATTCG CCCTTAAGCT AGCTTAATTA AATCCGACGC CGCCATCTCT
241    AGGCCCGCGC CGGCCCCCTC GCACAGACTT GTGGGAGAAG CTCGGCTACT CCCCTGCCCC
301    GGTTAATTTG CATATAATAT TTCCTAGTAA CTATAGAGGC TTAATGTGCG ATAAAAAGACA
361    GATAATCTGT TCTTTTTAAT ACTAGCTACA TTTTACATGA TAGGCTTGGA TTTCTATAAG
421    AGATACAAAT ACTAAATTAT TATTTTAAAA AACAGCACAA AAGGAAACTC ACCCTAACTG
481    TAAAGTAATT GTGTGTTTTG AGACTATAAA TATCCCTTGG AGAAAAGCCT TGTATCGGT
541    ACCATAACTT CGTATAGCAT ACATTATACG AAGTTATGAG CTCCGAACCT ATGACCTCAA
601    CAAATCAAGA GTTTGTGAG GTCATAGGTT CGTTTTTGAT ATCGAATTCC CACGGGGTTG
661    GGGTTGCGCC TTTTCCAAGG CAGCCCTGGG TTTGCGCAGG GACGCGGCTG CTCTGGGCGT
721    GGTTCCGGGA AACGCAGCGG CGCCGACCTT GGGTCTCGCA CATTCTTCAC GTCCGTTTCG
781    AGCGTCACCC GGATCTTCGC CGCTACCCTT GTGGGCCCCC CGGCGACGCT TCCTGCTCCG
841    CCCCTAAGTC GGAAGGTTT CTTGCGGTTT GCGGCGTGCC GGACGTGACA AACGGAAGCC
901    GCACGTCTCA CTAGTACCCT CGCAGACGGA CAGCGCCAGG GAGCAATGGC AGCGCGCCGA
961    CCGCGATGGG CTGTGGCCAA TAGCGGCTGC TCAGCGGGGC GCGCCGAGAG CAGCGGCCGG
1021   GAAGGGGCGG TCGGGGAGG GGGGTGTGGG GCGGTAGTGT GGGCCCTGTT CCTGCCCGCG
1081   SAAGTTTCCG CATTCTGCAA GCCTCCGGAG CCGACGTCCG CAGTCGGCTC CCTCGTTGAC
1141   CGAATCACCG ACCTCTCTCC CCAGGGGGAT CCACCGGTAT GGTGAGCAAG GCGAGGAGG
1201   ATAACATGGC CATCATCAAG GAGTTCATGC GCTTCAAGGT GCACATGGAG GGCTCCGTGA
1261   ACGGCCACGA GTTCGAGATC GAGGGCGAGG GCGAGGGCCG CCCCTACGAG GGCACCCAGA
1321   CCGCCAAGCT GAAGGTGACC AAGGGTGGCC CCCTGCCCTT CGCCTGGGAC ATCCTGTCCC
1381   CTCAGTTCAT GTACGGCTCC AAGGCCTACG TGAAGCACCC CGCCGACATC CCCGACTACT
1441   TGAAGCTGTC CTTCCCCGAG GGCTTCAAGT GGGAGCGCGT GATGAACTTC GAGGACGGCG
1501   GCGTGGTGAC CGTGACCCAG GACTCCTCCC TGCAGGACGG CGAGTTCATC TACAAGGTGA
1561   AGCTGCGCGG CACCAACTTC CCCTCCGACG GCCCCGTAAT GCAGAAGAAG ACCATGGGCT
1621   GGGAGGCCTC CTCCGAGCGG ATGTACCCCG AGGACGGCGC CCTGAAGGGC GAGATCAAGC
1681   AGAGGCTGAA GCTGAAGGAC GGCGGCCACT ACGACGCTGA GGTCAAGACC ACCTACAAGG
1741   CCAAGAAGCC CGTGCGAGTG CCCGGCGCCT ACAACGTCAA CATCAAGTTG GACATCACCT
1801   CCCACAACGA GGACTACACC ATCGTGGAAC AGTACGAACG CGCCGAGGGC CGCCACTCCA
1861   CCGGCGGCAT GGACGAGCTG TACAAGTAAG TTTAAACGTC GACAATCAAC CTCTGGATTA
1921   CAAAATTTGT GAAAGATTGA CTGGTATTCT TAACTATGTT GCTCCTTTTA CGCTATGTGG
1981   ATACGCTGCT TTAATGCCTT TGTATCATGC TATTGCTTCC CGTATGGCTT TCATTTTCTC
2041   CTCCTTGTAT AAATCCTGGT TGCTGTCTCT TTATGAGGAG TTGTGGCCCC TTGTCAGGCA
2101   ACGTGCGCTG GTGTGCACATG TGTTTGCTGA CGCAACCCCC ACTGTTGGG GCATFGCCAC
2161   CACCTGTCAG CTCCTTTCCG GGACTTTCGC TTTCCCCCTC CCTATTGCCA CGCGGAACT
2221   CATCGCCGCC TGCCTTGCCC GCTGCTGGAC AGGGGCTCGG CTGTTGGGCA CTGACAATTC
2281   CGTGGTGTG TCGGGGAAGC TGACGTCCCT TCCATGGCTG CTCGCCTGTG TTGCCACCTG
2341   GATTCTGCGC GGGACGTCC TCTGCTACGT CCCTTCGGCC CTCAATCCAG CGGACCTTCC
2401   TTCCCGCGGC CTGCTGCCGG CTCTGCGGCC TCTTCCGCGT CTTGAGATC TGCTCGACT
2461   GTGCCTTCTA GTTGCCAGCC ATCTGTTGTT TGCCCTCCC CCGTGCCTTC CTTGACCCTG
2521   GAAGGTGCCA CTCCCCTGT CTTTCTCTAA TAAAATGAGG AAATTGCATC GCATTGTCTG
2581   AGTAGGTGTC ATTCTATTCT GGGGGGTGGG GTGGGGCAGG ACAGCAAGGG GGAGGATTGG
2641   GAAGACAATA GCAGGCATGC TGGGGACTCG AGTTAAGGGC GAATTCCTCGA TTAGGATCTT
2701   CCTAGAGCAT GGCTACGTAG ATAAGTAGCA TGGCGGGTTA ATCATTAACT ACAAGGAACC
2761   CCTAGTGATG GAGTTGGCCA CTCCCTCTCT GCGCGCTCGC TCGCTCACTG AGGCCGGGCG
2821   ACCAAAGGTC GCCCGACGCC CGGGCTTTGC CCGGGCGGCC TCAGTGAGCG AGCGAGCGCG
2881   CAGCTGGGCC TCAGTGAGCG AGCGAGCGCG CAGCTGCATT AATGAATCGG CCAACGCGCG
2941   GGGAGAGGCG GTTTGCGTAT TGGGCGCTCT TCCGCTTCTT CGCTCACTGA CTCGCTGCGC
3001   TCGGTCGTTT GGCTGCGGCG AGCGGTATCA GCTCACTCAA AGGCGGTAAT ACGGTTATCC
3061   ACAGAATCAG GGGATAACGC AGGAAAGAAC ATGTGAGCAA AAGGCCAGCA AAAGGCCAGG
3121   AACCGTAAAA AGGCCGCGTT GCTGGCGTTT TTCCATAGGC TCCGCCCCCT TGACGAGCAT
3181   CACAAAATC GACGCTCAAG TCAGAGGTTG CGAAACCCGA CAGGACTATA AAGATACCAG
3241   GCGTTTTCCC CTGGAAGCTC CCTCGTGCGC TCTCCTGTTC CGACCTGCC GCTTACCGGA

```

3301 TACCTGTCCG CCTTTCTCCC TTCGGGAAGC GTGGCGCTTT CTCATAGCTC ACGCTGTAGG
3361 TATCTCAGTT CGGTGTAGGT CGTTTCGCTCC AAGCTGGGCT GTGTGCACGA ACCCCCCGTT
3421 CAGCCCGACC GCTGCGCCTT ATCCGGTAAC TATCGTCTTG AGTCCAACCC GGTAAAGACAC
3481 GACTTATCGC CACTGGCAGC AGCCACTGGT AACAGGATTA GCAGAGCGAG GTATGTAGGC
3541 GGTGCTACAG AGTTCTTGAA GTGGTGGCCT AACTACGGCT ACACTAGAAG AACAGTATTT
3601 GGTATCTGCG CTCTGCTGAA GCCAGTTACC TTCGGAAAAA GAGTTGGTAG CTCTTGATCC
3661 GGCAAACAAA CCACCGCTGG TAGCGGTGGT TTTTTTGTTT GCAAGCAGCA GATTACGCGC
3721 AGAAAAAAG GATCTCAAGA AGATCCTTTG ATCTTTTCTA CGGGGTCTGA CGCTCAGTGG
3781 AACGAAAAC CACGTTAAGG GATTTTGGTC ATGAGATTAT CAAAAAGGAT CTTCACCTAG
3841 ATCCTTTTAA ATTA AAAATG AAGTTTTAAA TCAATCTAAA GTATATATGA GTAAACTTGG
3901 TCTGACAGTT ACCAATGCTT AATCAGTGAG GCACCTATCT CAGCGATCTG TCTATTTCTG
3961 TCATCCATAG TTGCCTGACT CCCCCTCGTG TAGATAACTA CGATACGGGA GGGCTTACCA
4021 TCTGGCCCCA GTGCTGCAAT GATACCGCGA GACCCACGCT CACCGGCTCC AGATTTATCA
4081 GCAATAAACC AGCCAGCCGG AAGGGCCGAG CGCAGAAGTG GTCCTGCAAC TTTATCCGCC
4141 TCCATCCAGT CTATTAATTG TTGCCGGGAA GCTAGAGTAA GTAGTTCGCC AGTTAATAGT
4201 TTGCGCAACG TTGTTGCCAT TGCTACAGGC ATCGTGGTGT CACGCTCGTC GTTTGGTATG
4261 GCTTCATTCA GCTCCGGTTC CCAACGATCA AGGCGAGTTA CATGATCCCC CATGTTGTGC
4321 AAAAAAGCGG TTAGCTCCTT CGGTCCTCCG ATCGTTGTCA GAAGTAAGTT GGCCGAGTG
4381 TTATCACTCA TGTTTATGGC AGCACTGCAT AATTCTCTTA CTGTCAATGCC ATCCGTAAGA
4441 TGCTTTTCTG TGACTGGTGA GTACTCAACC AAGTCATTCT GAGAATAGTG TATGCGCGGA
4501 CCGAGTTGCT CTTGCCCGGC GTCAATACGG GATAATACCG CGCCACATAG CAGAACTTTA
4561 AAAGTGCTCA TCATTGGA AAAACGTTCTTCG GGGCGAAAAAC TCTCAAGGAT CTTACCCTG
4621 TTGAGATCCA GTTCGATGTA ACCCACTCGT GCACCAACT GATCTTCAGC ATCTTTTACT
4681 TTCACCAGCG TTTCTGGGTG AGCAAAAACA GGAAGGCAAAA ATGCCGCAAAA AAAGGGAATA
4741 AGGGCGACAC GGAATGTTG AATACTCATA CTCTTCCTTT TTCAATATTA TTGAAGCATT
4801 TATCAGGGTT ATTGTCTCAT GAGCGGATAC ATATTTGAAT GTATTTAGAA AAATAAACAA
4861 ATAGGGGTTT CGCGCACATT TCCCGGAAAA ATGCCACCTG ACGTCTAAGA AACCATTTT
4921 ATCATGACAT TAACCTATAA AAATAGGCGT ATCACGAGGC CCTTTCGTCT CGCGGTTTC
4981 GGTGATGACG GTGAAAACCT CTGACACATG CAGCTCCCGG AGACGGTCAC AGCTTGCTG
5041 TAAGCGGATG CCGGGAGCAG ACAAGCCCGT CAGGGCGCGT CAGCGGGTGT TGGCGGGTGT
5101 CGGGGCTGGC TTAACTATGC GGCATCAGAG CAGATTGTAC TGAGAGTGCA CCATATGCGG
5161 TGTGAAATAC CGCACAGATG CGTAAGGAGA AAATACCGCA TCAGGCGATT CCAACATCCA
5221 ATAAATCATA CAGGCAAGGC AAAGAATTAG CAAAATTAAG CAATAAAGCC TCAGAGCATA
5281 AAGCTAAATC GGTGTACCA AAAACATTAT GACCCTGTAA TACTTTTGCG GGAGAAGCCT
5341 TTATTTCAAC GCAAGGATAA AAATTTTATG AACCTCATA TATTTTAAAT GCAATGCCTG
5401 AGTAATGTGT AGGTAAAGAT TCAAACGGGT GAGAAAGGCC GGAGACAGTC AAATCACCAT
5461 CAATATGATA TTCAACCGTT CTAGCTGATA AATTCATGCC GGAGAGGGTA GCTATTTTTG
5521 AGAGGTCTCT ACAAAGGCTA TCAGGTCATT GCCTGAGAGT CTGGAGCAAAA CAAGAGAATC
5581 GATGAACGGT AATCGTAAAA CTAGCATGTC AATCATATGT ACCCCGGTTG ATAATCAGAA
5641 AAGCCCCAAA AACAGGAAGA TTGTATAAGC AAATATTTAA ATTGTAAGCG TTAATATTTT
5701 GTTAAAATTC GCGTTAAATT TTTGTTAAAT CAGCTCATTT TTTAACCAAT AGGCCGAAAT
5761 CGGCAAAATC CCTTATAAAT CAAAAGAATA GACCGAGATA GGGTTGAGTG TTGTTCCAGT
5821 TTGGAACAAG AGTCCACTAT TAAAGAACGT GGACTCCAAC GTCAAAGGGC GAAAAACCGT
5881 CTATCAGGGC GATGGCCAC TACGTGAACC ATCACCTTAA TCAAGTTTTT TGGGGTCGAG
5941 GTGCCGTAAA GCACTAAATC GGAACCTTAA AGGGAGCCCC CGATTTAGAG CTGACGGGG
6001 AAAGCCGGCG AACGTGGCGA GAAAGGAAGG GAAGAAAGCG AAAGGAGCGG GCGCTAGGGC
6061 GCTGGCAAGT GTAGCGGTCA CGCTGCGCGT AACCACCACA CCCGCCGCGC TTAATGCGCC
6121 GCTACAGGGC GCGTACTATG GTTGCTTTGA CGAGCACGTA TAACGTGCTT TCCTCGTTAG
6181 AATCAGAGCG GGAGCTAAAC AGGAGGCCGA TTAAAGGGAT TTTAGACAGG AACGGTACGC
6241 CAGAATCCTG AGAAGTGT TTATAATCAG TGAGGCCACC GAGTAAAAGA GTCTGTCCAT
6301 CACGCAAATT AACCGTTGTC GCAATACTTC TTTGATTAGT AATAACATCA CTGCTGAG
6361 TAGAAGAACT CAAACTATCG GCCTTGCTGG TAATATCCAG AACAATATTA CCGCCAGCCA
6421 TTGCAACGGA ATCGCCATTC GCCATTACAG CTGCGCAACT GTTGGGAAGG GCGATCGGTG
6481 CGGGCCTCTT CGCTATTACG C

8.2 References

- ACLAND, G. M., AGUIRRE, G. D., BENNETT, J., ALEMAN, T. S., CIDECIYAN, A. V., BENNICELLI, J., DEJNEKA, N. S., PEARCE-KELLING, S. E., MAGUIRE, A. M., PALCZEWSKI, K., HAUSWIRTH, W. W. & JACOBSON, S. G. 2005. Long-term restoration of rod and cone vision by single dose rAAV-mediated gene transfer to the retina in a canine model of childhood blindness. *Mol Ther*, 12, 1072-82.
- ACLAND, G. M., AGUIRRE, G. D., RAY, J., ZHANG, Q., ALEMAN, T. S., CIDECIYAN, A. V., PEARCE-KELLING, S. E., ANAND, V., ZENG, Y., MAGUIRE, A. M., JACOBSON, S. G., HAUSWIRTH, W. W. & BENNETT, J. 2001. Gene therapy restores vision in a canine model of childhood blindness. *Nat Genet*, 28, 92-5.
- AIT-ALI, N., FRIDLICH, R., MILLET-PUEL, G., CLERIN, E., DELALANDE, F., JAILLARD, C., BLOND, F., PERROCHEAU, L., REICHMAN, S., BYRNE, L. C., OLIVIER-BANDINI, A., BELLALOU, J., MOYSE, E., BOUILLAUD, F., NICOL, X., DALKARA, D., VAN DORSSELAER, A., SAHEL, J. A. & LEVEILLARD, T. 2015. Rod-derived cone viability factor promotes cone survival by stimulating aerobic glycolysis. *Cell*, 161, 817-32.
- ALDER, V. A., BEN-NUN, J. & CRINGLE, S. J. 1990. PO₂ profiles and oxygen consumption in cat retina with an occluded retinal circulation. *Invest Ophthalmol Vis Sci*, 31, 1029-34.
- AMES, A., 3RD, LI, Y. Y., HEHER, E. C. & KIMBLE, C. R. 1992. Energy metabolism of rabbit retina as related to function: high cost of Na⁺ transport. *J Neurosci*, 12, 840-53.
- AQUIRRE, G., FARBER, D., LOLLEY, R., FLETCHER, R. T. & CHADER, G. J. 1978. Rod-cone dysplasia in Irish setters: a defect in cyclic GMP metabolism in visual cells. *Science*, 201, 1133-4.
- ARANGO-GONZALEZ, B., TRIFUNOVIC, D., SAHABOGLU, A., KRANZ, K., MICHALAKIS, S., FARINELLI, P., KOCH, S., KOCH, F., COTTET, S., JANSSEN-BIENHOLD, U., DEDEK, K., BIEL, M., ZRENNER, E., EULER, T., EKSTROM, P., UEFFING, M. & PAQUET-DURAND, F. 2014. Identification of a common non-apoptotic cell death mechanism in hereditary retinal degeneration. *PLoS One*, 9, e112142.
- ARSHAVSKY, V. Y. & BURNS, M. E. 2012. Photoreceptor signaling: supporting vision across a wide range of light intensities. *J Biol Chem*, 287, 1620-6.
- AZUMA, M., SAKAMOTO-MIZUTANI, K., NAKAJIMA, T., KANAAMI-DAIBO, S., TAMADA, Y. & SHEARER, T. R. 2004. Involvement of calpain isoforms in retinal degeneration in WBN/Kob rats. *Comp Med*, 54, 533-42.
- BAINBRIDGE, J. W., MEHAT, M. S., SUNDARAM, V., ROBBIE, S. J., BARKER, S. E., RIPAMONTI, C., GEORGIADIS, A., MOWAT, F. M., BEATTIE, S. G., GARDNER, P. J., FEATHERS, K. L., LUONG, V. A., YZER, S., BALAGGAN, K., VISWANATHAN, A., DE RAVEL, T. J., CASTEELS, I., HOLDER, G. E., TYLER, N., FITZKE, F. W., WELEBER, R. G., NARDINI, M., MOORE, A. T., THOMPSON, D. A., PETERSEN-JONES, S. M., MICHAELIDES, M., VAN DEN

- BORN, L. I., STOCKMAN, A., SMITH, A. J., RUBIN, G. & ALI, R. R. 2015. Long-term effect of gene therapy on Leber's congenital amaurosis. *N Engl J Med*, 372, 1887-97.
- BANIN, E., GOOTWINE, E., OBOLENSKY, A., EZRA-ELIA, R., EJZENBERG, A., ZELINGER, L., HONIG, H., ROSOV, A., YAMIN, E., SHARON, D., AVERBUKH, E., HAUSWIRTH, W. W. & OFRI, R. 2015. Gene Augmentation Therapy Restores Retinal Function and Visual Behavior in a Sheep Model of CNGA3 Achromatopsia. *Mol Ther*, 23, 1423-33.
- BIEL, M. & MICHALAKIS, S. 2007. Function and dysfunction of CNG channels: insights from channelopathies and mouse models. *Mol Neurobiol*, 35, 266-77.
- BIEL, M., SEELIGER, M., PFEIFER, A., KOHLER, K., GERSTNER, A., LUDWIG, A., JAISSE, G., FAUSER, S., ZRENNER, E. & HOFMANN, F. 1999. Selective loss of cone function in mice lacking the cyclic nucleotide-gated channel CNG3. *Proc Natl Acad Sci U S A*, 96, 7553-7.
- BLAESE, R. M., CULVER, K. W., MILLER, A. D., CARTER, C. S., FLEISHER, T., CLERICI, M., SHEARER, G., CHANG, L., CHIANG, Y., TOLSTOSHEV, P., GREENBLATT, J. J., ROSENBERG, S. A., KLEIN, H., BERGER, M., MULLEN, C. A., RAMSEY, W. J., MUUL, L., MORGAN, R. A. & ANDERSON, W. F. 1995. T lymphocyte-directed gene therapy for ADA- SCID: initial trial results after 4 years. *Science*, 270, 475-80.
- BOERTH, N. J. & LINCOLN, T. M. 1994. Expression of the catalytic domain of cyclic GMP-dependent protein kinase in a baculovirus system. *FEBS Lett*, 342, 255-60.
- BORER, R. A., LEHNER, C. F., EPPENBERGER, H. M. & NIGG, E. A. 1989. Major nucleolar proteins shuttle between nucleus and cytoplasm. *Cell*, 56, 379-90.
- BOWES, C., LI, T., DANCIGER, M., BAXTER, L. C., APPLEBURY, M. L. & FARBER, D. B. 1990. Retinal degeneration in the rd mouse is caused by a defect in the beta subunit of rod cGMP-phosphodiesterase. *Nature*, 347, 677-80.
- BOYE, S. E., BOYE, S. L., LEWIN, A. S. & HAUSWIRTH, W. W. 2013. A comprehensive review of retinal gene therapy. *Mol Ther*, 21, 509-19.
- BRAUN, R. D., LINSENMEIER, R. A. & GOLDSTICK, T. K. 1995. Oxygen consumption in the inner and outer retina of the cat. *Invest Ophthalmol Vis Sci*, 36, 542-54.
- BRINGMANN, A., PANNICKE, T., GROSCHE, J., FRANCKE, M., WIEDEMANN, P., SKATCHKOV, S. N., OSBORNE, N. N. & REICHENBACH, A. 2006. Muller cells in the healthy and diseased retina. *Prog Retin Eye Res*, 25, 397-424.
- BROWN, E. J. & BALTIMORE, D. 2003. Essential and dispensable roles of ATR in cell cycle arrest and genome maintenance. *Genes Dev*, 17, 615-28.
- BRUHN, C. 2014. Gene therapy: First success and many unanswered questions. *Thieme- DMW - Deutsche Medizinische Wochenschrift* 139, 1916-18.
- BUSH, R. A., KONONEN, L., MACHIDA, S. & SIEVING, P. A. 2000. The effect of calcium channel blocker diltiazem on photoreceptor degeneration in the rhodopsin Pro213His rat. *Invest Ophthalmol Vis Sci*, 41, 2697-701.

- CARVALHO, L. S. & VANDENBERGHE, L. H. 2015. Promising and delivering gene therapies for vision loss. *Vision Res*, 111, 124-33.
- CARVALHO, L. S., XU, J., PEARSON, R. A., SMITH, A. J., BAINBRIDGE, J. W., MORRIS, L. M., FLIESLER, S. J., DING, X. Q. & ALI, R. R. 2011. Long-term and age-dependent restoration of visual function in a mouse model of CNGB3-associated achromatopsia following gene therapy. *Hum Mol Genet*, 20, 3161-75.
- CASTEEL, D. E., SMITH-NGUYEN, E. V., SANKARAN, B., ROH, S. H., PILZ, R. B. & KIM, C. 2010. A crystal structure of the cyclic GMP-dependent protein kinase I{beta} dimerization/docking domain reveals molecular details of isoform-specific anchoring. *J Biol Chem*, 285, 32684-8.
- CAVAZZANA-CALVO, M., HACEIN-BEY, S., DE SAINT BASILE, G., GROSS, F., YVON, E., NUSBAUM, P., SELZ, F., HUE, C., CERTAIN, S., CASANOVA, J. L., BOUSSO, P., DEIST, F. L. & FISCHER, A. 2000. Gene therapy of human severe combined immunodeficiency (SCID)-X1 disease. *Science*, 288, 669-72.
- CHECK, E. 2002a. Regulators split on gene therapy as patient shows signs of cancer. *Nature*, 419, 545-6.
- CHECK, E. 2002b. A tragic setback. *Nature*, 420, 116-8.
- CIDECIYAN, A. V. 2010. Leber congenital amaurosis due to RPE65 mutations and its treatment with gene therapy. *Prog Retin Eye Res*, 29, 398-427.
- CIDECIYAN, A. V., JACOBSON, S. G., BELTRAN, W. A., SUMAROKA, A., SWIDER, M., IWABE, S., ROMAN, A. J., OLIVARES, M. B., SCHWARTZ, S. B., KOMAROMY, A. M., HAUSWIRTH, W. W. & AGUIRRE, G. D. 2013. Human retinal gene therapy for Leber congenital amaurosis shows advancing retinal degeneration despite enduring visual improvement. *Proc Natl Acad Sci U S A*, 110, E517-25.
- CLIBY, W. A., ROBERTS, C. J., CIMPRICH, K. A., STRINGER, C. M., LAMB, J. R., SCHREIBER, S. L. & FRIEND, S. H. 1998. Overexpression of a kinase-inactive ATR protein causes sensitivity to DNA-damaging agents and defects in cell cycle checkpoints. *EMBO J*, 17, 159-69.
- DE VENTE, J., STEINBUSCH, H. W. & SCHIPPER, J. 1987. A new approach to immunocytochemistry of 3',5'-cyclic guanosine monophosphate: preparation, specificity, and initial application of a new antiserum against formaldehyde-fixed 3',5'-cyclic guanosine monophosphate. *Neuroscience*, 22, 361-73.
- DE WINTER, F., HOYNG, S., TANNEMAAT, M., EGGERS, R., MASON, M., MALESSY, M. & VERHAAGEN, J. 2013. Gene therapy approaches to enhance regeneration of the injured peripheral nerve. *Eur J Pharmacol*, 719, 145-52.
- DEGUCHI, A., THOMPSON, W. J. & WEINSTEIN, I. B. 2004. Activation of protein kinase G is sufficient to induce apoptosis and inhibit cell migration in colon cancer cells. *Cancer Res*, 64, 3966-73.
- DEJNEKA, N. S., SURACE, E. M., ALEMAN, T. S., CIDECIYAN, A. V., LYUBARSKY, A., SAVCHENKO, A., REDMOND, T. M., TANG, W., WEI, Z., REX, T. S., GLOVER, E., MAGUIRE, A. M., PUGH, E. N., JR., JACOBSON, S. G. & BENNETT, J. 2004.

- In utero gene therapy rescues vision in a murine model of congenital blindness. *Mol Ther*, 9, 182-8.
- DEMONTIS, G. C., LONGONI, B., GARGINI, C. & CERVETTO, L. 1997. The energetic cost of photoreception in retinal rods of mammals. *Arch Ital Biol*, 135, 95-109.
- DHAR, S. K. & ST CLAIR, D. K. 2009. Nucleophosmin blocks mitochondrial localization of p53 and apoptosis. *J Biol Chem*, 284, 16409-18.
- DING, X. Q., HARRY, C. S., UMINO, Y., MATVEEV, A. V., FLIESLER, S. J. & BARLOW, R. B. 2009. Impaired cone function and cone degeneration resulting from CNGB3 deficiency: down-regulation of CNGA3 biosynthesis as a potential mechanism. *Hum Mol Genet*, 18, 4770-80.
- DONNELLY, M. L., HUGHES, L. E., LUKE, G., MENDOZA, H., TEN DAM, E., GANI, D. & RYAN, M. D. 2001. The 'cleavage' activities of foot-and-mouth disease virus 2A site-directed mutants and naturally occurring '2A-like' sequences. *J Gen Virol*, 82, 1027-41.
- DONOVAN, M. & COTTER, T. G. 2002. Caspase-independent photoreceptor apoptosis in vivo and differential expression of apoptotic protease activating factor-1 and caspase-3 during retinal development. *Cell Death Differ*, 9, 1220-31.
- DOONAN, F., DONOVAN, M. & COTTER, T. G. 2003. Caspase-independent photoreceptor apoptosis in mouse models of retinal degeneration. *J Neurosci*, 23, 5723-31.
- DRAGER, U. C. & HUBEL, D. H. 1978. Studies of visual function and its decay in mice with hereditary retinal degeneration. *J Comp Neurol*, 180, 85-114.
- DRYJA, T. P., FINN, J. T., PENG, Y. W., MCGEE, T. L., BERSON, E. L. & YAU, K. W. 1995. Mutations in the gene encoding the alpha subunit of the rod cGMP-gated channel in autosomal recessive retinitis pigmentosa. *Proc Natl Acad Sci U S A*, 92, 10177-81.
- EKSANDH, L., KOHL, S. & WISSINGER, B. 2002. Clinical features of achromatopsia in Swedish patients with defined genotypes. *Ophthalmic Genet*, 23, 109-20.
- EZRA-ELIA, R., BANIN, E., HONIG, H., ROSOV, A., OBOLENSKY, A., AVERBUKH, E., HAUSWIRTH, W. W., GOOTWINE, E. & OFRI, R. 2014. Flicker cone function in normal and day blind sheep: a large animal model for human achromatopsia caused by CNGA3 mutation. *Doc Ophthalmol*, 129, 141-50.
- FAIN, G. L. & LISMAN, J. E. 1999. Light, Ca²⁺, and photoreceptor death: new evidence for the equivalent-light hypothesis from arrestin knockout mice. *Invest Ophthalmol Vis Sci*, 40, 2770-2.
- FARBER, D. B. & LOLLEY, R. N. 1974. Cyclic guanosine monophosphate: elevation in degenerating photoreceptor cells of the C3H mouse retina. *Science*, 186, 449-51.
- FEIL, R., FEIL, S. & HOFMANN, F. 2005. A heretical view on the role of NO and cGMP in vascular proliferative diseases. *Trends Mol Med*, 11, 71-5.
- FISCHER, A., HACEIN-BEY, S. & CAVAZZANA-CALVO, M. 2002. Gene therapy of severe combined immunodeficiencies. *Nat Rev Immunol*, 2, 615-21.

- FLOTTE, T. R., ZEITLIN, P. L., REYNOLDS, T. C., HEALD, A. E., PEDERSEN, P., BECK, S., CONRAD, C. K., BRASS-ERNST, L., HUMPHRIES, M., SULLIVAN, K., WETZEL, R., TAYLOR, G., CARTER, B. J. & GUGGINO, W. B. 2003. Phase I trial of intranasal and endobronchial administration of a recombinant adeno-associated virus serotype 2 (rAAV2)-CFTR vector in adult cystic fibrosis patients: a two-part clinical study. *Hum Gene Ther*, 14, 1079-88.
- FOX, D. A., POBLENZ, A. T. & HE, L. 1999. Calcium overload triggers rod photoreceptor apoptotic cell death in chemical-induced and inherited retinal degenerations. *Ann N Y Acad Sci*, 893, 282-5.
- GAMM, D. M., FRANCIS, S. H., ANGELOTTI, T. P., CORBIN, J. D. & UHLER, M. D. 1995. The type II isoform of cGMP-dependent protein kinase is dimeric and possesses regulatory and catalytic properties distinct from the type I isoforms. *J Biol Chem*, 270, 27380-8.
- GAVRIELI, Y., SHERMAN, Y. & BEN-SASSON, S. A. 1992. Identification of programmed cell death in situ via specific labeling of nuclear DNA fragmentation. *J Cell Biol*, 119, 493-501.
- GENEAD, M. A., FISHMAN, G. A., RHA, J., DUBIS, A. M., BONCI, D. M., DUBRA, A., STONE, E. M., NEITZ, M. & CARROLL, J. 2011. Photoreceptor structure and function in patients with congenital achromatopsia. *Invest Ophthalmol Vis Sci*, 52, 7298-308.
- GENG, Y., WALLS, K. C., GHOSH, A. P., AKHTAR, R. S., KLOCKE, B. J. & ROTH, K. A. 2010. Cytoplasmic p53 and activated Bax regulate p53-dependent, transcription-independent neural precursor cell apoptosis. *J Histochem Cytochem*, 58, 265-75.
- GORE, M. E. 2003. Adverse effects of gene therapy: Gene therapy can cause leukaemia: no shock, mild horror but a probe. *Gene Ther*, 10, 4-4.
- GU, S. M., THOMPSON, D. A., SRIKUMARI, C. R., LORENZ, B., FINCKH, U., NICOLETTI, A., MURTHY, K. R., RATHMANN, M., KUMARAMANICKAVEL, G., DENTON, M. J. & GAL, A. 1997. Mutations in RPE65 cause autosomal recessive childhood-onset severe retinal dystrophy. *Nat Genet*, 17, 194-7.
- HACEIN-BEY-ABINA, S., GARRIGUE, A., WANG, G. P., SOULIER, J., LIM, A., MORILLON, E., CLAPPIER, E., CACCAVELLI, L., DELABESSE, E., BELDJORD, K., ASNAFI, V., MACINTYRE, E., DAL CORTIVO, L., RADFORD, I., BROUSSE, N., SIGAUX, F., MOSHOUS, D., HAUER, J., BORKHARDT, A., BELOHRADSKY, B. H., WINTERGERST, U., VELEZ, M. C., LEIVA, L., SORENSEN, R., WULFFRAAT, N., BLANCHE, S., BUSHMAN, F. D., FISCHER, A. & CAVAZZANA-CALVO, M. 2008. Insertional oncogenesis in 4 patients after retrovirus-mediated gene therapy of SCID-X1. *J Clin Invest*, 118, 3132-42.
- HAGSTROM, S. A., DUYAO, M., NORTH, M. A. & LI, T. 1999. Retinal degeneration in *tulp1*^{-/-} mice: vesicular accumulation in the interphotoreceptor matrix. *Invest Ophthalmol Vis Sci*, 40, 2795-802.

- HAINDL, M., HARASIM, T., EICK, D. & MULLER, S. 2008. The nucleolar SUMO-specific protease SENP3 reverses SUMO modification of nucleophosmin and is required for rRNA processing. *EMBO Rep*, 9, 273-9.
- HARPER, J. W. & ELLEDGE, S. J. 2007. The DNA damage response: ten years after. *Mol Cell*, 28, 739-45.
- HARTONG, D. T., BERSON, E. L. & DRYJA, T. P. 2006. Retinitis pigmentosa. *Lancet*, 368, 1795-809.
- HAWKINS, R. K., JANSEN, H. G. & SANYAL, S. 1985. Development and degeneration of retina in rds mutant mice: photoreceptor abnormalities in the heterozygotes. *Exp Eye Res*, 41, 701-20.
- HOFMANN, F. 2005. The biology of cyclic GMP-dependent protein kinases. *J Biol Chem*, 280, 1-4.
- HOFMANN, F., FEIL, R., KLEPPISCH, T. & SCHLOSSMANN, J. 2006. Function of cGMP-dependent protein kinases as revealed by gene deletion. *Physiol Rev*, 86, 1-23.
- HOFMANN, F. & WEGENER, J. W. 2013. cGMP-dependent protein kinases (cGK). *Methods Mol Biol*, 1020, 17-50.
- HOON, M., OKAWA, H., DELLA SANTINA, L. & WONG, R. O. 2014. Functional architecture of the retina: development and disease. *Prog Retin Eye Res*, 42, 44-84.
- HURLEY, P. J. & BUNZ, F. 2007. ATM and ATR: components of an integrated circuit. *Cell Cycle*, 6, 414-7.
- HUTTL, S., MICHALAKIS, S., SEELIGER, M., LUO, D. G., ACAR, N., GEIGER, H., HUDL, K., MADER, R., HAVERKAMP, S., MOSER, M., PFEIFER, A., GERSTNER, A., YAU, K. W. & BIEL, M. 2005. Impaired channel targeting and retinal degeneration in mice lacking the cyclic nucleotide-gated channel subunit CNGB1. *J Neurosci*, 25, 130-8.
- IKAWA, M., TANAKA, N., KAO, W. W. & VERMA, I. M. 2003. Generation of transgenic mice using lentiviral vectors: a novel preclinical assessment of lentiviral vectors for gene therapy. *Mol Ther*, 8, 666-73.
- JACOBSON, S. G., ALEMAN, T. S., CIDECIYAN, A. V., SUMAROKA, A., SCHWARTZ, S. B., WINDSOR, E. A., TRABOULSI, E. I., HEON, E., PITTLER, S. J., MILAM, A. H., MAGUIRE, A. M., PALCZEWSKI, K., STONE, E. M. & BENNETT, J. 2005. Identifying photoreceptors in blind eyes caused by RPE65 mutations: Prerequisite for human gene therapy success. *Proc Natl Acad Sci U S A*, 102, 6177-82.
- JACOBSON, S. G., CIDECIYAN, A. V., AGUIRRE, G. D., ROMAN, A. J., SUMAROKA, A., HAUSWIRTH, W. W. & PALCZEWSKI, K. 2015a. Improvement in vision: a new goal for treatment of hereditary retinal degenerations. *Expert Opin Orphan Drugs*, 3, 563-575.
- JACOBSON, S. G., CIDECIYAN, A. V., RATNAKARAM, R., HEON, E., SCHWARTZ, S. B., ROMAN, A. J., PEDEN, M. C., ALEMAN, T. S., BOYE, S. L., SUMAROKA, A., CONLON, T. J., CALCEDO, R., PANG, J. J., ERGER, K. E., OLIVARES, M. B., MULLINS, C. L., SWIDER, M., KAUSHAL, S., FEUER, W. J., IANNACCONE, A., FISHMAN, G. A., STONE, E. M., BYRNE, B. J. & HAUSWIRTH, W. W. 2012.

- Gene therapy for leber congenital amaurosis caused by RPE65 mutations: safety and efficacy in 15 children and adults followed up to 3 years. *Arch Ophthalmol*, 130, 9-24.
- JACOBSON, S. G., CIDECIYAN, A. V., ROMAN, A. J., SUMAROKA, A., SCHWARTZ, S. B., HEON, E. & HAUSWIRTH, W. W. 2015b. Improvement and decline in vision with gene therapy in childhood blindness. *N Engl J Med*, 372, 1920-6.
- JARCHAU, T., HAUSLER, C., MARKERT, T., POHLER, D., VANDERKERCKHOVE, J., DE JONGE, H. R., LOHMANN, S. M. & WALTER, U. 1994. Cloning, expression, and in situ localization of rat intestinal cGMP-dependent protein kinase II. *Proc Natl Acad Sci U S A*, 91, 9426-30.
- JOBLING, A. I., VESSEY, K. A., WAUGH, M., MILLS, S. A. & FLETCHER, E. L. 2013. A naturally occurring mouse model of achromatopsia: characterization of the mutation in cone transducin and subsequent retinal phenotype. *Invest Ophthalmol Vis Sci*, 54, 3350-9.
- KAUFMANN, K. B., BUNING, H., GALY, A., SCHAMBACH, A. & GREZ, M. 2013. Gene therapy on the move. *EMBO Mol Med*, 5, 1642-61.
- KEMP-HARPER, B. & FEIL, R. 2008. Meeting report: cGMP matters. *Sci Signal*, 1, pe12.
- KIM, J. J., CASTEEL, D. E., HUANG, G., KWON, T. H., REN, R. K., ZWART, P., HEADD, J. J., BROWN, N. G., CHOW, D. C., PALZKILL, T. & KIM, C. 2011. Co-crystal structures of PKG I β (92-227) with cGMP and cAMP reveal the molecular details of cyclic-nucleotide binding. *PLoS One*, 6, e18413.
- KLASSEN, H. 2016. Stem cells in clinical trials for treatment of retinal degeneration. *Expert Opin Biol Ther*, 16, 7-14.
- KOCH, S., SOTHILINGAM, V., GARCIA GARRIDO, M., TANIMOTO, N., BECIROVIC, E., KOCH, F., SEIDE, C., BECK, S. C., SEELIGER, M. W., BIEL, M., MUHLFRIEDEL, R. & MICHALAKIS, S. 2012. Gene therapy restores vision and delays degeneration in the CNGB1(-/-) mouse model of retinitis pigmentosa. *Hum Mol Genet*, 21, 4486-96.
- KOHL, S., BAUMANN, B., BROGHAMMER, M., JAGLE, H., SIEVING, P., KELLNER, U., SPEGAL, R., ANASTASI, M., ZRENNER, E., SHARPE, L. T. & WISSINGER, B. 2000. Mutations in the CNGB3 gene encoding the beta-subunit of the cone photoreceptor cGMP-gated channel are responsible for achromatopsia (ACHM3) linked to chromosome 8q21. *Hum Mol Genet*, 9, 2107-16.
- KOHL, S., MARX, T., GIDDINGS, I., JAGLE, H., JACOBSON, S. G., APFELSTEDT-SYLLA, E., ZRENNER, E., SHARPE, L. T. & WISSINGER, B. 1998. Total colourblindness is caused by mutations in the gene encoding the alpha-subunit of the cone photoreceptor cGMP-gated cation channel. *Nat Genet*, 19, 257-9.
- KOHL, S., VARSANYI, B., ANTUNES, G. A., BAUMANN, B., HOYNG, C. B., JAGLE, H., ROSENBERG, T., KELLNER, U., LORENZ, B., SALATI, R., JURKLIES, B., FARKAS, A., ANDREASSON, S., WELEBER, R. G., JACOBSON, S. G., RUDOLPH, G., CASTELLAN, C., DOLLFUS, H., LEGIUS, E., ANASTASI, M., BITOUN, P., LEV, D., SIEVING, P. A., MUNIER, F. L., ZRENNER, E., SHARPE, L. T., CREMERS, F. P. & WISSINGER, B. 2005. CNGB3 mutations account for 50% of all cases with autosomal recessive achromatopsia. *Eur J Hum Genet*, 13, 302-8.

- KOHL, S., ZOBOR, D., CHIANG, W. C., WEISSCHUH, N., STALLER, J., GONZALEZ MENENDEZ, I., CHANG, S., BECK, S. C., GARCIA GARRIDO, M., SOTHILINGAM, V., SEELIGER, M. W., STANZIAL, F., BENEDICENTI, F., INZANA, F., HEON, E., VINCENT, A., BEIS, J., STROM, T. M., RUDOLPH, G., ROOSING, S., HOLLANDER, A. I., CREMERS, F. P., LOPEZ, I., REN, H., MOORE, A. T., WEBSTER, A. R., MICHAELIDES, M., KOENEKOOP, R. K., ZRENNER, E., KAUFMAN, R. J., TSANG, S. H., WISSINGER, B. & LIN, J. H. 2015. Mutations in the unfolded protein response regulator ATF6 cause the cone dysfunction disorder achromatopsia. *Nat Genet*, 47, 757-65.
- KOHN, D. B. 2000. Gene therapy for XSCID: the first success of gene therapy. *Pediatr Res*, 48, 578.
- KOMAROMY, A. M., ALEXANDER, J. J., ROWLAN, J. S., GARCIA, M. M., CHIODO, V. A., KAYA, A., TANAKA, J. C., ACLAND, G. M., HAUSWIRTH, W. W. & AGUIRRE, G. D. 2010. Gene therapy rescues cone function in congenital achromatopsia. *Hum Mol Genet*, 19, 2581-93.
- KOMMONEN, B., PENN, J. S., KYLMA, T., KARHUNEN, U., DAWSON, W. W., TOLMAN, B. & UKKOLA, T. 1994. Early morphometry of a retinal dystrophy in Labrador retrievers. *Acta Ophthalmol (Copenh)*, 72, 203-10.
- KUHN, M. 2003. Structure, regulation, and function of mammalian membrane guanylyl cyclase receptors, with a focus on guanylyl cyclase-A. *Circ Res*, 93, 700-9.
- KUMAR, M. S., MASTHAN, K. M., BABU, N. A. & DASH, K. C. 2013. Gene therapy in oral cancer: a review. *J Clin Diagn Res*, 7, 1261-3.
- LANDGRAF, W., HOFMANN, F., PELTON, J. T. & HUGGINS, J. P. 1990. Effects of cyclic GMP on the secondary structure of cyclic GMP dependent protein kinase and analysis of the enzyme's amino-terminal domain by far-ultraviolet circular dichroism. *Biochemistry*, 29, 9921-8.
- LAURA, R. P. & HURLEY, J. B. 1998. The kinase homology domain of retinal guanylyl cyclases 1 and 2 specifies the affinity and cooperativity of interaction with guanylyl cyclase activating protein-2. *Biochemistry*, 37, 11264-71.
- LI, Y., BHUIYAN, M., MOHAMMAD, R. M. & SARKAR, F. H. 1998a. Induction of apoptosis in breast cancer cells by TPA. *Oncogene*, 17, 2915-20.
- LI, Z., DULLMANN, J., SCHIEDLMEIER, B., SCHMIDT, M., VON KALLE, C., MEYER, J., FORSTER, M., STOCKING, C., WAHLERS, A., FRANK, O., OSTERTAG, W., KUHLCHE, K., ECKERT, H. G., FEHSE, B. & BAUM, C. 2002. Murine leukemia induced by retroviral gene marking. *Science*, 296, 497.
- LI, Z. Y., WONG, F., CHANG, J. H., POSSIN, D. E., HAO, Y., PETTERS, R. M. & MILAM, A. H. 1998b. Rhodopsin transgenic pigs as a model for human retinitis pigmentosa. *Invest Ophthalmol Vis Sci*, 39, 808-19.
- LIU, X., LIU, Z., JANG, S. W., MA, Z., SHINMURA, K., KANG, S., DONG, S., CHEN, J., FUKASAWA, K. & YE, K. 2007. Sumoylation of nucleophosmin/B23 regulates its subcellular localization, mediating cell proliferation and survival. *Proc Natl Acad Sci U S A*, 104, 9679-84.

- LOWE, D. G., DIZHOOR, A. M., LIU, K., GU, Q., SPENCER, M., LAURA, R., LU, L. & HURLEY, J. B. 1995. Cloning and expression of a second photoreceptor-specific membrane retina guanylyl cyclase (RetGC), RetGC-2. *Proc Natl Acad Sci U S A*, 92, 5535-9.
- LUNDSTROM, K. 2015. Special Issue: Gene Therapy with Emphasis on RNA Interference. *Viruses*, 7, 4482-7.
- LUO, D. G., XUE, T. & YAU, K. W. 2008. How vision begins: an odyssey. *Proc Natl Acad Sci U S A*, 105, 9855-62.
- MA, H., THAPA, A., MORRIS, L. M., MICHALAKIS, S., BIEL, M., FRANK, M. B., BEBAK, M. & DING, X. Q. 2013. Loss of cone cyclic nucleotide-gated channel leads to alterations in light response modulating system and cellular stress response pathways: a gene expression profiling study. *Hum Mol Genet*, 22, 3906-19.
- MAMASUEW, K., MICHALAKIS, S., BREER, H., BIEL, M. & FLEISCHER, J. 2010. The cyclic nucleotide-gated ion channel CNGA3 contributes to coolness-induced responses of Grueneberg ganglion neurons. *Cell Mol Life Sci*, 67, 1859-69.
- MCLAUGHLIN, M. E., SANDBERG, M. A., BERSON, E. L. & DRYJA, T. P. 1993. Recessive mutations in the gene encoding the beta-subunit of rod phosphodiesterase in patients with retinitis pigmentosa. *Nat Genet*, 4, 130-4.
- MEDAWAR, P. B. 1948. Immunity to homologous grafted skin; the fate of skin homografts transplanted to the brain, to subcutaneous tissue, and to the anterior chamber of the eye. *Br J Exp Pathol*, 29, 58-69.
- MICHALAKIS, S., GEIGER, H., HAVERKAMP, S., HOFMANN, F., GERSTNER, A. & BIEL, M. 2005. Impaired opsin targeting and cone photoreceptor migration in the retina of mice lacking the cyclic nucleotide-gated channel CNGA3. *Invest Ophthalmol Vis Sci*, 46, 1516-24.
- MICHALAKIS, S., MUHLFRIEDEL, R., TANIMOTO, N., KRISHNAMOORTHY, V., KOCH, S., FISCHER, M. D., BECIROVIC, E., BAI, L., HUBER, G., BECK, S. C., FAHL, E., BUNING, H., PAQUET-DURAND, F., ZONG, X., GOLLISCH, T., BIEL, M. & SEELIGER, M. W. 2010. Restoration of cone vision in the CNGA3^{-/-} mouse model of congenital complete lack of cone photoreceptor function. *Mol Ther*, 18, 2057-63.
- MICHALAKIS, S., MUHLFRIEDEL, R., TANIMOTO, N., KRISHNAMOORTHY, V., KOCH, S., FISCHER, M. D., BECIROVIC, E., BAI, L., HUBER, G., BECK, S. C., FAHL, E., BUNING, H., SCHMIDT, J., ZONG, X., GOLLISCH, T., BIEL, M. & SEELIGER, M. W. 2012. Gene therapy restores missing cone-mediated vision in the CNGA3^{-/-} mouse model of achromatopsia. *Adv Exp Med Biol*, 723, 183-9.
- MICHALAKIS, S., XU, J., BIEL, M. & DING, X. Q. 2013. Detection of cGMP in the degenerating retina. *Methods Mol Biol*, 1020, 235-45.
- MOLDAY, R. S. 1998. Photoreceptor membrane proteins, phototransduction, and retinal degenerative diseases. The Friedenwald Lecture. *Invest Ophthalmol Vis Sci*, 39, 2491-513.
- MOWAT, F. M., PETERSEN-JONES, S. M., WILLIAMSON, H., WILLIAMS, D. L., LUTHERT, P. J., ALI, R. R. & BAINBRIDGE, J. W. 2008. Topographical

- characterization of cone photoreceptors and the area centralis of the canine retina. *Mol Vis*, 14, 2518-27.
- MURGA, M., BUNTING, S., MONTANA, M. F., SORIA, R., MULERO, F., CANAMERO, M., LEE, Y., MCKINNON, P. J., NUSSENZWEIG, A. & FERNANDEZ-CAPETILLO, O. 2009. A mouse model of ATR-Seckel shows embryonic replicative stress and accelerated aging. *Nat Genet*, 41, 891-8.
- NARFSTROM, K., VAEGAN, KATZ, M., BRAGADOTTIR, R., RAKOCZY, E. P. & SEELIGER, M. 2005. Assessment of structure and function over a 3-year period after gene transfer in RPE65^{-/-} dogs. *Doc Ophthalmol*, 111, 39-48.
- NARFSTROM, K., WRIGSTAD, A. & NILSSON, S. E. 1989. The Briard dog: a new animal model of congenital stationary night blindness. *Br J Ophthalmol*, 73, 750-6.
- NEGOESCU, A., GUILLERMET, C., LORIMIER, P., BRAMBILLA, E. & LABAT-MOLEUR, F. 1998. Importance of DNA fragmentation in apoptosis with regard to TUNEL specificity. *Biomed Pharmacother*, 52, 252-8.
- NGHIEM, P., PARK, P. K., KIM, Y., VAZIRI, C. & SCHREIBER, S. L. 2001. ATR inhibition selectively sensitizes G1 checkpoint-deficient cells to lethal premature chromatin condensation. *Proc Natl Acad Sci U S A*, 98, 9092-7.
- NISHIDA, H., TATEWAKI, N., NAKAJIMA, Y., MAGARA, T., KO, K. M., HAMAMORI, Y. & KONISHI, T. 2009. Inhibition of ATR protein kinase activity by schisandrin B in DNA damage response. *Nucleic Acids Res*, 37, 5678-89.
- NOELL, W. K. 1951. The effect of iodoacetate on the vertebrate retina. *J Cell Physiol*, 37, 283-307.
- OKAWA, H., HOON, M., YOSHIMATSU, T., DELLA SANTINA, L. & WONG, R. O. 2014. Illuminating the multifaceted roles of neurotransmission in shaping neuronal circuitry. *Neuron*, 83, 1303-18.
- OZAKI, T., ISHIGURO, S., HIRANO, S., BABA, A., YAMASHITA, T., TOMITA, H. & NAKAZAWA, M. 2013. Inhibitory peptide of mitochondrial mu-calpain protects against photoreceptor degeneration in rhodopsin transgenic S334ter and P23H rats. *PLoS One*, 8, e71650.
- PALCZEWSKI, K., SOKAL, I. & BAEHR, W. 2004. Guanylate cyclase-activating proteins: structure, function, and diversity. *Biochem Biophys Res Commun*, 322, 1123-30.
- PANG, J. J., ALEXANDER, J., LEI, B., DENG, W., ZHANG, K., LI, Q., CHANG, B. & HAUSWIRTH, W. W. 2010. Achromatopsia as a potential candidate for gene therapy. *Adv Exp Med Biol*, 664, 639-46.
- PANG, J. J., DENG, W. T., DAI, X., LEI, B., EVERHART, D., UMINO, Y., LI, J., ZHANG, K., MAO, S., BOYE, S. L., LIU, L., CHIODO, V. A., LIU, X., SHI, W., TAO, Y., CHANG, B. & HAUSWIRTH, W. W. 2012. AAV-mediated cone rescue in a naturally occurring mouse model of CNGA3-achromatopsia. *PLoS One*, 7, e35250.
- PAQUET-DURAND, F., AZADI, S., HAUCK, S. M., UEFFING, M., VAN VEEN, T. & EKSTROM, P. 2006. Calpain is activated in degenerating photoreceptors in the rd1 mouse. *J Neurochem*, 96, 802-14.

- PAQUET-DURAND, F., BECK, S., MICHALAKIS, S., GOLDMANN, T., HUBER, G., MUHLFRIEDEL, R., TRIFUNOVIC, D., FISCHER, M. D., FAHL, E., DUETSCH, G., BECIROVIC, E., WOLFRUM, U., VAN VEEN, T., BIEL, M., TANIMOTO, N. & SEELIGER, M. W. 2011. A key role for cyclic nucleotide gated (CNG) channels in cGMP-related retinitis pigmentosa. *Hum Mol Genet*, 20, 941-7.
- PAQUET-DURAND, F., HAUCK, S. M., VAN VEEN, T., UEFFING, M. & EKSTROM, P. 2009. PKG activity causes photoreceptor cell death in two retinitis pigmentosa models. *J Neurochem*, 108, 796-810.
- PAYNE, A. M., DOWNES, S. M., BESSANT, D. A., TAYLOR, R., HOLDER, G. E., WARREN, M. J., BIRD, A. C. & BHATTACHARYA, S. S. 1998. A mutation in guanylate cyclase activator 1A (GUCA1A) in an autosomal dominant cone dystrophy pedigree mapping to a new locus on chromosome 6p21.1. *Hum Mol Genet*, 7, 273-7.
- PENG, C., RICH, E. D. & VARNUM, M. D. 2004. Subunit configuration of heteromeric cone cyclic nucleotide-gated channels. *Neuron*, 42, 401-10.
- PERRAULT, I., ROZET, J. M., CALVAS, P., GERBER, S., CAMUZAT, A., DOLLFUS, H., CHATELIN, S., SOUJED, E., GHAZI, I., LEOWSKI, C., BONNEMAISON, M., LE PASLIER, D., FREZAL, J., DUFIER, J. L., PITTLER, S., MUNNICH, A. & KAPLAN, J. 1996. Retinal-specific guanylate cyclase gene mutations in Leber's congenital amaurosis. *Nat Genet*, 14, 461-4.
- PETTERS, R. M., ALEXANDER, C. A., WELLS, K. D., COLLINS, E. B., SOMMER, J. R., BLANTON, M. R., ROJAS, G., HAO, Y., FLOWERS, W. L., BANIN, E., CIDECIYAN, A. V., JACOBSON, S. G. & WONG, F. 1997. Genetically engineered large animal model for studying cone photoreceptor survival and degeneration in retinitis pigmentosa. *Nat Biotechnol*, 15, 965-70.
- PFEIFER, A., ASZODI, A., SEIDLER, U., RUTH, P., HOFMANN, F. & FASSLER, R. 1996. Intestinal secretory defects and dwarfism in mice lacking cGMP-dependent protein kinase II. *Science*, 274, 2082-6.
- PFEIFER, A., RUTH, P., DOSTMANN, W., SAUSBIER, M., KLATT, P. & HOFMANN, F. 1999. Structure and function of cGMP-dependent protein kinases. *Rev Physiol Biochem Pharmacol*, 135, 105-49.
- PFISTER, J. A. & D'MELLO, S. R. 2015. Insights into the regulation of neuronal viability by nucleophosmin/B23. *Exp Biol Med (Maywood)*, 240, 774-86.
- PIERCE, E. A. 2001. Pathways to photoreceptor cell death in inherited retinal degenerations. *Bioessays*, 23, 605-18.
- PITTLER, S. J. & BAEHR, W. 1991. Identification of a nonsense mutation in the rod photoreceptor cGMP phosphodiesterase beta-subunit gene of the rd mouse. *Proc Natl Acad Sci U S A*, 88, 8322-6.
- POKORNY, J., SMITH, V. C., PINCKERS, A. J. & COZIJNSEN, M. 1982. Classification of complete and incomplete autosomal recessive achromatopsia. *Graefes Arch Clin Exp Ophthalmol*, 219, 121-30.
- REICHENBACH, A. & BRINGMANN, A. 2013. New functions of Muller cells. *Glia*, 61, 651-78.

- REICHER, S., SEROUSSI, E. & GOOTWINE, E. 2010. A mutation in gene CNGA3 is associated with day blindness in sheep. *Genomics*, 95, 101-4.
- ROBERTSON, B. H., GRUBMAN, M. J., WEDDELL, G. N., MOORE, D. M., WELSH, J. D., FISCHER, T., DOWBENKO, D. J., YANSURA, D. G., SMALL, B. & KLEID, D. G. 1985. Nucleotide and amino acid sequence coding for polypeptides of foot-and-mouth disease virus type A12. *J Virol*, 54, 651-60.
- ROGAKOU, E. P., NIEVES-NEIRA, W., BOON, C., POMMIER, Y. & BONNER, W. M. 2000. Initiation of DNA fragmentation during apoptosis induces phosphorylation of H2AX histone at serine 139. *J Biol Chem*, 275, 9390-5.
- ROOSING, S., THIADENS, A. A., HOYNG, C. B., KLAVER, C. C., DEN HOLLANDER, A. I. & CREMERS, F. P. 2014. Causes and consequences of inherited cone disorders. *Prog Retin Eye Res*, 42, 1-26.
- ROSENBERG, S. A., AEBERSOLD, P., CORNETTA, K., KASID, A., MORGAN, R. A., MOEN, R., KARSON, E. M., LOTZE, M. T., YANG, J. C., TOPALIAN, S. L. & ET AL. 1990. Gene transfer into humans--immunotherapy of patients with advanced melanoma, using tumor-infiltrating lymphocytes modified by retroviral gene transduction. *N Engl J Med*, 323, 570-8.
- RUTH, P., PFEIFER, A., KAMM, S., KLATT, P., DOSTMANN, W. R. & HOFMANN, F. 1997. Identification of the amino acid sequences responsible for high affinity activation of cGMP kinase Ialpha. *J Biol Chem*, 272, 10522-8.
- SAARI, J. C. 2000. Biochemistry of visual pigment regeneration: the Friedenwald lecture. *Invest Ophthalmol Vis Sci*, 41, 337-48.
- SAMULSKI, R. J., CHANG, L. S. & SHENK, T. 1987. A recombinant plasmid from which an infectious adeno-associated virus genome can be excised in vitro and its use to study viral replication. *J Virol*, 61, 3096-101.
- SANCAR, A., LINDSEY-BOLTZ, L. A., UNSAL-KACMAZ, K. & LINN, S. 2004. Molecular mechanisms of mammalian DNA repair and the DNA damage checkpoints. *Annu Rev Biochem*, 73, 39-85.
- SCHON, C., BIEL, M. & MICHALAKIS, S. 2013. Gene replacement therapy for retinal CNG channelopathies. *Mol Genet Genomics*, 288, 459-67.
- SCHON, C., HOFFMANN, N. A., OCHS, S. M., BURGOLD, S., FILSER, S., STEINBACH, S., SEELIGER, M. W., ARZBERGER, T., GOEDERT, M., KRETZSCHMAR, H. A., SCHMIDT, B. & HERMS, J. 2012. Long-term in vivo imaging of fibrillar tau in the retina of P301S transgenic mice. *PLoS One*, 7, e53547.
- SEDELNIKOVA, O. A., HORIKAWA, I., ZIMONJIC, D. B., POPESCU, N. C., BONNER, W. M. & BARRETT, J. C. 2004. Senescing human cells and ageing mice accumulate DNA lesions with unrepairable double-strand breaks. *Nat Cell Biol*, 6, 168-70.
- SHAMIR, M. H., OFRI, R., BOR, A., BRENNER, O., REICHER, S., OBOLENSKY, A., AVERBUKH, E., BANIN, E. & GOOTWINE, E. 2010. A novel day blindness in sheep: epidemiological, behavioural, electrophysiological and histopathological studies. *Vet J*, 185, 130-7.

- SHUART, N. G., HAITIN, Y., CAMP, S. S., BLACK, K. D. & ZAGOTTA, W. N. 2011. Molecular mechanism for 3:1 subunit stoichiometry of rod cyclic nucleotide-gated ion channels. *Nat Commun*, 2, 457.
- SIDJANIN, D. J., LOWE, J. K., MCELWEE, J. L., MILNE, B. S., PHIPPEN, T. M., SARGAN, D. R., AGUIRRE, G. D., ACLAND, G. M. & OSTRANDER, E. A. 2002. Canine CNGB3 mutations establish cone degeneration as orthologous to the human achromatopsia locus ACHM3. *Hum Mol Genet*, 11, 1823-33.
- SOKAL, I., ALEKSEEV, A. & PALCZEWSKI, K. 2003. Photoreceptor guanylate cyclase variants: cGMP production under control. *Acta Biochim Pol*, 50, 1075-95.
- STEINBERG, R. H. 1985. Interactions between the retinal pigment epithelium and the neural retina. *Doc Ophthalmol*, 60, 327-46.
- SUBER, M. L., PITTLER, S. J., QIN, N., WRIGHT, G. C., HOLCOMBE, V., LEE, R. H., CRAFT, C. M., LOLLEY, R. N., BAEHR, W. & HURWITZ, R. L. 1993. Irish setter dogs affected with rod/cone dysplasia contain a nonsense mutation in the rod cGMP phosphodiesterase beta-subunit gene. *Proc Natl Acad Sci U S A*, 90, 3968-72.
- SUNDIN, O. H., YANG, J. M., LI, Y., ZHU, D., HURD, J. N., MITCHELL, T. N., SILVA, E. D. & MAUMENEE, I. H. 2000. Genetic basis of total colourblindness among the Pingelapese islanders. *Nat Genet*, 25, 289-93.
- SZEBENI, A., HERRERA, J. E. & OLSON, M. O. 1995. Interaction of nucleolar protein B23 with peptides related to nuclear localization signals. *Biochemistry*, 34, 8037-42.
- TAKEMOTO, N., TACHIBANAKI, S. & KAWAMURA, S. 2009. High cGMP synthetic activity in carp cones. *Proc Natl Acad Sci U S A*, 106, 11788-93.
- TANAKA, J., MARKERINK-VAN ITTERSUM, M., STEINBUSCH, H. W. & DE VENETE, J. 1997. Nitric oxide-mediated cGMP synthesis in oligodendrocytes in the developing rat brain. *Glia*, 19, 286-97.
- THIADENS, A. A., ROOSING, S., COLLIN, R. W., VAN MOLL-RAMIREZ, N., VAN LITH-VERHOEVEN, J. J., VAN SCHOONEVELD, M. J., DEN HOLLANDER, A. I., VAN DEN BORN, L. I., HOYNG, C. B., CREMERS, F. P. & KLAVER, C. C. 2010a. Comprehensive analysis of the achromatopsia genes CNGA3 and CNGB3 in progressive cone dystrophy. *Ophthalmology*, 117, 825-30 e1.
- THIADENS, A. A., SOMERVUO, V., VAN DEN BORN, L. I., ROOSING, S., VAN SCHOONEVELD, M. J., KUIJPERS, R. W., VAN MOLL-RAMIREZ, N., CREMERS, F. P., HOYNG, C. B. & KLAVER, C. C. 2010b. Progressive loss of cones in achromatopsia: an imaging study using spectral-domain optical coherence tomography. *Invest Ophthalmol Vis Sci*, 51, 5952-7.
- TOSI, J., DAVIS, R. J., WANG, N. K., NAUMANN, M., LIN, C. S. & TSANG, S. H. 2011. shRNA knockdown of guanylate cyclase 2e or cyclic nucleotide gated channel alpha 1 increases photoreceptor survival in a cGMP phosphodiesterase mouse model of retinitis pigmentosa. *J Cell Mol Med*, 15, 1778-87.
- TRAPANI, I., PUPPO, A. & AURICCHIO, A. 2014. Vector platforms for gene therapy of inherited retinopathies. *Prog Retin Eye Res*, 43, 108-28.

- TRAVIS, G. H. 1998. Mechanisms of cell death in the inherited retinal degenerations. *Am J Hum Genet*, 62, 503-8.
- TRIFUNOVIC, D., DENGLER, K., MICHALAKIS, S., ZRENNER, E., WISSINGER, B. & PAQUET-DURAND, F. 2010. cGMP-dependent cone photoreceptor degeneration in the cpfl1 mouse retina. *J Comp Neurol*, 518, 3604-17.
- TSANG, S. H., GOURAS, P., YAMASHITA, C. K., KJELDBYE, H., FISHER, J., FARBER, D. B. & GOFF, S. P. 1996. Retinal degeneration in mice lacking the gamma subunit of the rod cGMP phosphodiesterase. *Science*, 272, 1026-9.
- VAANDRAGER, A. B., EHLERT, E. M., JARCHAU, T., LOHMANN, S. M. & DE JONGE, H. R. 1996. N-terminal myristoylation is required for membrane localization of cGMP-dependent protein kinase type II. *J Biol Chem*, 271, 7025-9.
- VESKE, A., NILSSON, S. E., NARFSTROM, K. & GAL, A. 1999. Retinal dystrophy of Swedish briard/briard-beagle dogs is due to a 4-bp deletion in RPE65. *Genomics*, 57, 57-61.
- WANG, D. & GAO, G. 2014. State-of-the-art human gene therapy: part I. Gene delivery technologies. *Discov Med*, 18, 67-77.
- WEBER, S., BERNHARD, D., LUKOWSKI, R., WEINMEISTER, P., WORNER, R., WEGENER, J. W., VALTCHEVA, N., FEIL, S., SCHLOSSMANN, J., HOFMANN, F. & FEIL, R. 2007. Rescue of cGMP kinase I knockout mice by smooth muscle specific expression of either isozyme. *Circ Res*, 101, 1096-103.
- WEGENER, J. W., NAWRATH, H., WOLFSGRUBER, W., KUHBANDNER, S., WERNER, C., HOFMANN, F. & FEIL, R. 2002. cGMP-dependent protein kinase I mediates the negative inotropic effect of cGMP in the murine myocardium. *Circ Res*, 90, 18-20.
- WERNET, W., FLOCKERZI, V. & HOFMANN, F. 1989. The cDNA of the two isoforms of bovine cGMP-dependent protein kinase. *FEBS Lett*, 251, 191-6.
- WILLET, K. & BENNETT, J. 2013. Immunology of AAV-Mediated Gene Transfer in the Eye. *Front Immunol*, 4, 261.
- WILSKER, D. & BUNZ, F. 2007. Loss of ataxia telangiectasia mutated- and Rad3-related function potentiates the effects of chemotherapeutic drugs on cancer cell survival. *Mol Cancer Ther*, 6, 1406-13.
- WRIGHT, A. F., CHAKAROVA, C. F., ABD EL-AZIZ, M. M. & BHATTACHARYA, S. S. 2010. Photoreceptor degeneration: genetic and mechanistic dissection of a complex trait. *Nat Rev Genet*, 11, 273-84.
- WRIGSTAD, A., NARFSTROM, K. & NILSSON, S. E. 1994. Slowly progressive changes of the retina and retinal pigment epithelium in Briard dogs with hereditary retinal dystrophy. A morphological study. *Doc Ophthalmol*, 87, 337-54.
- XU, J., MORRIS, L., THAPA, A., MA, H., MICHALAKIS, S., BIEL, M., BAEHR, W., PESHENKO, I. V., DIZHOOR, A. M. & DING, X. Q. 2013. cGMP accumulation causes photoreceptor degeneration in CNG channel deficiency: evidence of cGMP

- cytotoxicity independently of enhanced CNG channel function. *J Neurosci*, 33, 14939-48.
- YANG, R. B., ROBINSON, S. W., XIONG, W. H., YAU, K. W., BIRCH, D. G. & GARBERS, D. L. 1999. Disruption of a retinal guanylyl cyclase gene leads to cone-specific dystrophy and paradoxical rod behavior. *J Neurosci*, 19, 5889-97.
- YU, L., SUN, C., SONG, D., SHEN, J., XU, N., GUNASEKERA, A., HAJDUK, P. J. & OLEJNICZAK, E. T. 2005. Nuclear magnetic resonance structural studies of a potassium channel-charybdotoxin complex. *Biochemistry*, 44, 15834-41.
- ZHANG, X. & COTE, R. H. 2005. cGMP signaling in vertebrate retinal photoreceptor cells. *Front Biosci*, 10, 1191-204.
- ZULLIGER, R., CONLEY, S. M. & NAASH, M. I. 2015. Non-viral therapeutic approaches to ocular diseases: An overview and future directions. *J Control Release*, 219, 471-87.

9 Danksagung

Mein größter Dank gilt meiner gesamten Familie, die immer für mich da ist und mich stets unterstützt.

Ich danke Herrn PD Dr. Michalakis für die Möglichkeit an diesem Projekt zu arbeiten. Zudem möchte ich mich für die Betreuung und die hilfreichen wissenschaftlichen Ratschläge bedanken. Herrn Prof. Biel möchte ich danken, dass ich diese Arbeit in seinem Arbeitskreis durchführen konnte.

Ich danke Andrea Künzel und Michael Stadlmeier (AK Carrell) wie auch Daniela Meilinger (AK Leonhardt) für die hervorragende Zusammenarbeit.

Ich danke auch meinen fleißigen Studenten Theresa, Franziska und Veronika die mir tatkräftig zur Seite standen und tolle Arbeit geleistet haben. Nana auch dir möchte ich danken auch wenn wir nur ganz kurz zusammen gearbeitet haben.

Weiter möchte ich mich bei all denen bedanken die mir den Laboralltag versüßt und auch manchmal versalzen haben. Für gute wie auch schlechte wissenschaftliche Tipps, für kritische und dumme Fragen und natürlich für den ein oder anderen Weinabend. Dieser Dank gilt dem ganzen AK allerdings besonders zu erwähnen sind selbstverständlich Henne, Spahno, Rasmus, Hassan, Franzl, Krause und Sybi. Was wäre diese Zeit ohne euch gewesen ;).

Ganz besonderer Dank geht an Meike: ohne dich wäre ich schon oft nicht weiter gekommen du bist die beste große Schwester die man sich wünschen kann, die zu jeder Tages- und Nachtzeit bereit steht.